Human Adipose-derived Mesenchymal Stem Cells in a 3D Spheroid Culture System –

Extracellular Matrix Development, Adipogenic Differentiation, and Secretory Properties

Humane mesenchymale Stammzellen aus dem Fettgewebe in einem 3D Sphäroid Kultursystem –

Entwicklung der Extrazellulärmatrix, adipogene Differenzierung und sekretorische Eigenschaften

Doctoral thesis for a doctoral degree
at the Graduate School of Life Sciences,
Julius-Maximilians-Universität Würzburg,

submitted by
Christiane Höfner

from
Neuendettelsau, Germany

Würzburg, 2019

Submitted on: .....

Office stamp

Members of the Thesis Committee:

Chairperson: Prof. Dr. Thomas Dandekar

Primary Supervisor: Prof. Dr. Torsten Blunk

Supervisor (Second): Prof. Dr. Norbert Schütze

Supervisor (Third): PD Dr. Matthias Becker

Date of Public Defence: .....

Date of Receipt of Certificates:.....

In Liebe und Dankbarkeit für meine Eltern

Table of Contents

Summary

Human adipose-derived mesenchymal stromal/stem cells (ASCs) exhibit great therapeutic potential, ranging from the capability to differentiate into mesenchymal lineages to anti-inflammatory and immunomodulatory properties, what make them promising candidates for cellular therapies. Routine culture of ASCs under conventional 2D conditions encompasses the loss of their intrinsic 3D microenvironment and leads to impaired regenerative capacity of cells. Thus, the cultivation of ASCs as self-assembled 3D aggregates, called spheroids, with cells residing and interacting in their own matrix appears an attractive tool to enhance their therapeutic potential. The resemblance to physiological cell-cell and cell-matrix interactions within these multicellular aggregates leads to a higher similarity to real tissue, making them not only a promising approach in regenerative medicine, but also an emerging trend in their use as building blocks for tissue engineering. Especially for adipose tissue engineering to overcome the still tremendous clinical need for the development of adequate implants to repair soft tissue defects, 3D spheroids of abundant and easy to isolate ASCs appear to be an attractive tool. Before their effective use in regenerative medicine and adipose tissue engineering can be approached, however, an extensive characterization with regard to structural features, differentiation capability, and secretory properties is indispensable. For this purpose, in the first part of this thesis, the spheroid formation process and the participating cell-cell and cell-ECM interactions were addressed. The reproducible and well controlled assembly of ASCs into spheroids employing the liquid overlay technique was achieved within 24 h. Regarding the development of ECM components, fibronectin was the first matrix protein to be detected very early during assembly. An influence of this early expression of fibronectin on initial cell aggregation was demonstrated by the specific antibody-blocking of β1-integrin, one cellular receptor responsible for fibronectin binding. A dependence of spheroid formation on cell-cell interaction via cadherins, however, could not be shown for the ASCs. Thus, in addition to a detailed description of spheroid formation, first insights into the underlying mechanisms were shown.

The effective use of ASC-based spheroids as building blocks for adipose tissue engineering requires insights into ECM development and an efficient adipogenic induction. Thus, in the second part of this work, the focus was on the extracellular matrix development in ASC spheroids, and furthermore, on the adipogenic differentiation in comparison to conventional 2D culture regarding different induction protocols. Differentiated spheroids exhibited an ECM composition representing an adipogenic phenotype with laminin, collagen type I, IV, and VI as

major parts of the ECM framework with a distinct resemblance to native fat. Furthermore, a superior differentiation capability upon a short inductive stimulus of spheroids compared to 2D cultured cells could be demonstrated with regard to triglyceride content and adipogenic marker gene expression. This fact together with their feature to present adipose-like microtissues make them promising material-free modules for adipose tissue engineering approaches.

It is now known that the ECM not only act as an inert supportive scaffold, but also influences cellular processes, including differentiation, through interaction with cellular receptors. As laminin, one major ECM component of the basement membrane of mature adipocytes, was detected very early in the ECM of differentiating ASC spheroids, its possible influence on adipogenesis was further investigated. For this purpose, a shRNA-mediated knockdown of the *LAMA4* gene encoding for the laminin α4 chain of the adipo-specific laminin-8 heterotrimer was performed. Although a stable knockdown of *LAMA4* could be achieved in the ASCs, no direct correlation to the adipogenic differentiation capability of the cells could be established, since the reduced expression of this single laminin gene was not consistently reflected in the expression of the total laminin on protein level.

The enhanced therapeutic potential of mesenchymal stem cells in a 3D environment was shown to be not only restricted to their improved differentiation capacity, but also comes along with enhanced anti-inflammatory and immunomodulatory properties via paracrine secretion. To confirm this also for ASCs, in the last part of this thesis, gene expression of ASC-based spheroids, regarding several anti-inflammatory, anti-apoptotic, and anti-cancer related cytokines, were examined. Compared to 2D monolayers, a significant upregulation in the expression of the respective cytokines was observed in 3D spheroids. For one major anti-inflammatory factor, prostaglandin E2, the enhanced secretion of ASCs cultured in a 3D environment could also be confirmed on secretion level.

The identification of spheroid-intrinsic factors contributing to the improved therapeutic potential of cells in a 3D environment is still pending. A PCR array for screening of cell junction-related genes was used as a first attempt to identify alterations in cell-cell interactions in ASCs cultured as 3D spheroids that might be responsible for their enhanced therapeutic potential. Distinct differences in the expression of cell junction-related genes between 3D spheroids and 2D monolayers could be detected. These results may serve as a basis for further research to get closer to a comprehensive understanding of the role of cell-cell and cell-ECM interactions in a 3D spheroid culture system.

In summary, the results of this work contribute to a comprehensive characterization of ASC-based spheroids regarding structural features, differentiation capability and secretory properties. It has been shown that ASCs of 3D spheroids not only exhibit an elevated differentiation capability as well as an upregulated expression of genes encoding for multiple cytokines, but are also able to form adipose-like micro tissues. Thus, these results may ultimately further the effective application of ASC-based spheroids in regenerative medicine and adipose tissue engineering approaches.

Zusammenfassung

Humane mesenchymale Stammzellen aus dem Fettgewebe (ASCs) verfügen über ein großes therapeutisches Potenzial. Dieses reicht von ihrer Fähigkeit zur Differenzierung entlang der mesenchymalen Linien bis hin zu entzündungshemmenden und immunmodulatorischen Eigenschaften, was sie zu vielversprechenden Kandidaten im Einsatz für die regenerative Zelltherapie macht. Die Routinekultur dieser Zellen unter herkömmlichen 2D-Kulturbedingungen führt durch den Verlust der Umgebung in einem dreidimensionalen Gewebeverbund zur Beeinträchtigung ihrer regenerativen Fähigkeiten. Die Kultivierung in dreidimensionalen Zellaggregaten (Sphäroiden), in denen die Zellen in einem mehr physiologischen 3D Verbund innerhalb ihrer sekretierten Matrix interagieren können, erscheint somit als geeignete Möglichkeit das therapeutische Potential von ASCs zu steigern. Dies macht ASC-basierte Sphäroide nicht nur zu einem vielversprechenden Ansatz in der regenerativen Medizin im Allgemeinen, sondern auch zu einem innovativen Tool in ihrer Verwendung als „Bausteine“ für das Konzept des Tissue Engineerings. Insbesondere im Bereich des Fettgewebe-Engineerings besteht ein immenser klinischer Bedarf an der Entwicklung geeigneter Implantate für die Rekonstruktion von Weichteildefekten. Hierfür erscheinen Sphäroide aus den leicht und in ausreichender Menge zu isolierenden ASCs besonders attraktiv. Der effektive Einsatz solcher Sphäroide in der regenerativen Medizin, sowie im Fettgewebe-Engineering, erfordert jedoch zunächst ihre umfassende Charakterisierung in Bezug auf Strukturmerkmale, Differenzierungsfähigkeit und sekretorische Eigenschaften. Dazu wurden im ersten Teil dieser Arbeit der Prozess der Sphäroidbildung sowie die daran beteiligten Zell-Zell- und Zell-ECM-Interaktionen untersucht. Mit Hilfe der sogenannten Liquid-Overlay Technik gelang die reproduzierbare und kontrollierte Zusammenlagerung der ASCs in dreidimensionale Sphäroide innerhalb von 24 h. Hinsichtlich der Entwicklung von Extrazellulärmatrix-Komponenten während der Sphäroidbildung zeigte sich Fibronektin als die Matrix-Komponente, welche als Erste während des Prozesses zu detektieren war. Durch das Blockieren des Fibronektin-spezifischen β1-Integrins mittels eines spezifischen Antikörpers konnte ein Einfluss dieser frühen Fibronektin-Expression auf den Verlauf der Zellaggregation gezeigt werden. Bei dem hier blockierten β1-Integrin handelt es sich um einen zellulären Rezeptor, welcher maßgeblich an der Fibronektinbindung beteiligt ist. Eine Abhängigkeit der Sphäroidbildung von der Zell-Zell Interaktion mittels Cadherine konnte hingegen für die ASCs nicht nachgewiesen werden. Somit konnten im ersten Abschnitt neben einer detaillierten

Beschreibung der ASC-Sphäroidbildung zusätzlich erste Erkenntnisse über die dem Prozess zugrundeliegenden Mechanismen gewonnen werden.

Der effektive Einsatz von ASC-basierten Sphäroiden als Bausteine für das Fettgewebe-Engineering erfordert Kenntnisse sowohl über die Entwicklung der ECM als wichtigen gewebe-inhärenten Faktor, als auch über eine effiziente adipogene Induktion. Somit lag der Fokus im zweiten Teil dieser Arbeit auf der Charakterisierung der Extrazellulärmatrix in den ASC-Sphäroiden, sowie auf deren Fähigkeit zur adipogenen Differenzierung im Vergleich zur konventionellen 2D-Kultur unter der Verwendung verschiedener Induktionsprotokolle. Differenzierte Sphäroide weisen mit Laminin, Kollagen Typ I, IV und VI als nachgewiesenen Hauptbestandteilen eine Fettgewebs-spezifische Matrixzusammensetzung auf, die eine ausgeprägte Ähnlichkeit zu der des nativen Fettgewebes zeigt. Darüber hinaus konnte eine verbesserte Differenzierungsfähigkeit der ASC-Sphäroide nach einem kurzen induktiven Stimulus gegenüber der 2D kultivierten Zellen gezeigt werden. Dies wurde sowohl hinsichtlich des Triglyceridgehalts, sowie der Expression adipogener Markergene nachgewiesen. Diese verbesserte Differenzierbarkeit und die Möglichkeit mit den Sphäroiden fettgewebeähnliche Mikrogewebe herzustellen, machen diese Zellaggregate zu vielversprechenden Bausteinen für Ansätze im Fettgewebe-Engineering.

Inzwischen ist bekannt, dass die Extrazellulärmatrix nicht nur als inertes, unterstützendes Gerüst wirkt, sondern auch zelluläre Prozesse, einschließlich der Differenzierung, durch die Interaktion mit zellulären Rezeptoren beeinflusst. Laminin als wichtige ECM Komponente der Basalmembran reifer Adipozyten konnte in der ECM der adipogen differenzierenden Sphäroide im Gegensatz zu 2D Kulturen zu einem sehr frühen Zeitpunkt der Adipogenese nachgewiesen werden. Um einen positiven Einfluss des Laminins auf den Prozess der adipogenen Differenzierung weitergehend zu untersuchen, wurde ein shRNA-vermittelter Knockdown eines spezifischen Laminin-Gens, welches für die Lamininkette α4 des adipospezifischen Laminin-8 Heterotrimers kodiert, durchgeführt. Obwohl ein stabiler Knockdown des *LAMA4* Gens in den ASCs erreicht wurde, so konnte dennoch keine direkte Korrelation zur adipogenen Differenzierungsfähigkeit der Zellen festgestellt werden, da die reduzierte Expression dieses einzelnen Laminin-Gens sich nicht konsequent in der Expression des Gesamtlaminins auf Proteinebene durchsetzte.

Das verbesserte therapeutische Potenzial mesenchymaler Stammzellen in einer dreidimensionalen Umgebung beschränkt sich nicht nur auf ihre verbesserte Differenzierungsfähigkeit, sondern umfasst auch die parakrine Sekretion der Zellen, die

angiogene, anti-apoptotische, entzündungshemmende und immunmodulatorische Eigenschaften vermittelt. Um dies auch für ASCs zu bestätigen, wurden im letzten Teil dieser Arbeit die Genexpression von ASC-basierten Sphäroiden im Vergleich zu 2D kultivierten Zellen untersucht. Durch mRNA Genexpressionsanalysen konnte für ausgewählte entzündungshemmende, anti-apoptotische und anti-tumor wirksame Zytokine eine signifikant höhere Expression in den Sphäroiden gegenüber der 2D Kultur gezeigt werden. Für einen der wichtigsten entzündungshemmenden Faktoren, Prostaglandin E2, konnte eine erhöhte Sekretion von ASCs, kultiviert als 3D Sphäroide, auch auf Sekretionsebene bestätigt werden.

Die Identifizierung intrinsischer Faktoren, welche zu dem verbesserten therapeutischen Potenzial der Zellen in einer dreidimensionalen Umgebung beitragen, ist noch ausstehend. Zur Untersuchung des Einflusses von Zell-Zellkontakten diente ein PCR-Array zum Screening hierfür relevanter Gene. Durch den Vergleich der beiden Kulturbedingungen, 2D Monolayer und 3D Sphäroide, sollten mögliche Unterschiede in den ASCs festgestellt werden können, welche eventuell für das verbesserte therapeutische Potenzial der Sphäroide mitunter verantwortlich sind. Dabei konnten eindeutige Unterschiede zwischen ASCs aus der 3D bzw. 2D-Kultur festgestellt werden. Diese Ergebnisse bilden die Grundlage für weitere Untersuchungen auf diesem Gebiet, um einem umfassenden Verständnis der Rolle von Zell-Zell- und Zell-ECM-Interaktionen in einem 3D-Sphäroid-Kultursystem näherzukommen.

Zusammengefasst tragen die Ergebnisse dieser Arbeit zu einer umfangreichen Charakterisierung der ASC Sphäroide hinsichtlich struktureller Merkmale, Differenzierungsfähigkeit und sekretorischer Eigenschaften bei. Es wurde gezeigt, dass ASCs der 3D Sphäroide nicht nur eine verbesserte Differenzierungsfähigkeit, sowie eine erhöhte Expression von Genen aufweisen, welche für verschiedene Zytokine codieren, sondern ebenso in der Lage sind Fettgewebs-ähnliche Mikrogewebe zu bilden. Diese Erkenntnisse tragen dadurch insgesamt zur Förderung der ASC Sphäroide in ihrer effektiven Anwendung in der regenerativen Medizin und im Bereich des Fettgewebe-Engineerings bei.

1 Introduction

1.1 Adipose tissue

Adipose tissue is a type of highly specialized loose connective tissue which exists in two major forms in humans: white adipose tissue (WAT) and brown adipose tissue (BAT). Most prominent at birth, BAT is responsible for heat generation, especially to overcome the rapid temperature drop that occurs at birth. By cleaving triglycerides heat is generated, which is further transferred through the tissue vasculature to warm the new-born (1–3). In adult humans BAT is found only in small amounts as a gradual replacement by WAT takes place during the aging process (4,5). With a proportion of 10-29% of body weight in normal-weight adult humans, WAT is the most abundant tissue in humans and the focus of this work, so that in the further course fatty or adipose tissue always means white adipose tissue (6). WAT is distributed throughout the whole human body, so that it is mainly differed by type and depot between subcutaneous and intraabdominal (omental, retroperitoneal, visceral) fatty tissue, however it occurs also at other sites (e.g. bone marrow, intramuscular, pericardial, retroorbital and periarticular regions) (7). For decades WAT was viewed only as a passive organ relegated to serve primarily as an energy reservoir through storing a large amount of triacylglycerols. Besides the most prominent function as an energy regulator of the body through the controlled storage and release, maintaining normal body contours and providing mechanical protection for other organs are additional properties of fatty tissue (8–10). However, adipose tissue is much more than a passive organ with a high energy density and has far more functions than those previously mentioned. As a source of multiple autocrine, paracrine and endocrine factors such as proteins (named adipokines), fatty acids, steroid hormones and prostaglandins, fatty tissue is also considered an endocrine organ with metabolic function involved not only in energy homeostasis, but also in various other processes including blood pressure, regulation of immune function and angiogenesis (5,10–12).

On the cellular level, WAT is predominantly composed of mature adipocytes containing large lipid droplets. These lipid-laden cells have already reached their terminal differentiation state and are therefore incapable of further proliferating. Besides mature adipocytes, endothelial cells, pericytes, smooth muscle cells, fibroblasts, macrophages, progenitor cells committed to the adipogenic lineage as well as mesenchymal stem cells are all further cellular components of the WAT, which could be found in the stromal vascular fraction (SVF) of the tissue (4,9).

One further characteristic feature of the adipose tissue is a well-defined and dense capillary network. Because of the high metabolic rate, each adipocyte is in contact with at least one capillary. This extensive system of blood vessels together with lymph nodes and nerves which is supported by an extracellular matrix composed of different collagen types and other ECM proteins forms along with the respective cells a complex tissue that has been underestimated for years (3,5,10,11,13,14).

1.2 Adipose tissue engineering

Disease, trauma, tumor resection and congenital defects of the subcutaneous adipose tissue are all reasons that can affect the function, but mainly impair a natural human appearance. For plastic surgeons and clinicians these pathologies and defects of the adipose tissue still remain a reconstructive challenge. According to the American Society of Plastic Surgeons, breast reconstruction, burn care, cleft lip / palate repair, tumor removal and treatment from dog bites are the most common reconstructive procedures. In particular, from 2009 to 2014, the Agency for Health Care Research and Quality reported an increase in breast reconstruction after mastectomy by 62% (15,16). Implant or flap-based soft tissue reconstruction are the two major reconstruction options for breast adipose tissue deficits. Both methods are invasive procedures in which a large number of complications have to be considered, so that both surgeons and patients are interested in minimally invasive alternative methods (15,17,18). In plastic surgery the use of autologous fat grafting (AFG) increases as a safe, resourceful and minimally invasive method. After harvesting patients´ own fat via liposuction, the tissue is deposited into the defect site via syringe injections. There are several advantages in comparison to implant- or flap-based soft tissue reconstruction like minimal scarring, no foreign body reaction and a short patient recovery time, so that this method is the actual gold standard of care for example for breast reconstruction (19). Despite the positive outcome of this method in the short term, the long-term results are often unpredictable. Due to the lack of sufficient revascularization and the resulting limited oxygen and nutrient supply, the chances of a long-term viability of the tissue are reduced, which often leads to tissue resorption (19–21).

To overcome the tremendous clinical need of improved therapeutic approaches, the field of adipose tissue engineering evolved to find novel solutions for the previously discussed problems through the development of bioactive tissue constructs equivalent to native fat in terms of its cellular and extracellular structure (3,4,9). Approaches in tissue engineering pursue

the general principle of seeding cells, isolated from patients own tissue and further cultured in a laboratory to obtain larger amounts, onto a supporting scaffold, which may then be implanted into the patient at the needed site. Back in the patient the cells grow, a tissue develops, scaffold material degrades or is absorbed and finally a new tissue mass remains which now restore the previously defect site (4,22,23). For this purpose, tissue engineering strategies normally incorporate cell sources, biomaterial scaffolds and a microenvironment to provide the appropriate cues and signals for growth and tissue formation (3).

Cell source. There are several criteria that make an ideal cell source for adipose tissue engineering. Autologous cells should be available in sufficient quantities either by direct harvest or by propagation in vitro without losing their differentiation potential. To avoid donor site morbidity and further complications accompanying invasive surgeries, minimally invasive procedures of harvesting are preferable. Furthermore, the ability for standardization of the harvesting and processing procedure is beneficial (9). With regard to these characteristics, mature adipocytes seem obvious to repair soft tissue defects. However, through their susceptibility to mechanical damage during the aspiration procedure because of their lipid filled cytoplasm most attempt using mature adipocytes were unsuccessful. Besides the mechanical damage, their terminally differentiated state with the resulting lack of further proliferation and differentiation further discourages their use in tissue engineering methods (1,4,21,24). A cell source that appears to be better suited for tissue engineering approaches than mature adipocytes are preadipocytes, precursor cells which are already committed to the adipogenic lineage (25). These cells are capable of both proliferating to obtain sufficient quantities and of differentiating to obtain the tissue of interest (26–28). However, after elevated numbers of passages for in vitro propagation a loss of their differentiation capacity could emerge, what is a great disadvantage of the preadipocytes for their use in fat tissue engineering (29). The use of embryonic stem cells with their indefinite proliferation potential and their property to differentiate into a wide variety of cells, including adipocytes, would be a possibility to overcome the limitations of the previously mentioned cell sources (30). However, ethical concerns and legal constraints are reasons for the limited number of studies using embryonic stem cells in the context of adipose tissue engineering (9,31,32). Adult mesenchymal stem cells (MSCs), also termed mesenchymal stromal cells derived from the stromal vascular fraction of the adipose tissue (ASCs) or isolated from bone marrow aspirates (BMSCs), are therefore the most commonly used cell source for cell-based tissue engineering approaches. Their easy isolation and further expansion in the lab together with their self-renewing feature for several generations and their multipotent

differentiation capacity in vitro make them an attractive cell source for cell-based therapies in many tissue engineering applications (4,9,33).

Biomaterial scaffolds. With the aim to restore soft tissue defects, scaffolds take over the task of supporting cells in their attachment, migration, interaction, proliferation as well as differentiation (34–36). Furthermore, they serve as mechanical support for the cells and the newly formed extracellular matrix. They have to be biocompatible and should be degraded proportional to the formation of newly developed adipose tissue (15). One can distinguish between synthetic and natural biomaterial-based scaffolds. Synthetic material-based scaffolds like for example polylactic acid, polyglycolic acid and poly (lactic-co-glycolic) acid (PLA, PGA, PLGA), all of them extensively investigated and used for adipose tissue regeneration, have the advantage of being tailored and specifically designed for adjustment of mechanical/chemical properties as well as degradation (37). But also, many natural biomaterials have been widely examined and used for a plenty of studies concerning the engineering of adipose tissue. The natural biomaterials used in this context range from collagen and hyaluronic acid, which are the two most common naturally derived biomaterials for scaffolds in tissue engineering, to chitosan, silk, fibrin and even decellularized extracellular matrix (ECM) (15). In the form of decellularized adipose tissue (DAT), the latter has gained more and more significance as scaffold material in the field of soft tissue engineering (15). Due to the ability of closely mimicking the architecture as well as mechanical and biochemical properties of native adipose tissue, DAT would be highly suitable for the reconstruction of adipose tissue. However, the process of decellularization can also strip away more than just cells from the ECM, so that it is resulting in a suboptimal environment to repopulate with functional cells (38).

Microenvironment. The surrounding environment of a tissue construct also influences to a large extent its differentiation and rate of tissue formation. Several inducing and inhibiting factors, such as growth factors (endo- and exogenous) and hormones are known to affect the differentiation into the tissue of interest, here adipose tissue. The role of tissue-inherent conditions, especially cell-cell or cell-ECM interactions but also local pO_2 (normoxia, hypoxia) and pH should not be neglected as they may also contribute to an appropriate tissue formation but have not been fully elucidated yet (1).

1.3 Adipose-derived mesenchymal stromal/stem cells (ASCs)

Adipose tissue, is an abundant, easily accessible, and rich source of mesenchymal stem cells with multipotent properties, highly suitable for tissue engineering and regenerative medical applications (39,40). As an omnipresent tissue in humans, subcutaneous fat is easily accessible in large quantities by liposuction aspiration, which is a good starting material for adipose-derived mesenchymal stromal/stem cell (ASCs) isolation (41). This makes ASCs highly advantageous over MSCs isolated from bone marrow aspirates (BMSCs). Even though BMSCs are the most commonly used adult stem cells, their extraction procedure is painful, and the yield rate of cells is quite low (42). Compared to stem cells derived from the bone marrow, adipose tissue has been reported to contain 1000x the number of stem cells (per gram tissue) (43). Especially for adipose tissue engineering, which requires a high number of cells, fat tissue is therefore an attractive source for mesenchymal stem cells. Otherwise an extensive propagation would be necessary in vitro to obtain sufficient cell numbers what could possibly be accompanied by a decreasing differentiation capability (43).

The most commonly used method to isolate ASCs from adipose tissue first combines homogenization, enzymatic digestion and differential centrifugation in order to separate mature adipocytes from the pelleted stromal vascular fraction (SVF). The subsequent cultivation uses the ability of the cells to adhere to plastic and to proliferate in vitro to gain an enrichment of ASCs (39,44).

Mesenchymal stromal/stem cells derived from the stromal vascular fraction of adipose tissue have a multilineage potential and are known to differentiate into numerous cell lineages including adipogenic, osteogenic, chondrogenic, myogenic, cardiomyogenic, and neurogenic-like cell types upon treatment with established lineage specific factors (40). Due to their capacity for self-renewal and multilineage differentiation, these multipotent cells have a great potential for tissue engineering and regenerative medicine (39).

1.4 Adipogenic differentiation of ASCs

During the differentiation process of mesenchymal stromal/stem cells along the adipogenic lineage into mature adipocytes various changes regarding cell morphology and gene expression occur (39). Determination and terminal differentiation are the two phases adipogenesis can be subdivided in (Figure 1.1). In the first part of adipogenic differentiation, named determination phase, the commitment of the multipotent mesenchymal stem cells to the adipogenic lineage

take place. The so called preadipocytes no longer have the multipotent character of their precursor cells. The commitment to the adipogenic lineage lead to the loss of their differentiation potential into other cell types, while they still maintain their capacity to proliferate (9,45). During the subsequent terminal differentiation preadipocytes develop into mature adipocytes. Insulin sensitivity and secretion of adipocyte-specific proteins accompany the final differentiation process as well as the synthesis and accumulation of lipids, which finally occupy 90% of the cytoplasm (45).

Much of our knowledge about the differentiation along the adipogenic lineage was obtained through extensive investigations using mouse preadipocyte cell lines like 3T3-L1 or 3T3-F442A as adipocyte cell culture model (46,47). However, the cellular and molecular mechanisms of the second phase of adipogenesis are still better characterized than the early commitment of multipotent mesenchymal stem cells to the adipogenic lineage (45). Various changes in the expression of numerous genes take place in a chronological order during the differentiation of committed preadipocytes into lipid laden mature adipocytes. This strictly regulated process is accompanied by the development of early, intermediate, and late adipogenic markers. Growth arrested 3T3-L1 preadipocytes are reported to re-enter the cell cycle for further cell-doubling steps prior to final adipogenic differentiation, a process referred to as mitotic clonal expansion (MCE) (45,48). Whether this is an important step and therefore required for differentiation is still discussed controversially, however, it was reported for human primary preadipocytes that it is not a critical part during adipogenesis (45,49). After several rounds of MCE, the adipogenic gene expression program is initiated ultimately leading to final adipocyte differentiation. The adipogenic program requires a cascade of multiple transcription factors, which are involved in directing adipogenesis through the temporal regulation of several gene expression events (50,51). Two early adipogenic markers expressed during the terminal differentiation are members of the CCAAT/enhancer binding protein (C/EBP) family, i.e. C/EBPβ and C/EBPδ, which are responsible for the required growth arrest of the differentiating cells. Furthermore, C/EBPβ and C/EBPδ mediate the expression of another member of the C/EBP family, C/EBPα, as well as of the nuclear receptor superfamily, peroxisome proliferator-activated receptor γ (PPARγ), which is a critical step in adipogenesis (45,52). Playing a key role in adipogenic differentiation, PPARγ is not only essential for the process of adipogenesis itself, but also for the maintenance of the final differentiated state (53). While the expression of C/EBPβ and C/EBPδ decreases again in the further course of adipogenesis, C/EBPα and PPARγ coregulate each other to maintain their gene expression in order to generate terminally

differentiated mature adipocytes (52). Besides the activation of the two main transcription factors in the process of adipogenic differentiation, C/EBPα and PPARγ, one further key factor is also involved in gene expression and the regulation of triglyceride synthesis in mature adipocytes, the sterol regulatory element binding protein-1c (SREBP-1c)/adipocyte determination and differentiation factor 1 (ADD1), a helix-loop-helix-leucine zipper protein (54). The loss of a fibroblastic cell morphology accompanied by the development of a rounded-up cell shape as well as the metabolic characteristics of mature adipocytes are the consequences of the adipocyte-specific gene expression. This includes among others the expression of enzymes participating in the fatty acid and triacylglycerol metabolism like the lipoprotein lipase (LPL). Through its key role in lipid accumulation, the latter is required for the increased rate of *de novo* lipogenesis. One further main characteristic of mature adipocytes is their insulin sensitivity due the expression of numerous insulin receptors. The previously mentioned proteins, which are directly related either to the lipid metabolism or the insulin sensitivity, are not the only features of mature adipocytes. These also includes various regulatory proteins and further adipose specific tissue products, like for example the adipocyte specific fatty acid binding protein (aP2), the putative fatty acid transporter FAT/CD36, the lipid droplet-associated protein perilipin, the insulin-responsive glucose transporter GLUT 4 and secreted products like leptin, adipsin, adiponectin, tumor necrosis factor α (TNFα) and others. Among others, these are all factors which make the mature adipocytes what they are, namely both endocrine and paracrine/autocrine cells (54,55).

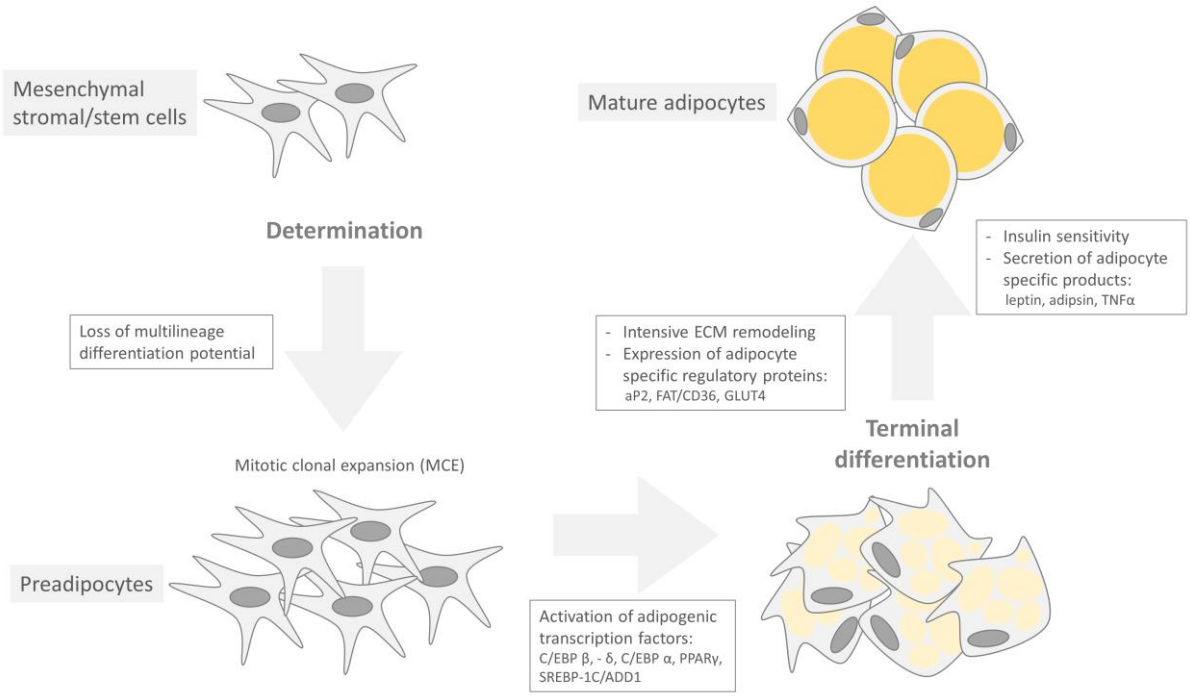

Figure 1.1: Adipogenic differentiation of ASCs.

The process of adipogenesis can be subdivided into two phases, called determination and terminal differentiation. In the first part the commitment of the multipotent mesenchymal stromal/stem cells to the adipogenic lineage take place. After further cell-doubling steps, also known as mitotic clonal expansion (MCE), committed preadipocytes start their final differentiation into lipid laden mature adipocytes, accompanied by changes in the expression of numerous genes as well as an intensive remodeling of the cell surrounding ECM. Adapted in part from Mahoney et al. 2018 (15).

Precursor cells in vivo surrounded by their natural microenvironment receive their signals for differentiation in form of stimulating and repressing cytokines. For inducing adipogenesis in vitro, however, the addition of soluble hormonal factors to the culture medium is required (9). Typically, a cocktail inducing differentiation of mesenchymal stem cells along the adipogenic lineage consists of at least three factors, a glucocorticoid (e.g. dexamethasone), a cyclic adenosine monophosphate (cAMP) level increasing agent such as phosphodiesterase inhibitors (e.g. isobutylmethylxanthine (IBMX)), and insulin or IGF-1 (insulin-like growth factor 1). The latter activates the phosphorylation of the cAMP response element binding protein (CREB) in preadipocytes to induce differentiation while regulating triglyceride synthesis through the sterol regulatory element-binding protein-1c (SREBP1c) (53,56,57). In addition to the three above mentioned factors, directing adipogenic differentiation, a PPARγ agonist, like for example the nonsteroidal anti-inflammatory drug indomethacin is often added in order to sustain adipogenesis (9,53).

However, not only the above mentioned various hormones and growth factors, but also cell-cell and especially, cell-matrix interactions can affect the differentiation process (9,54). Several extracellular matrix proteins form the non-cellular component of the adipose tissue. Through specific protein domains, which can bind to cellular receptors such as integrins, they can mediate cell-matrix adhesion as well as signal transduction into the cells. The ECM components can thus provide information to the cells in order to regulate cellular processes, including the differentiation along the adipogenic lineage (58,59). Exact mechanisms through which cell-matrix interactions can direct adipogenic differentiation, however, are poorly understood and still remain elusive.

1.5 The extracellular matrix (ECM)

1.5.1 The role of the ECM

Once considered an inert supportive scaffold with the main function of sustaining tissue and organ structure, it was recognized during the last two decades that the ECM is more than that, as its fundamental role in key aspects of cell biology became increasingly evident. Through direct or indirect action the extracellular matrix influences cell behavior and directs several cellular processes, thus, playing essential roles during the development but also having a major impact on tissue homeostasis and regeneration under physiological and pathological conditions (58,60).

At the cellular level, stem cells, which are located in a specific microenvironment, defined as their niche, are mainly responsible for tissue maintenance and regeneration. ECM is a key component in these stem cell niches, where it takes influence on various aspects of stem cell behavior including maintenance, proliferation, self-renewal, and differentiation (60,61). As part of their specific microenvironment, stem cells receive signals from their surrounding ECM deriving from cell-ECM interaction as well as soluble and ECM-bound factors to permit maintenance of stem cell homeostasis (62–65). Findings on the influence of ECM on stem cell regulation mainly result from studies using decellularized tissue. The preserved ECM is further used as a natural scaffold, which was shown to be able to guide seeded stem cells to differentiate into cell types found in the tissue from which the ECM originates. As already mentioned above, this is why the preserved ECM from decellularized tissue is often used as a scaffold in tissue engineering and for developing new cell therapy approaches (66–68).

However, not only stem cells are residing in der niche, but also all other cell types are in contact with this complex and dynamic network of macromolecules. This molecular scaffold is unique and specific to each tissue by varying in the amounts and organization of the different ECM components, thereby adapting to the particular needs of the cells in each tissue. The functional diversity and the different organization of ECM components also confers different physical, biochemical as well as mechanical properties to the ECM (Figure 1.2) (60,69,70).

Biochemical characteristics. These include both direct and indirect signaling properties, directly by binding to cells via cell-surface receptors or indirectly by non-canonical growth factor presentation (58). The direct binding of ECM molecules to cells is mediated by a number of cell receptors, including integrins, among others. Integrins are heterodimeric transmembrane receptors which are most frequently involved in direct ECM-cell interaction. They link the ECM to the internal cytoskeleton of the cell by binding directly to the ECM molecule and indirectly to actin via cytoplasmic binding proteins, and are therefore key factors in the adhesion and anchorage of the cells to their surrounding matrix (61,71). Besides the direct influence via cell-ECM interaction, the ECM can also regulate cell activity through the presentation of growth factors. For this purpose, several ECM components are either able to firmly bind growth factors making them unavailable and inactive, in order to function as a growth factor reservoir and regulating their local availability. Or they function as a distributor of growth factors after enzymatical remodeling, what leads to the release of factors that were otherwise in an insoluble state and not accessible for the cells (58).

Physical and mechanical characteristics. Rigidity, porosity, topography and insolubility are all features of the surrounding ECM that can direct various anchorage-dependent biological functions like cell division, tissue polarity and cell migration (72). Especially differences in the matrix stiffness, resulting from the varying composition of the ECM molecules can be sensed by the residing cells as external forces and thus influence the cellular behavior, a process known as mechanotransduction (73–76).

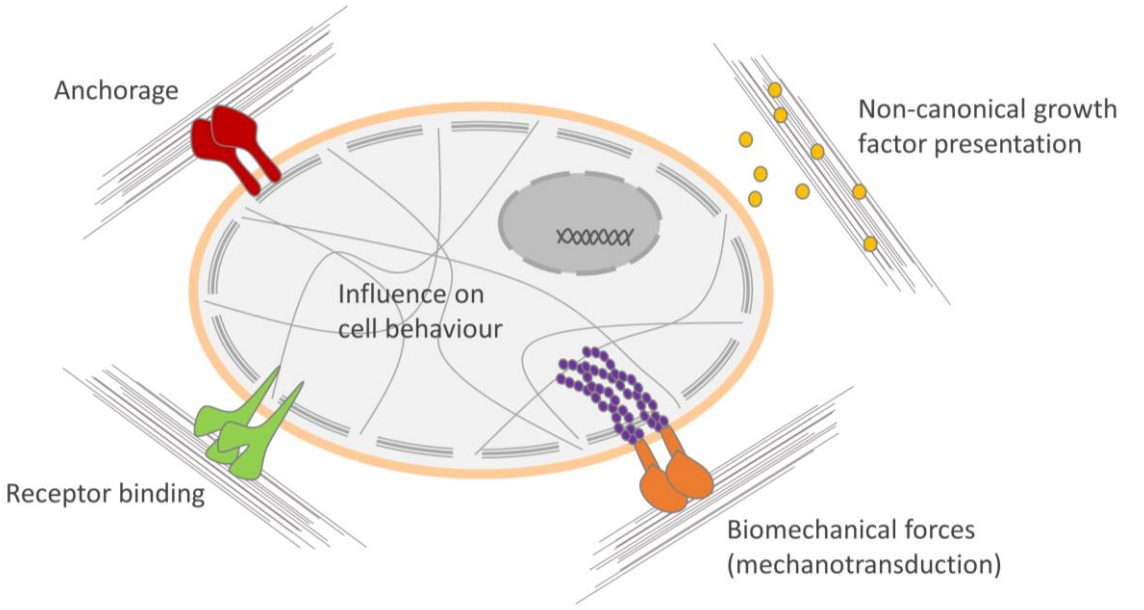

Figure 1.2: Extracellular matrix properties.
Different biochemical, mechanical, and physical characteristics of the ECM can either directly or indirectly influence cellular behavior and direct several cellular processes. Besides the direct influence via cell-ECM interaction, the ECM can also regulate cellular activity through the non-canonical presentation of growth factors. Anchorage-dependent biological functions can be influence by ECM features like rigidity, porosity, topography, and insolubility. Especially matrix stiffness can be sensed by the residing cells as external forces and thus influence cellular behavior (mechanotransduction). Adapted in part from Gattazzo et al. 2014 (77).

All of the above-mentioned properties are strongly interconnected, and one can influence the other. According to this, the cell-ECM interaction can be described as reciprocal, while the cells continuously remodel the ECM present in their microenvironment, these dynamic modifications of the ECM in turn direct cell behavior (58).

1.5.2 Components of the ECM

The extracellular matrix is a multi-component structure which is the product of the resident cells of each tissue. Subject to continuous processes like remodeling, assembly, and degradation, the ECM is by no means a static structure, but rather a highly dynamic system. Cells therefore spend a lot of energy to maintain their extracellular environment mediated by a balanced complement of constructive and destructive enzymes together with their enhancers and inhibitors. This controlled production and degradation of the ECM is enormously important for the proper functioning of a tissue or an organ and misregulation at this point can even contribute to disease (61,78,79).

Primary components of the extracellular matrix are fibrous structural proteins and proteoglycans. These include, among others, collagens, which are the most abundant proteins within the ECM, as well as non-collagenous glycoproteins (79). Both of them are described in more detail below. In addition to those already mentioned, glycosaminoglycans (GAGs) are also an important component of the ECM. These linear unbranched polymers of repeating disaccharides are attached to core proteins through covalent binding forming proteoglycans, responsible for binding and preservation of growth factors and cytokines, as well as water retention and gel properties for the ECM (80). In addition to the growth factors, there is a variety of further bioactive molecules, which together with their respective binding molecules, like decorin, perlecan, and biglycan, also contribute to an optimal function of the extracellular environment (80,81).

Collagens. With about 30% of total protein mass, collagens are the most abundant proteins in mammals with various functions including the maintenance of structural integrity in tissues (82). These trimeric matrix molecules are consisting of three polypeptide chains, referred to as α chains, of which either three identical chains can be interwoven forming a homotrimeric collagen molecule, or up to three different α chains resulting in heterotrimeric collagen molecules. To date, the collagen family comprises 28 members of collagen molecules with a high diversity originating from several α chains, various molecular isoforms and supramolecular structures for a single collagen type, and the use of alternative promotors and alternative splicing (82,83). A common structural feature of all collagens, however, is the presence of a triple helix that can reach from most of their structure to less than 10%. This common structural motif is composed of Gly-X-Y repeats, where X and Y are frequently proline and 4-hydroxyproline residues. This leads to a structure which is rod-shaped but flexible because of the presence of Gly-X-Y imperfections and interruptions associated at the molecular level with local regions of considerable plasticity, flexibility and molecular recognitions (82,84,85). The discovery of the first fibril-associated collagen with interrupted triple-helices (FACIT), collagen IX, showed that these triple-helical, referred to as collagenous domains, could be interspersed among non-collagenous domains (NC). Within one collagen molecule the NC domains can be frequently repeated and participate in the structural assembly as well as the conferring of biological activities to collagens (82,86).

Due to their complexity and structural diversity, the multidomain collagen proteins can be subdivided into several groups. First of all, a distinction is made between fibrillar and non-fibrillar collagens. Most of the collagen fibrils consist of several collagen types and are

therefore heterotypic (82). Other ECM molecules, like fibronectin, together with cellular receptors, such as integrins act as organizers for fibrillogenesis (87). On the other hand, there are the non-fibrillar collagens. In addition to the FACITs already mentioned, these include network-forming collagens and transmembrane collagen molecules consisting of a cytoplasmic, a transmembrane, and several triple-helical domains located in the ECM (82). An overview of the fibrillar and non-fibrillar collagens together with their respective subgroups is given in the following Table 1.1 (83,88).

Table 1.1: The collagen family – fibrillar and non-fibrillar collagens.

The collagen family	
Fibrillar collagens	Non-fibrillar collagens
Fibril-forming collagens: I, II, III, V, XI, XXIV, XXVII	Network-forming collagens: IV, VI, VIII, X
Anchoring fibril-forming collagens: VII	FACITs: IX, XII, XIV, XVI, XIX, XX, XXI, XXII, XXVI
	Transmembranous collagens: XIII, XVII, XXIII, XXV
	Endostatin precursor collagens: XV, XVIII

With regard to collagen molecules occuring in the ECM of adipose tissue, already 12 different types of collagen have been identified from rodent models, including collagen type I-VI, XI, XII, XIV, XV, XVIII and XXIII. With the exception of collagen type II, XI and XXIII, all of the above mentioned ones could be also found in the human visceral adipose tissue (79). However, the major constituents of the white adipose tissue are collagen molecules of type I, IV, and VI (89). While the fibril-forming collagen type I is found in the interstitial space, type IV collagen is the major collagen found in the basement membrane, an important structure which is discussed in more detail below. The third of the three main collagen components in WAT, collagen type VI, is characterized by the interaction with both collagen type I and IV, and therefore is supposed to be a key player in anchoring the basement membrane to the adipocytes as well as in the regulation of the structural organization of the adipose ECM (79).

As discussed previously, the ECM has not only structural functions, but also plays an important role in several cellular process including differentiation. This also applies to the collagen molecules for the adipogenic differentiation of mesenchymal stem cells, as shown by Ibrahimi et al. through the inhibition of collagen synthesis (90). Ethyl-3, 4-dihydroxybenzoate

(EDHB) is an inhibitor of the prolyl hydroxylase, which directs the conversion of proline residues into hydroxyproline during collagen synthesis (91). This in turn is responsible for the formation of the triple-helical molecule structure and the subsequent secretion of the procollagen into the extracellular space (88). A decreasing adipogenic differentiation of preadipocytes is the result of the inhibition of this key enzyme, indicating that the collagen synthesis and the insertion into the extracellular matrix is a requirement for the differentiation of the cells (90).

Non-collagenous glycoproteins. Besides the diverse family of collagen molecules, there is also a varied amount of non-collagenous proteins as part of the ECM, including several protein families with diverse origins (81). One of these protein families are the laminins, which were investigated in detail in the course of this work. They play a fundamental role in the architecture and function of the basement membrane and are highly essential taking into account that in their absence basement membranes do not form and embryo development is arrested at an early stage (78,92,93). Laminins are heterotrimeric glycoproteins consisting of α, β, and γ chains. Up to date, 5 α, 3 β, and 3 γ chains have been identifies in vertebrates (92). In addition to splicing variants of several chains, the variable compositions of the three polypeptide chains lead to numerous isoforms of laminin, however, the number of identified laminins is not as high as the number of possible combinations that can be created from the three polypeptide chains, since so far only 16 isoforms have been found (94).

The three polypeptide chains are held together by disulfide bonds to form either a Y-shaped, cruciform or rod-shaped structure (92). During laminin synthesis, the individual subunits are initially stabilized through the co-translational glycosylation in the rough endoplasmic reticulum and thus protected from degradation (95). The first step of the laminin trimer assembly is the stable association of the glycosylated β and γ chain. After the rate limiting step of binding the α chain to the dimeric complex in order to form a trimeric molecule, a terminal glycosylation step takes place in the Golgi organelle after which the laminin trimer is secreted into the extracellular space followed by the final proteolytic processing of its chains (95–97). The α chain is the largest one of the trimeric laminin molecules. They are modified at their C-terminal globular (G) domain which can be divided into 5 globular modules, termed LG1-5 (92). These LG modules mainly mediate the interaction of laminins with cell surface receptors such as integrins, while the N-terminal region is mainly responsible for the self-assembly of laminin trimers and their incorporation into the basement membrane (92). Through binding to cellular receptors like integrins and dystroglycans, laminins can interact with the cells and

thereby influence several cellular processes including cell proliferation, differentiation, adhesion and migration (98). Through binding of the α chain, the cytoplasmic part of the integrin can activate focal adhesion kinases (FAK), small rho GTPases and MAPK pathways to affect the cellular activities (99). A defective cell-laminin binding can even result in severe human diseases, such as muscular dystrophies and skin blistering disorders, what clarifies again that the ECM is not only an inert shaping structure (93). The occurrence of laminin isoforms is tissue specific and also mainly determined by the expression of the different α chains. Laminin isoforms 8 (α4β1γ1), 9 (α4β2γ1), and 14 (α4β2γ3), which all contain the α4 chain, are specific for cells of mesenchymal origin. To the main constituents of WAT further belong the two laminin isoforms 1 and 8 (100,101).

Apart from laminin, fibronectin represents also an important non-collagenous component of the ECM (102). It was the first example of a protein recognized to have dual functions, namely both structural and functional properties. This glycoprotein is forming fibrillar structures and participates in organizing the assembly of various other ECM components (103,104). As a complex molecule with several integrin- and heparin-binding sites it also mediates a wide variety of cellular interactions with the ECM. Fibronectin molecules usually exist as a dimer composed of nearly two identical ~ 250 kDa subunits linked covalently together near their C-termini by a pair of disulfide bonds. This non-collagenous matrix protein can exist in multiple forms, even if the respective molecules are all product of a single gene. Alternative splicing is the reason for as many as 20 fibronectin variants in humans (103).

1.5.3 ECM in adipose tissue and its dynamic development during adipogenesis

The extracellular matrix is also crucial for maintaining the structural and functional integrity of adipose tissue and represents an important mediator in the development of major adipocytes and the whole tissue formation (105). In 1963, Napolitano made the first observation of the ECM structure in adipose tissue examining the WAT development in rats (106). Various immunohistochemistry studies performed several years later, highlighted the presence of collagen IV, laminin, fibronectin and heparan sulphate proteoglycan surrounding human adipocytes, however, the fibronectin expression in subcutaneous adipocytes was shown to be quite low (107,108).

The basement membrane of mature adipocytes. During adipogenic differentiation cells have to remodel the interstitial matrix surrounding them (109,110). More specifically, they have to generate a supporting basement membrane-like structure, which surrounds mature adipocytes but is not yet present in the undifferentiated precursor cells (109). This basement membrane, also known as basal lamina, is a structure mainly known from epithelial cells but could be also found in several other cell types with mesenchymal origin, including osteoblasts and chondrocytes (61). Two fused sheet-like networks are reported to form the basement membrane. One of the two networks is composed of collagen type IV and the other one of laminins, to which the cells are integrated via their integrin and non-integrin matrix receptors (107). Nidogen/entactin as well as smaller amounts of other components like the proteoglycan perlecan (heparan sulfate proteoglycan) are further parts of the basement membrane (111). To build non-covalent bridges between type IV collagen and laminin, nidogen/entactin together with collagen VI serve as crosslinker, resulting in the double polymer network architecture of the basement membrane (111,112).

For maturing adipocytes, the development of the cell surrounding basement membrane is mandatory for survival. During adipogenic differentiation, cells start to store vast amounts of triglycerides which end up in a single fat droplet that nearly fills the entire cell volume. This makes them susceptible to mechanical stress what can easily lead to disruption. A strong external skeleton can decrease the transfer of mechanical stress from the outside to the inside of the cell and is therefore a requirement for cell survival. Therefore it is evident that the development of precursor cells into fat-storing, mature adipocytes should be accompanied by specific changes in the make-up of the ECM (79).

Dynamic ECM development during adipogenic differentiation. The adipogenic differentiation as a bi-phasic process with its early phase of commitment and the following terminal differentiation is accompanied by drastic morphological changes through the alteration from a fibroblastic to a rounded cell shape. This is reflected by an intense remodeling of the ECM from a fibrillar to a laminar structure (Figure 1.3) (79). Most of our previous knowledge concerning the dynamic changes in the protein composition of the ECM derives from the investigation during the in vitro differentiation along the adipogenic lineage of mouse preadipocyte cell lines (e.g. 3T3-L1). An emerging collagen network composed of type I, III, IV, V, and VI was shown during the adipogenic differentiation of murine cells compared to undifferentiated cells. Especially collagen IV and laminin were confined to close proximity of these cells located in the cell-surrounding basement membrane (109,110,113). These

observations were not restricted only to murine cells, but also for bovine pre-adipose cells, the expression of type I-VI collagens increased during differentiation (113). According to the development of the cell-associated ECM from a fibronectin enriched matrix into a basement membrane during the differentiation process, decreased amounts of pericellular and cellular fibronectin during adipogenesis were observed. A significant decrease of fibronectin in gene and protein expression during preadipocyte differentiation, could be also shown for humans via the investigation of in vitro cell culture models (105,114).

The alterations in ECM composition are not only due to the morphological changes of the differentiating cells during adipogenesis, but at the same time also have a great influence on the differentiation of the cells via interaction with respective receptors. In this context, an inhibitory effect of fibronectin on the adipogenic differentiation was reported, while enhancing features were observed for laminin and collagen type IV (115–117). Matrix metalloproteinases (MMPs), a family of zinc-dependent proteases, are partly responsible for the ECM remodeling during differentiation. Especially MMP-2 and MMP-9 are reported to be important for the differentiation of 3T3-L1 preadipocytes, so that the inhibition of these proteases leads to the blockage of adipogenesis (118).

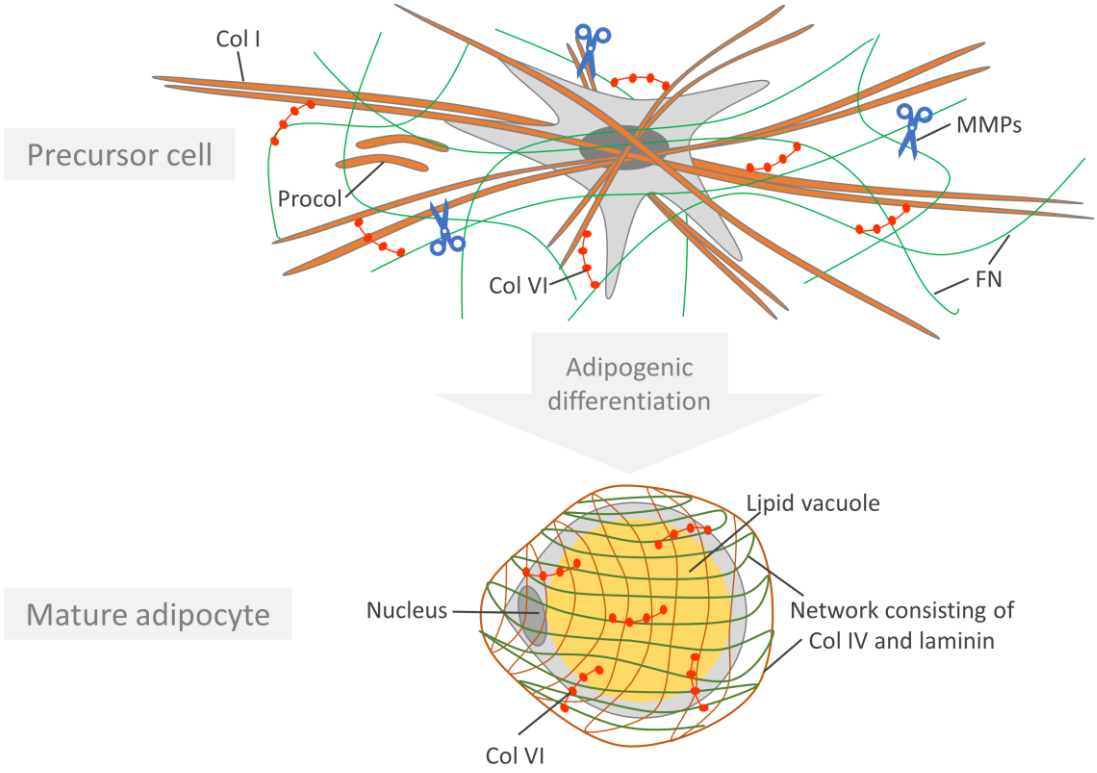

Figure 1.3: ECM development during adipogenic differentiation.

During the differentiation of a precursor cell into a mature adipocyte, accompanied by drastic morphological changes, an intense remodeling of the ECM from a fibrillar to a laminar structure takes place. The development

of a fibronectin (FN) enriched matrix into the supporting basement membrane of mature adipocytes, partly mediated by matrix metalloproteinases (MMPs) together with further constructive and destructive enzymes, is a prerequisite for the survival of the lipid laden cells. Two networks composed of collagen IV and laminin crosslinked through several proteins, e.g. collagen VI, form the adipocyte surrounding basement membrane. Adapted in part from Huang et al. 2012 (104).

More research is necessary in order to appreciate the exact composition and role of the ECM in adipose tissue physiology (105). The existing knowledge on the development of ECM and its participation in the differentiation process came almost exclusively from studies using 2D cell culture. However, it is easy to understand that the ECM in a 2D culture, in which the cells are almost exclusively in contact with the plastic plate, differ substantially from those of cells grown in a 3D environment (61). Therefore, establishing a 3D system which more closely resembles the in vivo condition is desirable for a meaningful in vitro analysis of in vivo cell-ECM interactions during the development of adipose tissue (77).

1.6 Multicellular spheroids

1.6.1 Spheroids as a three-dimensional (3D) cell culture model

To date, most of the findings in cell biology, including the ECM development described above, come from studies using traditional 2D culture techniques in which the cells of interest are cultured as 2D monolayers on a plastic plate. This easy and traditional culture condition provides a well-controlled and homogeneous cell environment which is highly artificial and less physiological and therefore, does not reflect the natural microenvironment of the cells (119,120). In vivo, cells interact not only with the neighboring cells, but also with the surrounding ECM, forming a complex system with a unique 3D organization. The complex communication network consisting of cell-cell and cell-ECM interactions together with several biochemical and mechanical signals are critical for normal cell physiology. This is also the reason why cells cultured as 2D monolayers, where cell to plastic interactions prevail rather than the crucial cell-cell and cell-ECM interactions, lose their tissue-specific properties and normal cell function (119,121,122). Compared to these traditional 2D monolayers, 3D multicellular aggregates, or spheroids are regarded as more physiological and exhibit higher similarity to real tissues in many aspects than monolayer cells (122,123). Many types of mammalian cells, including mesenchymal stromal/stem cells are able to aggregate into 3D

spheroid structures, so that this type of 3D culture model recently gained increasing recognition in biomedical research like in the field of oncology (124), stem cell biology (125–127), and even tissue engineering as discussed below (119,122). The in vitro culture of multicellular spheroids was originally described by Holtfreter (128) and Moscona (129) for embryonic stem cells 70 years ago (123).

3D spheroids are characterized by the fact that they are free of foreign material and the cells, with their own secreted ECM in which they reside and interact, create an in vivo like microenvironment (119,120). Complex cell-cell and cell-ECM interactions together with additional signals including mechanical forces and biochemical signals lead to alterations in cell shape, motility, proliferation and differentiation as well as gene expression in the spheroid forming cells (119,130,131). Some of these differences to cells cultured under 2D conditions are due to the marked differences in cell-cell as well as cell-matrix interactions. This makes 3D spheroids a suitable tool for the investigation of intercellular and cell-matrix interactions together with their influence on cellular behavior (120).

However, the spheroid culture has not only advantages over the traditional 2D culture, there are also some limitations. Because of the spheroidal structure, diffusion of nutrients, oxygen and waste through the interior of the spheroids is compromised in a size dependent manner and can lead to necrotic damage and limited cell viability in the spheroid core (123,132). So, the overall size of spheroids should not exceed a few hundred micrometers, which has to be considered in the formation of these cell aggregates (133,134).

1.6.2 Spheroid formation techniques in vitro

Since they are anchorage dependent cells, mesenchymal stromal/stem cells in suspension fall on the plastic surface by gravity and start to establish cell adhesion to the culture vessel. To achieve that the cells assemble and form multicellular aggregates, they need to be cultured under conditions which do not allow them to adhere to the solid surface (123). To date numerous methods for spheroid generation in vitro have been developed. The two traditionally used methods to facilitate cell aggregation are the spinner flask and the liquid overlay technique (123). The first one is based on constant stirring of a high-density cell suspension in order to maximize cell-cell contact while minimization of cellular attachment to the solid surface. This spinner culture can be scaled up to produce a large number of spheroids, however the resulting culture of cellular aggregates is very heterogeneous (119). The liquid overlay technique uses

agar to prevent cell attachment to the culture vessel and promotes cell-cell aggregation. Originally this easy method also leads to spheroids which are very heterogeneous in both size and shape, however, when performed in 96-well plates a more homogeneous population of spheroids can be generated as the spheroid size is then determined by the number of cells in each well (123,135). Furthermore, it allows the monitoring of individual spheroid formation and growth (119). For a large-scale production of spheroids, however, this method is rather unsuitable, due to the high effort required in the laboratory. One further method for spheroid generation is the well-known hanging drop technique. This method eliminates surface attachment by placing the cell suspension in a drop and further relies on the gravity-enforced self-assembly of the cells to produce spheroids (119,123,136,137). There are already approaches for the high-throughput production of spheroids with this method (138), however, it is difficult to track these spheroids during formation (119). Further methods for spheroid generation include the pellet culture, which uses centrifugal forces to maximize the opportunity for cell-cell adhesion as well as the culture on chitosan membranes to initiate 2D to 3D transition (119,123). Also, micro-fluidics are used to cause cells to aggregate, when they flow through a microchannel network into micro-chambers where they are exposed to microrotational flow (139). These and some other methods all have the same final aim of generating multicellular three-dimensional spheroids with a complex communication network for a variety of applications.

1.6.3 The spheroid formation process

The process of multicellular spheroid formation was first investigated on human hepatoma cell lines and reported by Lin et al. in 2006 (Figure 1.4) (140). In the beginning of spheroid formation long chain ECM fibers with multiple RGD motifs for cell-surface integrin binding, like fibronectin, are mainly responsible for the initial aggregation of dispersed cells. The following part of the formation process is also described as the delay phase, in which the upregulation of cadherin expression in the spheroid forming cells take place. Finally, homophilic cadherin-cadherin binding between the cells confers strong cell adhesion and the final compaction of the spheroids (122,140). In addition to cadherins, which are critical to self-assembly, also connexins are reported to take part in this process. Through the formation of gap junctions which directly couple cells to one another, they also possess an adhesive function and can contribute to the spheroid formation process together with the adhesive effects of cadherins (141). Although the adhesive molecules responsible for the spheroid formation process may

vary from cell to cell (142–144), it becomes increasingly clear that the surface adhesion molecules and the cytoskeletal network act together to control self-assembly. Furthermore, mechanical forces of cell-cell and cell-ECM interactions play a substantial role in this process (119,130).

1.6.4 Therapeutic potential of 3D spheroids

Human mesenchymal stromal/stem cells, including ASCs, are becoming increasingly important in the field of regenerative medicine. Due to their multifaceted therapeutic capabilities these cells are a promising approach to therapy for human diseases (145). This includes not only their potential to differentiate along mesenchymal lineages, but also their strong anti-inflammatory and immunomodulatory capabilities, which they can exhibit at sites of inflammation to promote wound healing and regeneration. That makes them promising candidates for therapy in regenerative medicine and inflammatory disease processes (145). However, both their ability to differentiate as well as their anti-inflammatory and immunomodulatory effects can be even enhanced through their culture as 3D multicellular spheroids (123,133,146). For example, bone marrow-derived MSC spheroids are reported to exhibit increased amounts of anti-inflammatory factors including prostaglandin E2 (PGE2), tumor necrosis factor (TNF)-α-stimulated gene/protein-6 (TSG-6), and stanniocalcin-(STC)-1 compared to conventional 2D monolayer culture (147). The secretion of all these factors lead to the conversion of lipopolysaccharide-stimulated macrophages from a primarily proinflammatory M1 phenotype to a more anti-inflammatory M2 phenotype (148).

Due to the increased anti-inflammatory and immunomodulatory effects as well as improved stemness and survival rates after transplantation, the pre-conditioning of MSCs under physiological conditions such as the 3D environment in multicellular spheroids, prior to transplantation is proved to optimize their therapeutic efficiency (146). This makes 3D spheroids not only highly attractive for cellular therapies and regenerative medicine, but they also gained more and more attention as a promising approach in the field of tissue engineering.

1.6.5 3D spheroids as building blocks in tissue engineering

Tissue engineering means the fabrication and development of adequate biological substitutes for the repair or complete replacement of injured or lost tissues and organs (133).

As discussed earlier, most of the tissue engineering approaches are based on biodegradable scaffold which are seeded with isolated cells. Here, scaffolds determine the 3D shape of the tissue substitutes while they serve as matrices for cell attachment. However, the cell-scaffold interaction was reported to rather resemble the artificial condition of a 2D culture where cells adhere to a plastic surface, than the physiological conditions in vivo (133). Physiological self-assembly of cells allowing instructive cell-cell contacts in a complex structure with 3D architecture already take place during embryonic development. In this case, cells are surrounded by their own secreted ECM that provides the above discussed biomechanical and biochemical cues. The combination of all these components determines cell differentiation and proliferation and ensures the homeostasis of the resulting tissue (133,149). To mimic these physiological conditions, there is an upcoming trend towards the use of spheroids as building blocks for tissue engineering (Figure 1.4). Due to their remarkable regenerative properties, including the improved differentiation capability compared to 2D monolayers (150–152), 3D spheroids become more and more important. Through the combination of multiple cell types in coculture spheroids it is also possible to mimic complex tissues (133).

Both scaffold-based and scaffold-free strategies are conceivable for the use of spheroids as building blocks. To embed spheroids into a biodegradable scaffold would combine the classical approach of an implantable 3D shaped matrix for the filling of the defect site with the improved regenerative properties of the 3D spheroids. These scaffolds would be useful for the initial fixation of the spheroids in the intended position during and immediately after implantation and further provide a defined geometry for their directed development into larger tissues (133). This approach of seeding biodegradable scaffolds with spheroids has been already used to engineer tissue constructs several times, for example to replace cartilage and skin. Also, Zhang et al. used a non-adhesive scaffold based on PLGA and chitosan, which stimulates the assembly of single seeded MSCs into spheroids. With this approach they showed an improved cartilage regeneration in vivo compared to an adhesive control scaffold overgrown with single cells (153). In vivo applications without using artificial scaffolds can avoid biocompatibility issues that occur with scaffold implantation and therefore, may represent a more physiological approach for tissue regeneration (133). Also freely implanted MSC spheroids were shown to be capable of repairing tissue defects in vivo, for example osteochondral ones in minipigs (154). Applied without using artificial scaffolds, 3D spheroids have one further advantage over single cells. 3D spheroids are less prone to wash out by body fluids, as the susceptibility to unwanted distribution of applied single cell suspensions constitutes a great disadvantage (155).

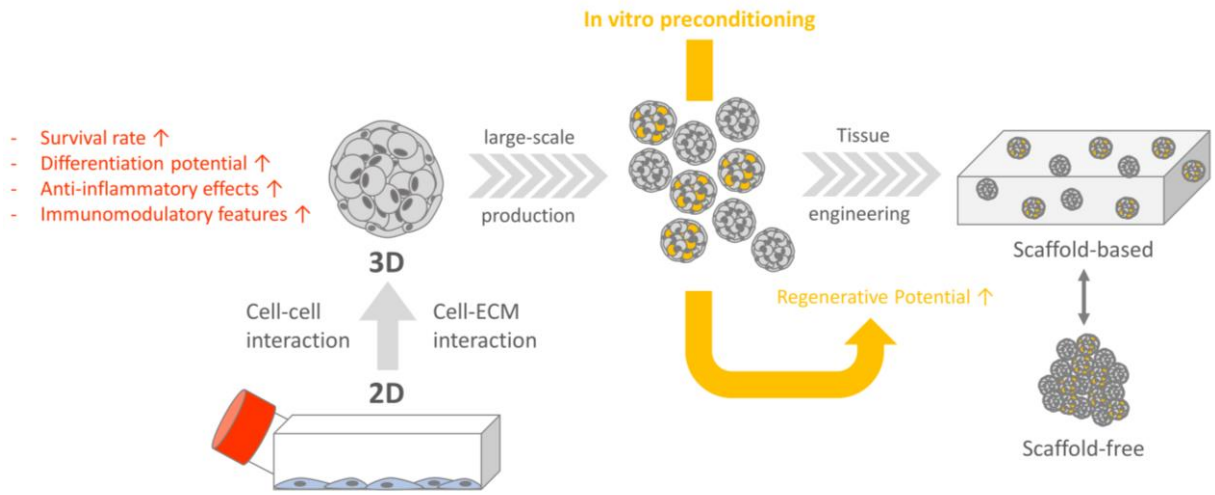

Figure 1.4: 3D spheroids as building blocks for tissue engineering.
Increased regenerative properties, including differentiation capability, anti-inflammatory, and immunomodulatory features, are the result of culturing MSCs as 3D multicellular aggregates compared to conventional 2D monolayers. After a large-scale production of spheroids with a defined size and structure, they can be further preconditioned in vitro for example through the addition of respective factors to the culture medium to start the differentiation into a specific lineage. Also, the combination of multiple cell types is possible in coculture spheroids to mimic complex tissues. Subsequently, the spheroids can be either embedded in, or seeded on external scaffolds to generate scaffold-based tissue substitutes or are directly implanted without using an artificial scaffold. Adapted in part from Laschke et al. 2017 (133).

The biological principle of tissue self-assembly also applies to 3D spheroids, which spontaneously fuse into larger tissue units when they are in close contact to each other. A directed fusion of multiple spheroids therefore opens up the possibility to synthesize scaffold-free macrotissues with a complex organ-like composition (133). There is a need of challenging technologies for the automized and controlled fusion of spheroids in order to engineer large tissue constructs in the future. Bioprinting is a rapidly evolving technology in this field (133). Here, spheroids as building blocks for organ printing can be deposited layer-by-layer to generate tissues with defined geometrical structures (156). This upcoming technology has already been proven to be suitable for the computer-controlled generation of distinct organ structures by fusion of multicellular spheroids (133,157). Another promising approach is the incorporation of magnetic microparticles into the multicellular spheroids, called magnetic organoid patterning. Through the application of externally magnetic field, spheroids are arranged and directed to fuse into a desired shape. However, it has to be considered that viability, phenotype, and function of the cells within the spheroids may be affected by the incorporated magnetic particles (133,158,159).

Overall, 3D spheroids represent highly suitable building blocks for tissue engineering. Emerging technologies allow high throughput production and direct fusion into distinct organ structures. Together with in vitro preconditioning strategies, which contribute to an improved regenerative capacity, this further strengthen the implementation of spheroid-based tissue engineering approaches. However, a complete understanding of the spheroid system is indispensable for their use in TE. Therefore, it is still a long way before spheroid-based approaches become reality in clinical practice, and there are many open questions for spheroid research that need to be clarified in future studies.

1.7 Goals of the thesis

Human adipose-derived mesenchymal stromal/stem cells (ASCs) are promising candidates for use as cellular therapies. Their therapeutic potential ranges from the capability to differentiate into mesenchymal lineages to anti-inflammatory and immunomodulatory properties, which drives their application in regenerative medicine and inflammatory disease therapy (145,160). Through their culture as multicellular spheroids, the therapeutic potential of mesenchymal stem cells was reported to be enhanced (123,133,146,161). Their possibility to self-assemble into cellular aggregates offer them an in vivo like microenvironment, where they reside and interact within their own secreted extracellular matrix. Intensive cell-cell and cell-matrix interactions contribute to a complex communication network in a three-dimensional organization, free of foreign material (162). The physiological resemblance of cell-cell and cell-matrix interactions within these cellular aggregates leads to the exhibition of a higher similarity to real tissue and therefore makes spheroids also an emerging trend in use as building blocks in tissue engineering (122,123,125,133). Due to their high abundance, and ease of isolation, ASCs are an ideal cell source to overcome the still tremendous clinical need for the development of adequate implants to repair oft tissue defects (39,40), however, ASC-derived spheroids have been rarely investigated so far for their use in adipose tissue engineering. In order to optimally exploit their therapeutic potential and to further their use in regenerative medicine, and adipose tissue engineering approaches, an extensive characterization of the spheroid model consisting of ASCs is indispensable. This includes a broad knowledge of their structural features, adipogenic differentiation capacity, as well as secretory properties. The underlying mechanisms of their enhanced therapeutic efficiency also remain to be elucidated. This work therefore includes the following objectives to further implement ASC-based spheroids as a promising approach in regenerative medicine and adipose tissue engineering:

1. The characterization of the spheroid formation process of ASCs and the participating cell-cell and cell-ECM interactions.
2. The investigation of the adipogenic differentiation capacity of ASC-based spheroids and the associated dynamic development of an adipo-specific extracellular matrix.
3. The evaluation of the influence of laminin on the differentiation capacity along the adipogenic lineage of ASCs.

4. The analysis of gene expression and secretory properties of ASC-based spheroids and the investigation of cell junctions as one possible driving force for the enhanced therapeutic potential of 3D spheroids.

1.7.1 Characterization of the spheroid formation process and investigations on the influence of cell-cell and cell-ECM interactions

Like many types of mammalian cells, also adipose-derived mesenchymal stromal/stem cells (ASCs) have the ability to aggregate into multicellular, three-dimensional spheroid structures. In order to further promote their use in regenerative medicine and tissue engineering approaches for the reasons mentioned above, a comprehensive understanding of the mechanisms contributing to the spheroid formation process is essential. Most of the previous knowledge regarding cellular aggregation into 3D spheroid structures resulted from studies using different carcinoma cells lines (140,143,163). Spheroid formation of ASCs, however, has been rarely investigated so far (150,164,165). Therefore, in this study, the individual spheroid formation of ASCs was monitored using the liquid overlay technique in a 96-well plate setup. The development of the extracellular matrix in which cells of the 3D spheroids reside and interact, and which is known to be involved in various aspects of cellular behavior, was examined by expression analyses and immunohistological investigations during spheroid formation. Furthermore, the influence of cell-cell and cell-matrix interactions on the formation process, by unspecific, as well as specific blocking of respective receptors, was addressed (see Chapter 4.1).

1.7.2 Elucidating the adipogenic differentiation capacity of ASC-based spheroids and the dynamic development of the ECM during adipogenesis

ASCs as a widely used cell source for adipose tissue engineering have been shown to be limited in their regenerative capacity when applied as single cells (166,167). In contrast, ASC 3D spheroids appear to be predestined as prefabricated, material-free building blocks in tissue engineering approaches for creation of tissues with proper three-dimensional organization. Their use as building blocks for soft tissue engineering, however, requires insights into ECM development and efficient adipogenic induction. To date only little is known about the ECM composition and development during the adipogenic differentiation process of ASC-derived

spheroids. The development of a tissue-specific ECM, however, must be considered as an important requirement in tissue engineering approaches (168). For this purpose, investigations on the dynamic ECM development during adipogenesis of ASC spheroids were performed. Furthermore, the ECM composition of differentiated spheroids was compared to native fat via immunohistological analyses, to assess the resemblance between the ECM of the two tissues. The comparison of the adipogenic differentiation capacity of ASCs cultured as 2D monolayers and 3D spheroids, as well as the elucidation of an induction protocol for the most effective differentiation of 3D spheroids in this study should further contribute to their implementation as building blocks for soft tissue engineering (see Chapter 4.2).

1.7.3 Investigating the influence of laminin on the differentiation capability of human ASCs

During the last two decades it was recognized that the ECM not only act as inert scaffold for sustaining tissue and organ structure. As part of the complex communication network of cells in their niche, the ECM influences several cellular processes, including differentiation, survival, and proliferation (61,166,167). Therefore, a tissue-specific ECM development is an important requirement for tissue engineering approaches, as already mentioned above. Changes in the ECM composition are not only the consequence of morphological changes during differentiation, but in turn influence differentiating cells via interaction with cellular receptors. Therefore, another objective of this study was to investigate whether the development of adipo-specific ECM components influences cell differentiation along the adipogenic lineage itself. For laminin, one major component of the basement membrane of mature adipocytes (107), a very early development during adipogenic differentiation was observed (see Chapter 4.2), thus the possible role of laminin in the adipogenic differentiation process was investigated. A shRNA-targeted knockdown of one respective laminin gene was performed to examine the involvement of this adipo-specific ECM component in directing adipogenic differentiation of ASCs. These investigations shall contribute to a closer understanding of how ECM components influence cellular process like adipogenic differentiation in ASCs and furthermore provide closer insight into possible mechanisms involved in an improved differentiation capacity of ASC-based spheroids compared to ASCs cultured as 2D monolayers (see Chapter 4.3).

1.7.4 Analyzing secretory properties of ASC-based spheroids and investigations on cellular junctions within the 3D constructs compared to 2D monolayers

The enhanced therapeutic potential of mesenchymal stem cells in a 3D environment is not only restricted to their improved differentiation capability, but also includes anti-inflammatory and immunomodulatory properties via paracrine secretion (147,148). Studies regarding the therapeutic potential of spheroids exerted by their secretion of relevant cytokines, were performed mainly with MSCs derived from the bone marrow (147,148,169). In contrast, investigations on paracrine secretion of ASC-based spheroids are scarce (170,171). Therefore, in this study, gene expression of ASC spheroids, namely for anti-inflammatory, anti-apoptotic, and anti-cancer related cytokines, were examined by mRNA expression analyses and compared to ASCs originating from 2D monolayers. The secretion of one major anti-inflammatory factor, prostaglandin E2, was also addressed on secretion level through the measurement with a specific enzyme-linked immunosorbent assay (ELISA). The identification of the underlying mechanisms and the driving forces for the increased therapeutic potential of cells in a 3D environment is still pending. The assumption exists that paracrine effects and differentiation capacity are related to niche specific settings, including cell-ECM and cell-cell interactions together with the involved cellular junctions. Therefore, in this study, a PCR array for screening cell junction related genes was used to investigate possible differences between ASCs cultured as 3D spheroids and conventional 2D monolayers. This served as a first attempt to provide possible explanations for the previously observed differences between ASC monolayers and 3D spheroids and should be the basis for further experiments to get closer to a comprehensive understanding of cell-cell and cell-ECM interactions in a three-dimensional spheroid culture (see Chapter 4.4).

2 Materials

2.1 Instruments

Table 2.1: Overview of used instruments.

Instrument	Supplier	Central office
Analytical balance	Ohaus	Zürich, Switzerland
Centrifuge Rotina 420 R	Hettich	Tuttlingen, Germany
Centrifuge SIGMA 1-14	SIGMA Laborzentrifugen GmbH	Osterode, Germany
CO_2 incubator	IBS Integra Biosciences	Fernwald, Germany
Confocal laser scanning microscop (CLSM) TCS-SP2 AOBS	Leica	Wetzlar, Germany
Cryostat CM 3050 S	Leica	Wetzlar, Germany
Fluorescence spectrometer Tecan GENios pro	Tecan	Crailsheim, Germany
Freezers	Liebherr	Biberach, Germany
Fridges	Liebherr	Biberach, Germany
Hemacytometer Neubauer	Paul Marienfeld GmbH	Lauda, Germany
Laminar flow box Typ HS18	Heraeus	Hanau, Germany
Orbital shaker Unimax 1010	Heidolph	Schwabach, Germany
Mastercycler® Gradient	Eppendorf	Hamburg, Germany
Magnetic stirrer	VWR	Darmstadt, Germany
Microscope BX51/ DP71 camera	Olympus	Hamburg, Germany
Microscope IX51/ XC30 camera	Olympus	Hamburg, Germany
NanoDrop 2000c	Thermo Scientific	Waltham, USA
pH-meter HI2210	Hanna Instruments	Kehl am Rhein, Germany
Pipettes Research® Plus	Eppendorf	Hamburg, Germany
Pipette controller accu-jet® pro	Brand	Wertheim, Germany
Pipette repetitive	Brand	Wertheim Germany

Instrument	Supplier	Central office
Real-Time PCR Detection System CFX96™	Bio-Rad	Munich, Germany
Spectrophotometer, MRX microplate reader	Dynatech Laboratories	Chantilly, USA
TissueLyser	Qiagen	Hilden, Germany
Thermomixer comfort MTP	Eppendorf	Hamburg, Germany
Thermomixer MHR 23	DITABIS	Pforzheim, Germany
Ultrasonic homogenizer SonoPlus	Bandelin	Berlin, Germany
Vortexer, IKAR MS3 basic	IKAR	Staufen, Germany
Waterbath	Memmert	Schwabach, Germany

2.2 Consumable materials

Table 2.2: Overview of used consumables.

Consumable	Supplier	Central office
Coverslips 24 x 60 mm	Menzel	Braunschweig, Germany
Combitips® Plus 2.5 mL	Eppendorf	Hamburg, Germany
Cryovials CryoPure 2.0 mL	Sarstedt	Nümbrecht, Germany
Glass pasteur pipettes	Brand	Wertheim, Germany
Hardshell PCR plates, 96-well, thin wall	Bio-Rad	Munich, Germany
Microseal® ´C´ Film	Bio-Rad	Munich, Germany
Microtome blades	Feather	Osaka, Japan
6- & 12-well plates	Greiner Bio-One	Frickenhausen, Germany
24-well plates	Thermo Scientific	Waltham, USA
96-well plates	TPP	Trasadingen, Switzerland
96-well plates black	Thermo Scientific	Waltham, USA
Parafilm®	Pechiney	Chicago, USA
PAP pen liquid blocker	Sigma-Aldrich	Munich, Germany
PCR-strips 8-tubes 0.2 mL	Carl Roth GmbH	Karlsruhe, Germany

Consumable	Supplier	Central office
Pipette filter tips	Sarstedt	Nümbrecht, Germany
Pipette tips	Starlab	Hamburg, Germany
Pipettes serological	Greiner Bio-One	Frickenhausen, Germany
Polypropylene Tubes 15 mL/50 mL	Greiner Bio-One	Frickenhausen, Germany
Reagent Reservoirs	VWR	Darmstadt, Germany
SafeSeal micro tubes 1.5 mL/2.0 mL	Sarstedt	Nümbrecht, Germany
Sample cup PE 2.5 mL	Hartenstein	Würzburg, Germany
Scalpels	Feather	Osaka, Japan
SuperFrost™ plus glass slides	R. Langenbrinck	Emmendingen, Germany
Syringe Filter Minisart® 0.2 µm	Sartorius AG	Göttingen, Germany
Tissue culture flasks T25 / T75 / T175	Greiner Bio-One	Frickenhausen, Germany

2.3 Chemicals

If not otherwise stated in Table 2.3 or the Methods section (Chapter 3), all chemicals and reagents utilized for the preparation of buffers and solutions were obtained from Sigma-Aldrich (Munich, Germany) and Carl Roth GmbH (Karlsruhe, Germany).

Table 2.3: Overview of used chemicals.

Chemical	Supplier	Central office
Ambion RNaseZAP	Life Technologies	Karlsruhe Germany
Antibody diluent, Dako REAL™	Dako	Hamburg, Germany
Aqua ad iniectabilia	B. Braun	Melsungen, Germany
BODIPY 493/503	Invitrogen	Karlsruhe, Germany
DAPI mounting medium Immunoselect®	Dako	Hamburg, Germany
Dulbecco´s phosphate-buffered saline (DPBS), no calcium, no magnesium	Life Technologies	Karlsruhe, Germany
Distilled water (DNase/RNase free)	Life Technologies	Karlsruhe, Germany

Chemical	Supplier	Central office
EGTA (Ethylenglycol-bis-(β-aminoethyl ether)-N,N,N´,N´-tetraacetic acid)	AppliChem	Darmstadt, Germany
Glycergel® Mounting Medium	Dako	Hamburg, Germany
Hematoxylin	Bio Optica	Milan, Italy
Hoechst 33258 dye	Polysciences	Warrington, USA
Human insulin	Promocell	Heidelberg, Germany
IBMX (3-Isobutyl-1-methylxanthine)	Serva Electrophoresis	Heidelberg, Germany
MESA GREEN qPCR™ Mastermix Plus for SYBR® Assay	Eurogentec	Cologne, Germany
Phosphate-buffered saline (Dulbecco A) tablets	Thermo Scientific	Waltham, USA
QIAzol Lysis Reagent	Qiagen	Hilden, Germany
RT^2 SYBR Green qPCR Mastermix	Qiagen	Hilden, Germany
Terralin Liquid® disinfectant	Schülke	Norderstedt, Germany
Thesit®	Gepepharm	Hennef, Germany
Tissue-Tek® O.C.T. compound	Sakura Finetek	Zoeterwonde, Netherlands
TRIzol® reagent	Life Technologies	Karlsruhe, Germany
Trypsin-EDTA 0.25%	Life Technologies	Karlsruhe, Germany

2.4 Antibodies

Table 2.4: Overview of used antibodies.

Antibody	Type/Source	Application/Dilution	Supplier
Anti-collagen I	Polyclonal IgG rabbit	IHC: 1:800	Abcam (ab34710)
Anti-collagen IV	Polyclonal IgG rabbit	IHC: 1:150	Abcam (ab19808)
Anti-collagen VI	Polyclonal IgG rabbit	IHC: 1:200	Abcam (ab6588)
Anti-E-cadherin	Monoclonal IgG mouse	Blocking: 10µg/mL	Santa Cruz Biotech. (sc-8426)

Antibody	Type/Source	Application/Dilution	Supplier
Anti-fibronectin	Polyclonal IgG rabbit	IHC: 1:500	Abcam (ab2413)
Anti-Integrin β1	Monoclonal IgG mouse	IHC: 1:50 Blocking: 10µg/mL	Santa Cruz Biotech. (sc-18845)
Anti-laminin	Polyclonal IgG rabbit	IHC: 1:200	Abcam (ab11575)
Anti-N-cadherin	Monoclonal IgG mouse	Blocking: 10µg/mL	Santa Cruz Biotech. (sc-8424)
IgG1 negative control	Polyclonal IgG mouse	IHC: according to primary antibody concentration	Dako (X0931)
IgG1 isotype control	Polyclonal IgG rabbit	IHC: according to primary antibody concentration	Dianova Clone pAK (DLN-13121)
Cy3-conjugated goat anti-rabbit secondary antibody	Polyclonal IgG goat	IHC: 1:400	Dianova (111-165-003)
Cy3-conjugated donkey anti-mouse secondary antibody	Polyclonal IgG donkey	IHC: 1:400	Dianova (715-165-150)

2.5 Primers and Plasmids

Table 2.5: Overview of used primers.

Gene	Gene Symbol	Unique Assay ID / Sequence	Supplier
aP2	*FABP4*	QT00203357	Qiagen
CD82	*CD82*	qHsaCID0013785	Bio-Rad
C/EBPα	*CEBPA*	QT01667694	Qiagen
Cldn-11	*CLDN11*	qHsaCED0041987	Bio-Rad
Collagen I	*COL1A1*	QT00037793	Qiagen
Collagen VI	*COL6A1*	QT00084343	Qiagen
COX-2	*PTGS2*	F: 5´-ACAGTCCACCAACTTACAAT-3` R: 5´-CAATCATCAGGCACAGGA-3´	Biomers
Cx 26	*GJB2*	qHsaCED0046305	Bio-Rad

Gene	Gene Symbol	Unique Assay ID / Sequence	Supplier
Cx 43	*GJA1*	qHsaCID0012977	Bio-Rad
EF1α	*EF1A1*	F: 5´-CCCCGACACAGTAGCATTTG-3` R: 5´-TGACTTTCCATCCCTTGAACC-3´	Biomers
Fibronectin	*FN1*	QT00038024	Qiagen
HPRT-1	*HPRT1*	QT00059066	Qiagen
IL-10	*IL10*	F: 5´-GTGATGCCCCAAGCTGAGA-3` R: 5´-CACGGCCTTGCTCTTGTTTT-3´	Biomers
IL-24	*IL24*	qHsaCID0011520	Bio-Rad
Jam-2	*JAM2*	qHsaCID0010183	Bio-Rad
Laminin α4	*LAMA4*	QT00032977	Qiagen
Laminin β1	*LAMB1*	QT00078162	Qiagen
Laminin γ1	*LAMC1*	QT00072142	Qiagen
N-Cadherin	*CDH2*	F: 5´-CCATCACTCGGCTTAATGGT-3` R: 5´-ACCCACAATCCTGTCCACAT-3´	Biomers
Notch-3	*NOTCH3*	qHsaCID0006529	Bio-Rad
Notch-4	*NOTCH4*	qHsaCID0037298	Bio-Rad
PPARγ	*PPARG1*	QT00029841	Qiagen
STC-1	*STC1*	F: 5´-AGGATGATTGCTGAGGTG-3` R: 5´-TGTTATAGTATCTGTTGGAGAAGT-3´	Biomers
TJP-2	*TJP2*	qHsaCID0006349	Bio-Rad
TRAIL	*TNFSF10*	qHsaCED0036477	Bio-Rad
TSG-6	*TSG6*	F: 5´-CATCTCGCAACTTACAAGC-3` R: 5´-AGACGGATTCCATAATCAATAATG-3´	Biomers

Three unique 29mer shRNA constructs, referred to as construct A, B, and C, in a retroviral GFP vector were used for the LAMA4 specific gene knockdown.

Table 2.6: Overview of the unique shRNA construct sequences.

Construct	ID	Sequence	Supplier
A	TG311803A (GI347205)	TTGGTCAGGTGACTCGCTTTGACATAGAA	OriGene Technologies, Rockville, USA
B	TG311803B (GI347206)	ATTAGAAGCCAGGAGAAATACAATGATGG	

Construct	ID	Sequence	Supplier
C	TG311803D (GI347208)	ACTGCCAGCGGAACACAACAGGAGAGCAC	

2.6 Cells

Table 2.7: Overview of used cells.

Cell Type	Source	Ref./Lot Number	Supplier
Adipose-derived stem cells	Human abdominal adipose tissue (female)	PT5006 Lot 0000407088 or Lot 0000421627	Lonza, Walkersville, USA
Phoenix™-ampho cells	kindly provided by AG Becker, ZEMM, Würzburg, Germany		

2.7 Cell culture media

Table 2.8: Overview of used cell culture media.

Medium	Composition
Basal medium (BM)	Dulbecco's Modified Eagle's Medium/Ham's F-12 (DMEM/F12, Invitrogen, Karlsruhe, Germany) supplemented with 1% penicillin/streptomycin (100 U/mL penicillin, 0.1 mg/mL streptomycin) and 10% fetal bovine serum (both from Invitrogen, Karlsruhe, Germany)
Growth medium (GM)	Preadipocyte basal medium-2 (PBM-2; Lonza, Walkersville, USA) supplemented with 1% penicillin/streptomycin (100 U/mL penicillin, 0.1 mg/mL streptomycin) and 10% fetal bovine serum (both from Invitrogen, Karlsruhe, Germany)
Differentiation medium (DM)	Growth medium with 1.7 µM insulin (Promocell, Heidelberg, Germany), 1 µM dexamethasone, 200 µM indomethacin (both from Sigma-Aldrich, Munich, Germany) and 500 µM 3-isobutyl-1-methylxanthin (IBMX; Serva Electrophoresis, Heidelberg, Germany)
Maintenance medium (MM)	Growth medium with 1.7 µM insulin (Promocell, Heidelberg, Germany)
Cryopreservation medium	Basal medium, supplemented with 5% Dimethyl sulfoxide (DMSO, Sigma-Aldrich, Munich, Germany)

2.8 Buffers and solutions

Table 2.9: Overview of used buffers and solutions.

Buffer / Solution	Composition
Adipogenic inducer stock solutions	Insulin (1.7 mM): 10 mg/mL dissolved in 30 mM HCl. IBMX (25 mM): 5.55 mg/mL dissolved in ddH_2O with a spatula tip of Na_2CO_3. Dexamethasone (10 mM): 3.925 mg/mL dissolved in abs. ethanol. Indomethacin (50 mM): 17.89 mg/mL dissolved in abs. ethanol.
Blocking solution (IHC)	1.5% BSA dissolved in PBS
BODIPY stock solution	1 mg/mL dissolved in PBS
Buffered formalin	3.7% formalin (37% stock solution) diluted in PBS
EGTA stock solution	38 mg/mL dissolved in ddH_2O (100 mM). pH adjusted to 7.4.
Hoechst 33258 stock solution	2 mg/mL dissolved in ddH_2O
ORO staining solution	0.5 g ORO dissolved in 100 mL isopropanol. Addition of 66.6 mL ddH2O. Filtered twice before use.
PBS	10 PBS (Dulbecco A) tablets are dissolved in 1 L ddH_2O
Phosphate saline buffer	50 mM ($Na_2HPO_4*2H_2O$ (178 g/mol), $NaH_2PO_4*H_2O$ (138 g/mol)), 2 mM $Na_2EDTA*2H_2O$, and 2 M NaCl dissolved in ddH_2O. pH adjusted to 7.4 with NaOH or HCl.
Resazurin solution	0.15 mg/mL resazurin sodium salt dissolved in PBS
TEN buffer	0.1 M NaCl, 1 mM EDTA, 10 mM Tris dissolved in ddH_2O; pH adjusted to 7.4.

2.9 Assay kits and multicomponent systems

Table 2.10:Overview of used assay kits.

Assay kit	Supplier	Central office
ImProm-II™ Reverse Transcription System	Promega	Mannheim, Germany
miRNeasy Mini Kit	Qiagen	Hilden, Germany
Prostaglandin E2 Parameter Assay Kit	R&D Systems	Minneapolis, USA
RT^2 First Strand Kit	Qiagen	Hilden, Germany

Assay kit	Supplier	Central office
RT^2 Profiler™ PCR Array	Qiagen	Hilden, Germany
Serum Triglyceride Determination Kit	Sigma-Aldrich	Munich, Germany

2.10 Software

Table 2.11: Overview of used software.

Software/Version	Supplier	Central office
CellSense™ 1.16	Olympus	Hamburg, Germany
GraphPad Prism Version 6.0	GraphPad Sofware	LaJolla, USA
Microsoft Office 2016	Microsoft	Redmond, USA

3 Methods

3.1 Cell culture of ASCs

3.1.1 Expansion of ASCs

Human ASCs were purchased from Lonza (Walkersville, USA; human adipose-derived stem cells). For expansion, cells were seeded in T175 tissue culture-treated plastic flasks with an initial seeding density of 5,000 cells/cm^2. The plastic adherent cells were cultured in basal medium (BM) consisting of Dulbecco´s Modified Eagle´s Medium/Ham´s F-12 (DMEM/F-12) (Invitrogen, Karlsruhe, Germany), supplemented with 10% fetal calf serum (FCS; Invitrogen) and 1% penicillin-streptomycin (Invitrogen) at 37°C and 5% CO_2, until confluence. Culture medium was changed every other day. For passaging or harvesting confluent cells for subsequent experiments, a 0.25% trypsin-EDTA solution (Invitrogen) was used. Cells in passage 4 or 5 were used for subsequent experiments.

3.1.2 2D monolayer culture

For experiments under conventional 2D culture conditions, unless otherwise stated, ASCs were seeded with a density of 25,000 cells/cm^2 in tissue culture-treated well plates (6-well and 24-well plates). From the moment of seeding into an experiment, ASCs were cultured in growth medium (GM) consisting of Preadipocyte Basal Medium-2 (PBM-2; Lonza) containing 10% FCS and 1% penicillin-streptomycin at 37°C and 5% CO_2.

3.1.3 3D spheroid culture

For 3D culture, multicellular spheroids were generated from the ASCs using the liquid overlay technique (Figure 3.1). For this purpose, tissue culture polystyrene 96-well plates were coated with 1.5% agarose diluted in DMEM/F-12 without supplementation. Unless otherwise stated, ASCs were seeded with 5,000 cells/well and cultured in growth medium on an orbital shaker at 50 rpm at 37°C and 5% CO_2. To prevent loss of spheroids during medium changes, only half of the medium volume was replaced with each medium change. Cells in 2D cultures were treated the same way for comparability.

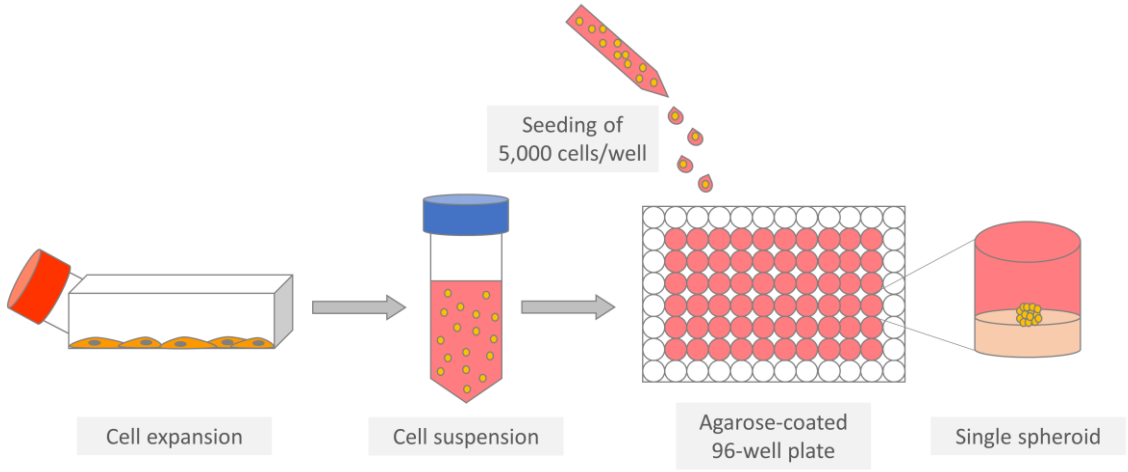

Figure 3.1: Generation of 3D spheroids using the liquid overlay technique.
After expansion, cells were seeded on a 96-well plate coated with 1.5% agarose with a density of 5,000 cells/well. The agarose layer prevented cell attachment to the surface of the culture plate. Due to the meniscus of the agarose layer and the agitation on an orbital shaker, the cells assembled in the center of the well and started to form one multicellular spheroid in each well. Modified from C. Muhr, doctoral thesis, 2012 (172).

The spheroid assembly process was monitored by microscopical images at different time points between 2 h and 48 h with an Olympus IX51 inverted light microscope equipped with a XC30 digital camera (Olympus, Hamburg, Germany). The diameter of spheroids was assessed using the Olympus cellSense™ Dimension Microscope Imaging Software. To analyze spheroid assembly over time the diameter of five independent spheroids was measured at each time point. As the spheroids do not have a uniformly round shape, the diameter of one spheroid was measured at four different sites of the spheroid and the mean value was calculated. To compare the assembly process of differently treated spheroids, the compactness index (CI) was determined. The CI was obtained by dividing the spheroid diameter by the diameter of the first measuring point after 2h of the same spheroid group. It was used as a parameter to normalize variations between the different spheroid groups that may have resulted from differences in the initially seeded cell number. The smaller the CI value, the greater the degree of compactness of the cell aggregates.

3.1.4 Inhibition of cadherin and integrin binding during spheroid formation

For unspecific inhibition of cadherin-binding the calcium chelator EGTA (ethylenglycol-bis-(β-aminoethyl ether)-N,N,N´,N´-tetraacetic acid; AppliChem, Darmstadt, Germany) was

added to the growth medium. To remove the extracellular calcium for blocking Ca^{2+}-dependent cadherins, ascending EGTA concentrations from 0.1 to 5.0 mM were added to the cell suspension directly before seeding the cells into the agarose-coated 96-well plates for spheroid formation. Spheroid forming ASCs in growth medium without the supplementation of EGTA served as control.

For a specific inhibition of N- and E-cadherin-, as well as β1-integrin-binding during spheroid assembly specific monoclonal antibodies were used for blocking. For this purpose, ASCs of the single cell suspension were pre-incubated with 10 µg/mL of the respective antibodies against N-cadherin (clone D-4, Santa Cruz Biotechnology, Texas, USA), E-cadherin (clone G-10, Santa Cruz Biotechnology, Texas, USA), and β1-integrin (clone P4G11, Santa Cruz Biotechnology, Texas, USA), which were added to the growth medium for 1 hour at 37°C prior to seeding into the agarose-coated 96-well plates. After pre-incubation the ASCs were seeded for spheroid assembly with 5,000 cells/well. The blocking antibody was added to the assembling cells in the same concentration as for the pre-incubation. ASCs with the respective isotype IgG1 control (Dako, Hamburg, Germany) added to the medium served as control.

The assembly process was observed over 48 hours by taken microscopical images at several time points with the Olympus IX51 inverted light microscope equipped with a XC30 digital camera (Olympus, Hamburg, Germany). Further analysis of spheroid assembly under the influence of the calcium chelator, as well as specific blocking antibodies, was carried out as described in the previous section.

3.1.5 shRNA-mediated gene silencing via retroviral transduction

The HuSH-29 shRNA vector (OriGene Technologies, Rockville, USA) was used for the shRNA-targeted knockdown of the laminin α4 encoding gene LAMA4. Three different shRNA sequences were used for the LAMA4 specific knockdown in human ASCs, referred to as construct A, B, and C. A non-effective 29mer scrambled shRNA construct served as control. For retroviral transduction, Phoenix™-ampho cells (kindly provided by AG Becker, Institute for Medical Radiation and Cell Research (MSZ) at the Center of Experimental Molecular Medicine (ZEMM), Würzburg, Germany) were first seeded into tissue culture treated 6-well plates with a seeding density of $1x10^6$ cells/well for Ca_2PO_4-transfection. The next day Phoenix™-ampho cells were Ca_2PO_4 transfected with 1.4 µg of the retroviral vector DNA, each containing one of the above-mentioned different shRNA constructs, in the presence of 25 µl

chloroquine. In parallel, human ASCs were seeded for retroviral transduction in basal medium (BM) into 6-well plates with a density of 30,000 cells/well. The next day, supernatants from transfected Phoenix™-ampho cells were harvested and passed through a 0.45 µm filter. One mL of BM was removed from each well with seeded ASCs and replaced by 1 mL of the retroviral supernatant. After the addition of 12 µg/mL polybrene to each well, cells were spun at 2,200 rpm at 32°C for 2 h. After centrifugation cells were incubated in a tissue culture incubator (37°C, 5% CO_2) for another day, before medium was replaced again by BM. To ensure uniform expression of the transduced shRNA construct, ASCs were cultured for one week in the presence of 10 µg/mL puromycin. After one week of antibiotic selection, when the cells reached confluence in the wells, transduced ASCs were used for subsequent analyses.

3.1.6 Adipogenic differentiation of 3D spheroids and 2D monolayers

After two days of cultivation in growth medium, adipogenic differentiation was induced (start of induction, designated day 0) by exchanging half of the medium with adipogenic differentiation medium (DM), i.e. growth medium with the hormonal inducers insulin (final concentration 1.7 µM; PromoCell, Heidelberg, Germany), dexamethasone (1 µM; Sigma-Aldrich, Steinheim, Germany), IBMX (500 µM; Serva-Electrophoresis, Heidelberg, Germany) and indomethacin (200 µM; Sigma-Aldrich). Two different induction regimes were performed under 2D as well as under 3D culture conditions. For permanent induction, the ASCs were kept in DM for 9 days until harvest. For short-term induction, cells were treated with DM for two days. Subsequently, the DM was replaced by maintenance medium (MM, growth medium supplemented with 1.7 µM insulin) by exchanging half of the medium for three times in order to minimize the concentration of the hormonal inducers. Non-induced control groups were cultured in growth medium during the whole culture time. The respective medium of each group was changed every other day until the end of the experiment.

3.2 Investigations on cell viability

3.2.1 Live/dead staining

Cell viability within the 3D spheroids was analyzed using live/dead staining (PromoKine, Heidelberg, Germany). Spheroids were washed three times with PBS and stained afterwards by

applying 100 µl of staining solution containing 4 μM ethidium bromide homodimer III (EthD) and 2 μM calcein acetoxymethyl ester (calcein) in PBS to each spheroid per well. After 1 hour of incubation in the dark, the staining solution was removed, and the spheroids were washed with PBS for another three times. The whole spheroids were analyzed either using an Olympus IX51 fluorescence microscope (Hamburg, Germany) (ex/em 460-490 nm/520nm and ex/em 510-550 nm/590 nm, respectively) and processed using the Olympus CellSens™ software. Furthermore, images were captured using a TCS-SP2 AOBS Leica confocal laser scanning microscope (CLSM) together with the Leica LCS Lite Software (Leica, Wetzlar, Germany).

3.2.2 Resazurin Assay

Resazurin as a cell permeable redox indicator was used to monitor viable cells within the 3D spheroids. Cells with an active metabolism can reduce resazurin into the fluorescent resorufin product. For this purpose, 20 µl of a resazurin solution (0.15 mg/mL resazurin sodium salt (Sigma-Aldrich, Munich, Germany) dissolved in DPBS) were added directly into each well of the 96-well plate containing cells in 100 µl growth medium. ASCs treated with 1% Triton X (Sigma-Aldrich) before served as negative control. Cells were further incubated with the supplemented resazurin for 4 h on an orbital shaker at 37°C and 5% CO_2. Subsequently, 100 µl of each well were transferred into a black 96-well plate for fluorescence measurement using a 560 nm excitation/590 nm emission filter set with a fluorescence spectrometer (Tecan GENios pro, Tecan Dtl. GmbH, Crailsheim, Germany).

3.3 Histology and immunohistochemistry

For histological and further immunohistochemical evaluation, 2D monolayers and 3D spheroids were fixed in 3.7% buffered formalin and stored until histological investigation in PBS. For a better visualization of the embedded spheroids for cryosectioning, spheroids were stained with methylene blue. Dehydration of 3D spheroids was performed by applying increasing sucrose concentrations from 10% to 40% for 30 min each prior to embedding in TissuTek® O.C.T. Compound (Sakura Finetek, Zoeterwonde, Netherlands). Spheroids were cut into 8 µm thick sections using a Leica CM3050 S cryostat (Leica Biosystems, Wetzlar, Germany). Histological and immunohistochemical analyses of 2D monolayers were performed directly in the 24-well plates.

3.3.1 Histological investigation of adipogenesis

For visualization of intracellular lipid accumulation of differentiating cells, 2D monolayers in tissue culture treated 24-well plates or cryosections of 3D spheroids were stained with the fat-soluble dye Oil Red O. After the Oil Red O working solution (0.5 g ORO (Sigma), 100 mL isopropanol (Sigma) and 66.6 mL H_2O) had been filtered through a 0.2 µm filter, 2D monolayers as well as spheroid sections were stained for 6 min. A counterstaining with Mayer´s Hematoxylin (Bio Optica, Milan, Italy) for visualization of nuclei was optionally performed. Before imaging, 3D spheroid sections were covered with Glycergel® mounting medium and coverslipped. Stained 2D monolayers were covered with PBS. Microscopical brightfield images of stained 3D spheroid sections were taken using a DP71 digital camera (Olympus, Hamburg, Germany) attached to an Olympus BX51 microscope. Phase contrast images were taken from 2D monolayers with an Olympus IX51 inverted light microscope equipped with a XC30 digital camera (Olympus, Hamburg, Germany).

3.3.2 Immunofluorescent staining

For immunohistochemical analysis of ECM components, cryosections of spheroids and native tissue, as well as 2D monolayers were stained with primary antibodies against collagen I (Col I; ab34710; polyclonal rabbit anti-Col I), collagen IV (Col IV; ab6586; polyclonal rabbit anti-Col IV), collagen VI (Col VI; ab6588; polyclonal rabbit anti-Col VI), laminin (Lam; ab11575; polyclonal rabbit anti-Lam) as well as fibronectin (FN; ab2413; polyclonal rabbit anti-FN) which were all purchased from Abcam (Cambridge, United Kingdom). Additionally, β1-integrin was investigated during spheroid formation using a specific primary antibody (Integrin β1, monoclonal mouse IgG, clone P4G11, sc-18845) purchased from Santa Cruz Biotechnology (Texas, USA). After blocking with 1% bovine serum albumin (BSA; Sigma-Aldrich, Munich Germany) for 20 min at room temperature, sections were incubated with the primary antibodies overnight in appropriate dilutions (Col I 1:800; Col IV 1:150; Col VI 1:200; Lam 1:200; FN 1:500; β1-integrin 1:50). After a washing step with PBS, the secondary antibody was applied for one hour (Cy3-conjugated AffiniPure goat anti-rabbit (1:400) or Cy3-conjugated AffiniPure donkey anti-mouse (1:400) both from Dianova, Hamburg, Germany). Spheroid cryosections were optionally stained with BODIPY® 493/503 (0.01 mg/mL in DMSO, Sigma-Aldrich) for lipid droplet visualization. Sample imaging of cryosections was performed with an Olympus BX51 microscope equipped with a DP71 digital camera (Olympus,

Hamburg, Germany) in combination with the Olympus cellSense™ Dimension Microscope Imaging Software. For imaging of 2D monolayers an Olympus IX51 inverted light microscope equipped with a XC30 digital camera (Olympus, Hamburg, Germany) was used.

3.4 Biochemical assays

For biochemical assays a total number of 3 biological replicates per sample were harvested and applied for each analysis. In 2D 1n consisted always of 2 wells of a 24-well plate and in 3D 1n was represented by a total of 20 spheroids. For the different analyses, different harvesting solutions were needed specified in the next sections.

3.4.1 Quantitative analysis of DNA content

For determination of total DNA content cells of 2D monolayers and 3D spheroids were harvested in phosphate-saline-buffer (50 mM phosphate buffer, 2 mM Na_2 EDTA*2 H_2O, 2 M NaCl, pH 7.4; all obtained from Carl Roth, Karlsruhe, Germany) and subsequently, sonicated with an ultrasonic homogenizer (Sonopuls, Bandelin electronic, Berlin, Germany). DNA quantification was performed using three biological replicates with one replicate consisting of 2 wells of a 24-well plate for 2D culture and an exact number of 20 spheroids for 3D culture, respectively. DNA content was determined by using the intercalating fluorescence dye Hoechst 33258 (Sigma). The fluorescence intensities were measured at an excitation wavelength of 365 nm and an emission wavelength of 458 nm with a fluorescence spectrometer (Tecan GENios pro, Tecan Dtl. GmbH, Crailsheim, Germany). Determination of unknown DNA contents was performed by correlating measured fluorescence intensities to the intensities of known DNA contents using standard dilutions of double-stranded DNA (from salmon sperm; Sigma)

3.4.2 Quantitative analysis of intracellular triglyceride content

Quantitative analysis of intracellular lipid accumulation during differentiation was performed by using the Serum Triglyceride Determination Kit from Sigma-Aldrich (Steinheim, Germany). ASCs of 2D monolayers and 3D spheroids were harvested in 0.5% aqueous Thesit solution (0.5% Thesit in H_2O; Gepepharm, Hennef, Germany) and sonicated with an ultrasonic homogenizer (Sonopuls, Bandelin electronic, Berlin, Germany). Intracellular triglyceride

content was also measured in three biological replicates, similar to the replicates of the DNA assay as described above. The assay was carried out according to the manufacturer`s instructions and measured with a Microplate ELISA-Reader (Dynatech Laboratories, EL Passo, USA) at 570 nm. Calculated triglyceride contents were normalized to the DNA content of the respective samples.

3.5 RNA isolation and real time qRT-PCR analysis

For gene expression analysis, total RNA from 2D cultured cells and 3D spheroids was harvested with TRIzol® reagent (Invitrogen). cDNA was synthesized using the IMProm-II™ Reverse Transcription System from Promega (Mannheim, Germany) followed by real-time quantitative PCR using the MESA GREEN qPCR MasterMix Plus Meteor*Taq* polymerase (Eurogentec; Seraing, Belgium). qRT-PCR was carried out with all the primers listed in Table 2.5. The following cycling protocol was applied: 95 °C for 15 minutes initial denaturation followed by 40 cycles at 95 °C for 15 seconds, 60 °C for 30 seconds, and 72 °C for 30 seconds. A melting curve analysis for qPCR product integrity was performed. mRNA expression levels were normalized either to the eukaryotic translation elongation factor 1 alpha (*EF1α*) (173), or to the hypoxanthine-guanine phosphoribosyltransferase (*HPRT1*) as a housekeeping gene for verification of the array hits. The $2^{-\Delta\Delta CT}$ method was used to determine the relative expression levels. The relative expression values were further normalized to the respective day 0, initial sample values, or respective 2D monolayers.

3.6 PCR array for expression analysis of cell junction related genes

For the analysis of cell junction related genes in ASCs cultured as 2D monolayers or 3D spheroids the RT2 Profiler ™ PCR Array “Human cell junction pathway finder” from Qiagen was used (Qiagen, Hilden, Germany). Three biological replicates of both 2D monolayers and 3D spheroids were harvested 72 h after seeding. For 2D cultured cells, 4 wells of a 24-well plate were pooled for one replicate in QIAzol™ lysis reagent (Qiagen). For 1n of 3D culture, a total amount of 60 spheroids were harvested in QIAzol™, respectively. Right before RNA isolation, cells of harvested 2D monolayers and 3D spheroids were disintegrated using a TissueLyzer (20 Hz, 2 min).

Total RNA was isolated using the miRNeasy Mini Kit from Qiagen according to manufacturer´s instructions. Subsequent cDNA synthesis was performed with the RT^2 First Strand Kit from Qiagen. Finally, the expression of cell junction related genes was analyzed with the above mentioned Qiagen PCR Array. Using the RT^2 SYBR® Green Mastermix, the process was carried out exactly according to the manufacturer's specifications for the performance with the Bio-Rad Real-Time PCR Detection System CFX96™. The following cycling protocol was applied: 95°C for 10 min to activate the polymerase followed by 40 cycles at 95°C for 15 sec and 60°C for 1 min. A melting curve analysis was performed afterwards to check PCR product integrity. The Qiagen GeneGlobe data analysis web tool was used to support the evaluation of the 84 genes examined in this array. mRNA expression levels were normalized to the hypoxanthine-guanine phosphoribosyltransferase 1 (*HPRT1*). The fold increase in expression levels for each gene was determined using the $2^{-\Delta\Delta CT}$ method. The obtained relative expression values of 3D spheroids were further normalized to the respective ones of 2D monolayers.

3.7 Quantitative analysis of secreted prostaglandin E2 (PGE2)

For the investigation of PGE2 secretion, cell culture medium from 3D spheroids and respective 2D monolayers was harvested after three days of culture. For 3D spheroids the medium of 10 single spheroids was pooled for 1n (total volume of 1 mL). For the respective 2D monolayers, 1n consisted of the pooled medium of 2 wells of a 48-well plate (total volume of 1mL). Secreted prostaglandin E2 was quantified using the Prostaglandin E2 Parameter Assay Kit from R&D Systems (Minneapolis, USA). The ELISA was performed according to the manufacturer´s instructions and finally measured with a Microplate ELISA-Reader (Dynatech Laboratories, EL Passo, USA) at 450 nm. Wavelength correction was performed at 570 nm. Measured PGE2 values were normalized to the total DNA content of the respective cells.

3.8 Statistics

Quantitative results are presented as mean value ± standard deviation (SD). Statistical significance was assessed by analysis of variance (one-way or two-way analysis of variance (ANOVA)) with subsequent multiple comparisons according to Bonferroni post-hoc test. A value of $p < 0.05$ was considered statistically significant. Statistical analysis was performed using GraphPad Prism 6 statistic software.

4 Results and Discussion

4.1 Spheroid formation of human ASCs

The use of 3D spheroids as building blocks for tissue engineering is an upcoming trend in future regenerative medicine. Especially for the application in soft tissue replacement, where it is usually required to restore larger volumes, e.g. for breast reconstruction, a large quantity of cells for spheroid formation is necessary, so that human adipose derived mesenchymal stromal/stem cells represent an ideal cell source, as they are of high abundancy and can be easily obtained from adipose tissue (174). Like many types of mammalian cells, also ASCs have the ability to aggregate and differentiate into multicellular 3D spheroids when cultured in suspension or a non-adhesive environment (122). During their assembly cells of these biomaterial-free spheroids are creating their own niche in which they are residing and interacting. Due to the spatial cell-cell and cell-ECM interaction within their created niche, 3D spheroids more closely represent the situation in vivo in comparison to conventional monolayer cultures. This makes 3D spheroids also advantageous over the currently frequently used biodegradable scaffolds seeded with isolated cells for tissue engineering applications. The type of cell-scaffold interaction more closely represents the artificial situation of cells cultured on a cell culture plate than the physiological interaction of cells among each other and with the surrounding extracellular matrix in vivo. Furthermore, the use of cell-seeded scaffolds always raises the issue of biocompatibility with regard to implantation of scaffold based tissue substitutes (3,140,150).

Besides their improved differentiation potential of 3D spheroids, also secretory properties with anti-inflammatory as well as immunomodulatory effects, contribute to spheroids suitability in regenerative medicine approaches and cellular therapies (145). To further extend the applications of ASC multicellular spheroids in this field, an extensive understanding of the molecular mechanisms contributing to the spheroid formation is of great importance. Inside the spheroids there exists a highly complex communication network, both between the cells themselves and with their surrounding matrix. Thus, spheroids are a great tool to investigate cell-cell and cell-ECM interactions to further understand the molecular forces for their improved regenerative potential, regarding differentiation and cytokine secretion.

As in natural processes like embryogenesis, morphogenesis and organogenesis, complex cell adhesion and differentiation contribute to the formation of multicellular spheroids

(119,151). Most of the previous findings concerning the formation process were gained from studies with different carcinoma cell lines (140,143,163). In these reports a three-step model with the involvement of cadherins and integrins is described for the spheroid-forming process. Thus, the spheroid formation in vitro starts with the initial loose formation of cellular aggregates through the binding to ECM molecules via integrins (step 1), followed by an upregulation of cadherin expression in the spheroid forming cells (step 2) and further spheroid compaction through enhanced cell-cell connection via homophilic cadherin binding (step 3) (123,140). This requirement for cadherins and integrin-binding to the ECM was also observed for other cell types, however, the ECM fiber and cadherin dependence may vary from cell to cell (122,142,144,175). This fact requires the investigations of the mechanisms contributing to the spheroid formation of human mesenchymal stem cells, in our case in particular of human adipose derived mesenchymal stromal/stem cells. Several groups are working with spheroids consisting of ASCs, however, they exclusively dealt with the augmentation of their therapeutic potency or differentiation but did not reveal the mechanisms of spheroid formation (150,164,165). Only Yeh et al. described a calcium dependent regulation of spheroid formation for ASCs grown on a chitosan membrane. At the same time, however, it was reported that the spheroid formation of adipose-derived as well as bone marrow-derived mesenchymal stromal/stem cells on chitosan membranes was quite different from that occurring in suspension or on non-adherent surfaces (176). Therefore, it is essential to analyse the formation process including the involved molecular mechanisms separately for each cell type and culture method.

According to this, the formation of 3D ASC spheroids on a non-adherent surface was investigated here. To the best of our knowledge, this is the first time of monitoring the individual spheroid formation of ASCs using the liquid overlay technique. Based on previous reports the influence of calcium-dependent cadherins as well as integrin-ECM binding were investigated in order to better understand the molecular mechanisms involved here. Furthermore, the development of the ECM as one major part of the 3D environment, spheroid forming cells are residing and interacting in, should be examined during spheroid formation to gain further insights in its involvement in various aspects of cellular behavior.

Altogether, these investigations should contribute to a detailed characterization of the 3D ASC spheroid model with the intention to strengthen their implementation in the field of regenerative medicine, including cellular therapies and tissue engineering approaches.

4.1.1 Self-assembly of ASCs into spheroid structures on a non-adherent surface

The self-assembly of ASCs to form single, three-dimensional spheroids was induced by seeding the cells in agarose-coated 96-well plates as described in the methods section. Because of the meniscus of the agarose layer and the gentle agitation on an orbital shaker, cells started to assemble in the center of the well. The non-adhesive surface forced the cells to attach to each other and form one multicellular spheroid in each well. The live/dead analysis of finally compacted cell aggregates showed viable cells in the entire spheroid with only single dead cells (Figure 4.1 A). To reveal the dynamics of assembly the morphology of ASCs during spheroid formation was documented through microscopic pictures which were taken at various time points during spheroid culture between 2 and 48 h after seeding the cells. A representative series of pictures from one single spheroid during the formation process is shown in Figure 4.1 B a) – e). Two hours after seeding, cells formed a loose cell aggregate which progressively underwent compaction during the next hours until the assembly process was completed after 24 h when spheroids reached their round shape with final compaction of the cells, as no further decrease of spheroid size could be observed in the following 24 h. Furthermore, it could be shown that all of the initially 5,000 seeded cells per well were part of the cell-aggregate, as no single cells could be found in the periphery of the assembled spheroids. This fact makes it possible to determine the final size of the spheroids via the initial number of seeded cells, which also achieves high reproducibility. Four hours after seeding was the earliest time point to harvest and fixate the assembling cell-aggregates without dissociating them again into single cells. This is the reason why histological analyses on cryosections from spheroids during the assembly process were only possible after four hours of spheroid formation. The hematoxylin staining of 8 µm cryosections from spheroids during the assembly process illustrated the development of a loose cell aggregate in the early phase of spheroid formation into a compact spheroid within 24 h (Figure 4.1 B, f – i). The arrows in image h) i) and j) of Figure 4.1 B indicated the tightly packed cells with a fibroblastic morphology in the outer layer of the finally assembled spheroids

Finally, ASCs were able to form viable, compact, and stable spheroids within 24 h. With the application of the liquid overlay technique in a 96-well plate setup, spheroids can be produced in a highly reproducible manner.

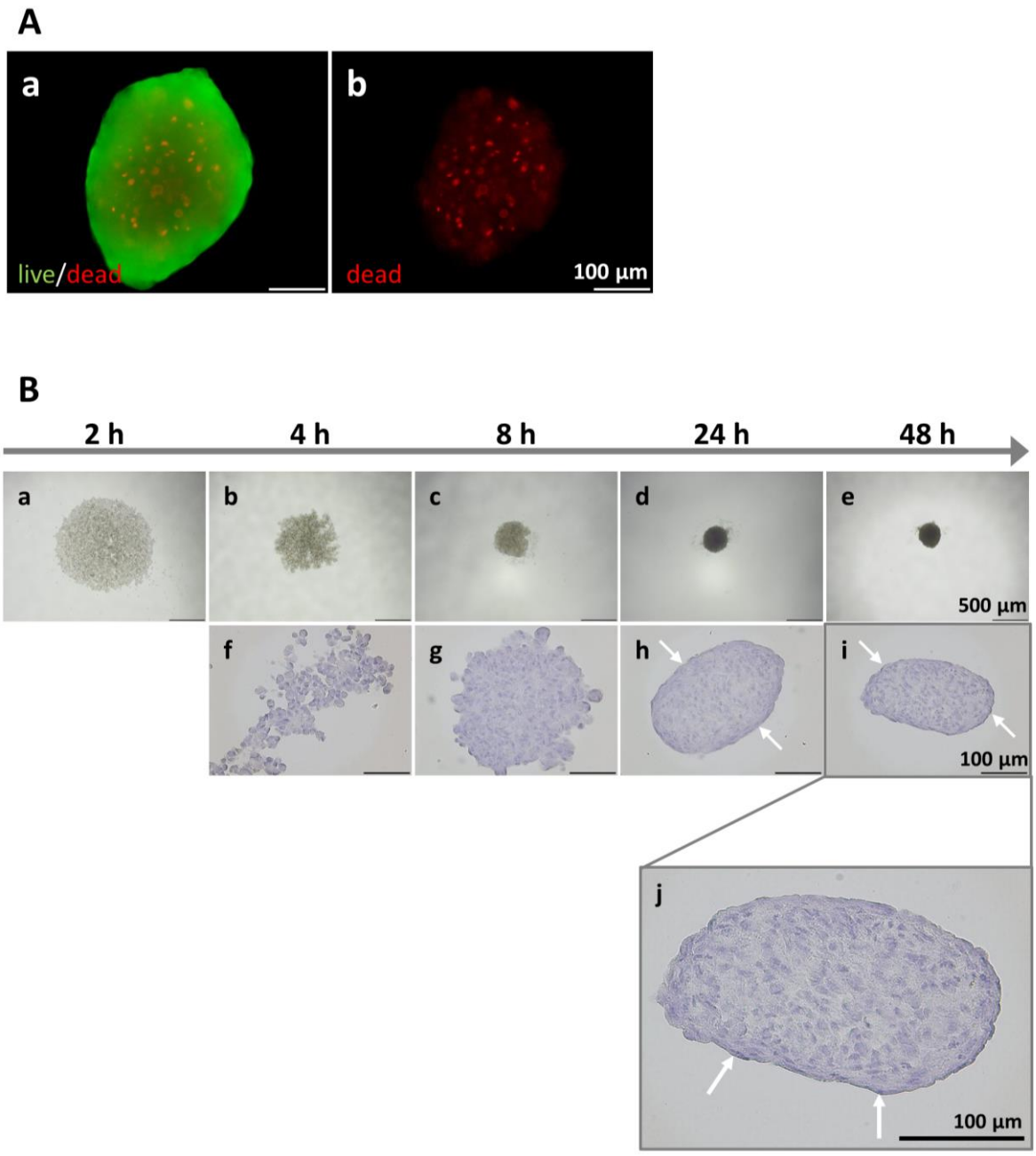

Figure 4.1: Formation of three-dimensional ASC spheroids.

A) a) Viability staining of a 3D spheroid after 48 h of assembly. Live cells were labeled with calcein acetoxymethyl ester in green and dead cells with ethidium bromide homodimer III (EthD) in red. For a clearer visualization, dead cells of this spheroid were separately shown in image **b)**. All images were taken in a 20-fold magnification, scale bars represent 100 µm. **B)** Morphology of ASC aggregates during spheroid formation. Images from whole spheroids were taken at various time points after seeding between 2 and 48 h **(a-e)**. The time course of the assembly process from one representative spheroid is shown here. Images from whole spheroids were taken at a 4-fold magnification; scale bars represent 500 µm. Hematoxylin staining of 8 µm cryosections of assembling spheroids at the respective time points **(h-i)**. Picture **j** shows an enlarged illustration of image **i** (*arrows* tightly packed cells in the outer layer of the spheroids). Images of hematoxylin stained cryosections were taken at a 20-fold magnification; scale bars represent 100 µm.

4.1.2 ECM development during spheroid formation

As 3D spheroids entail their own secreted matrix, which is important for spheroid formation via cell-integrin binding and further the cells are embedded and interacting in, a detailed description of the ECM development during spheroid assembly is one part of the characterization of the assembly process and the finally compacted spheroids. Here we investigated the development of three major ECM components (collagen I, VI and fibronectin) by immunohistological analyses on cryosections of assembling spheroids at various time points. The first row of images in Figure 4.2 A shows the development of the non-collagenous ECM protein fibronectin during the spheroid assembly between 4 and 48 h after seeding (Figure 4.2 A, a – d). Fibronectin could be already detected in the very beginning of spheroid formation, where it surrounded the assembling cells, followed by a strong increase of the fibronectin signal over time. The development of the fibrillar collagen I is shown in the second row of Figure 4.2 A (e – h). In contrast to fibronectin hardly any collagen I was detected in the beginning of spheroid formation. Only after 24 h a strong collagen I signal was observed in the already compact cell-aggregates which remained on a high level also in the following 24 h. The third row of Figure 4.2 A shows the increase of the network-forming, non-fibrillar collagen VI in the ECM of assembling spheroids (Figure 4.2 A, i - l). A slight signal was already detected in the beginning of spheroid formation. When spheroids reached their final size and compaction after 24 h, also collagen VI strongly increased and stayed constant until 48 h after seeding the cells for spheroid formation. Complementary to the histological analyses, the quantitative expression of these three ECM components was examined on mRNA level. Cells were harvested for mRNA isolation directly before seeding for spheroid formation (Start) as well as during spheroid formation after 2, 4, 8, 24 and 48 h of assembly. The expression levels of *EF1α* used as a housekeeping gene for quantitative real-time PCR, was used as a reference. The expression levels of *FN1*, *COL1A1* and *COL6A1* were determined relative to the start of seeding the cells on the agarose layer and are displayed in Figure 4.2 B. The expression analyses of these three ECM components revealed no statistically significant changes over time. This indicates that the differences observed in the histological analyses maybe were due to post-translational modifications differentially regulating final deposition of the ECM proteins into the extracellular space.

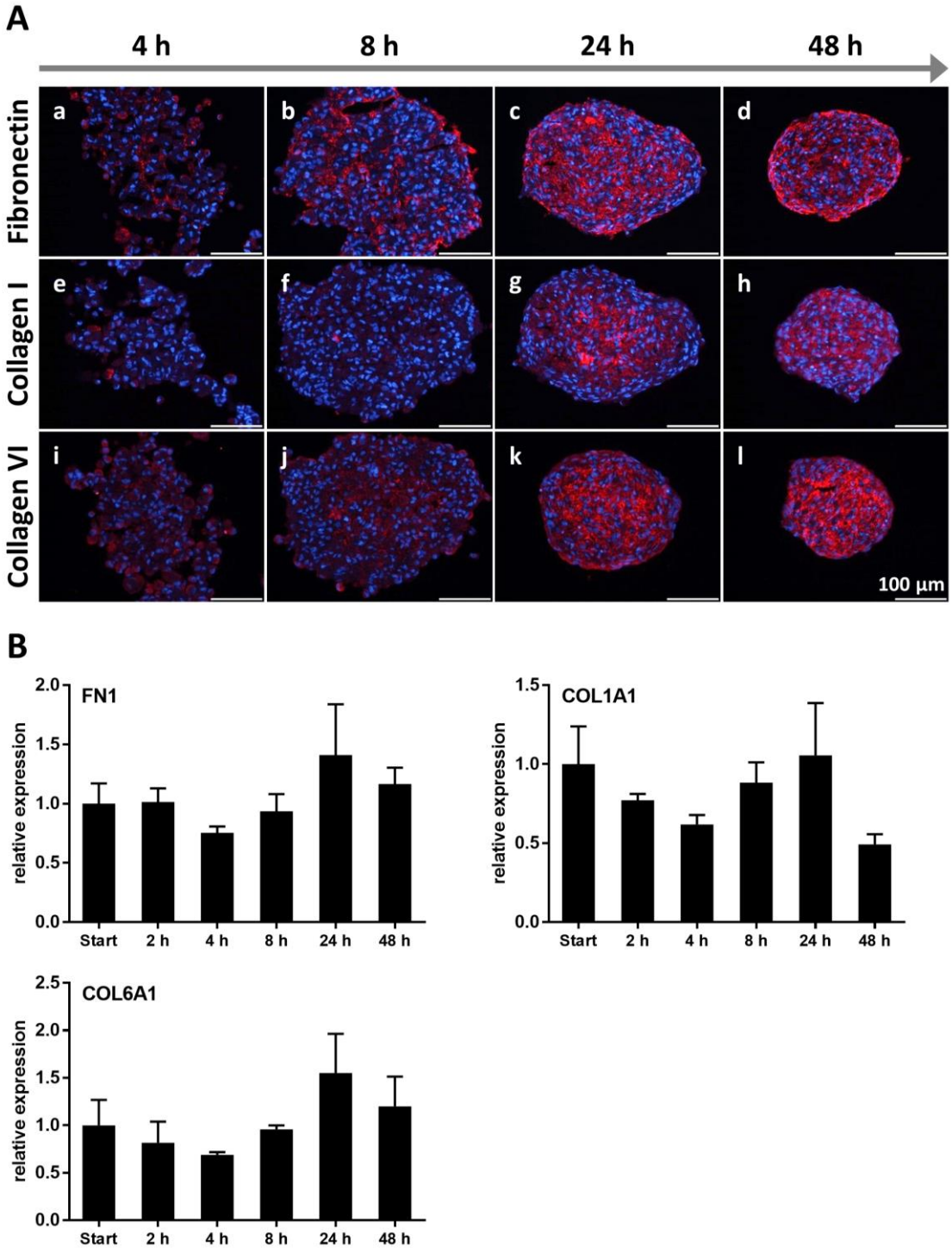

Figure 4.2: ECM development during spheroid formation.

A) Overlay fluorescence images of fibronectin **(a-d)**, collagen I **(e-h)**, collagen VI **(i-l)** (red) and 4´,6-diamidino-2-phenylindole (DAPI) nuclear counterstain (blue) from 8 µm cryosections of assembling 3D spheroids. Immunostaining was performed at different time points during spheroid formation between 4 and 48 h after seeding. Images were taken at a 20-fold magnification, scale bars represent 100 µm. **B)** Relative expression of *FN1*, *COL1A1* and *COL6A1* mRNA was determined by qRT-PCR. Total RNA for expression analysis was harvested directly before seeding the cells (Start) as well as during spheroid formation, 2, 4, 8, 24 and 48 h after seeding. Gene expression was normalized to *EF1α* as housekeeping gene. Expression levels were expressed

relative to the start of seeding cells on the agarose coated well plates. Values are expressed as mean with standard deviation (n=3).

4.1.3 Spheroid assembly with specific blocking of β1-integrin binding

Fibronectin was the only ECM component which was prominent already in the beginning of spheroid assembly as it was shown in Figure 4.3 A (a – d). Already after four hours of assembly a slight fibronectin signal was detected, which increased over time. The detected fibronectin surrounded the cells which started to bind to each other in order to begin the spheroid formation process. As one major adhesion molecule receptor, binding to fibronectin, the development of β1-integrin was simultaneously investigated during the assembly process by immunohistological analysis (Figure 4.3 A, e – h). Figure 4.3 A shows a concomitant development of fibronectin and β1-integrin directly in the beginning of spheroid aggregation. It is possible that the spheroid forming ASCs bound to the connecting fibronectin via β1-integrin, so that the detected signal increased with the growing abundancy of the detected fibronectin. To further elucidate whether fibronectin plays a role via β1-integrin binding of the cells in the spheroid formation process, the receptor was blocked with a specific antibody. Assembling spheroids with a respective isotype antibody added to the culture medium served as control group. Looking at the morphology of the spheroids during their formation, a delay in the assembly and compaction process was obvious in the β1-integrin blocked spheroids during the first 8 h compared to the control group (Figure 4.3 B). After 24 h the β1-integrin blocked cells reached the same size and compaction as the control group. Thus, blocking the fibronectin receptor resulted in a delay in the early phase of cell assembly, the final compaction process of the spheroids was not affected. This finding is corroborated by determination of the spheroids´ compactness index. The compactness index (CI) in Figure 4.3 C illustrates the progressive cell aggregation and compaction of the 3D spheroids over time. The smaller the index the more compacted are the assembling spheroids. The CI depicted a delayed spheroid assembly of the β1-integrin blocked ASCs within the first eight hours during the formation process. At every time point within the first eight hours the CI of the blocked spheroids was significantly higher than the CI of the control spheroids. This indicated a retarded aggregation and compaction of the blocked spheroids, however after eight hours a strong decrease in the CI was observed, so that also the blocked spheroids ended up with a comparable size and compaction to the control cell aggregates after 24 h.

Specific blocking of β1-integrin in order to prevent binding of the cells to fibronectin led to a delayed spheroid assembly in the first eight hours, so that fibronectin as one prominent ECM component in the beginning of the assembly process seemed to play a role in the initial cell aggregation and compaction.

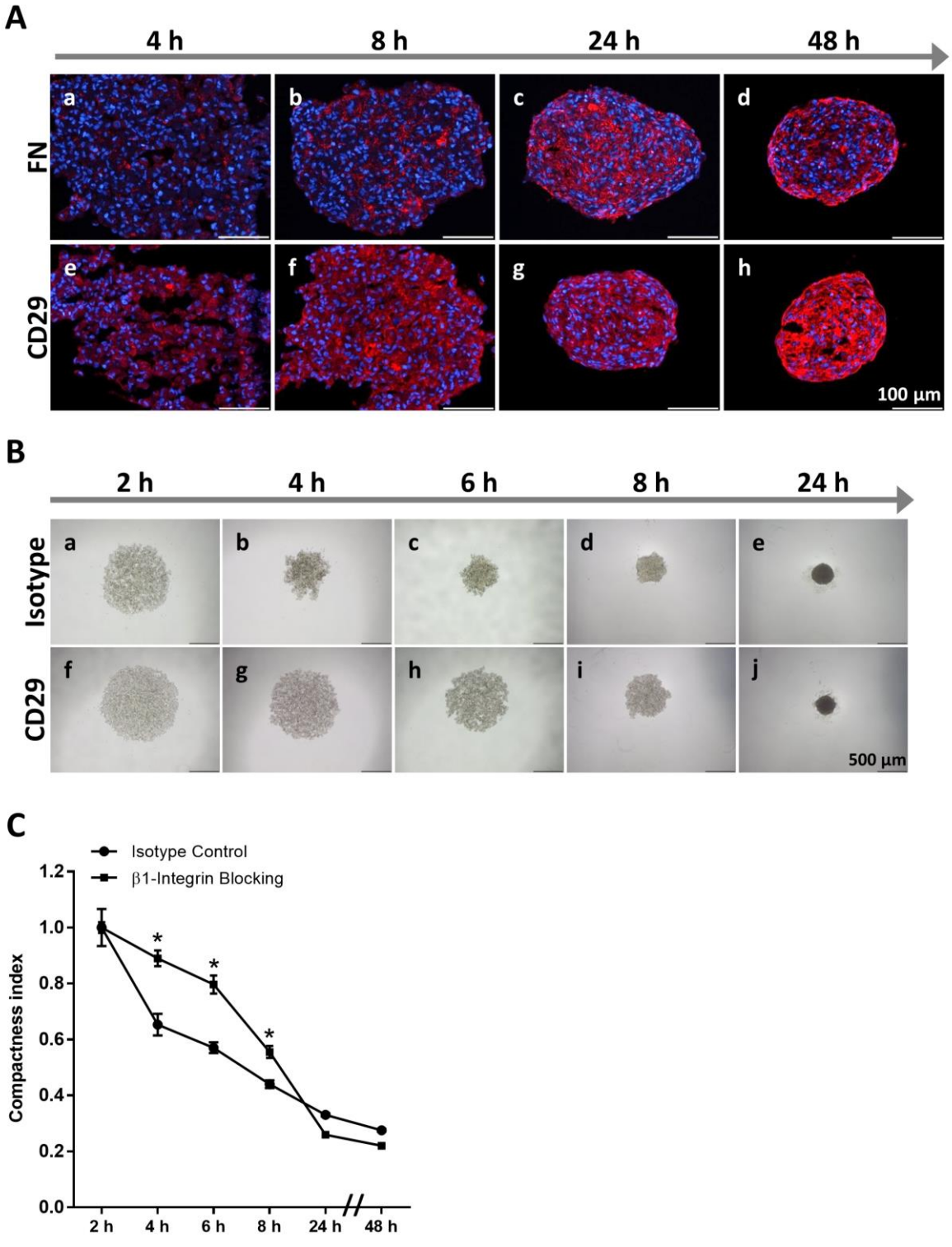

(Figure legend on the next page.)

Figure 4.3: Spheroid formation with specific blocking of β1-integrin (CD29).
A) Overlay fluorescence images of fibronectin **(a-d)**, CD29 **(e-h)** (red) and 4´,6-diamidino-2-phenylindole (DAPI) nuclear counterstain (blue) from 8 µm cryosections of assembling 3D spheroids. Immunostaining was performed at different time points during spheroid formation between 4 and 48 h after seeding. Images were taken at a 20-fold magnification, scale bars represent 100 µm. **B)** Morphology of ASC aggregates during spheroid formation with specific β1-integrin blocking **(f-j)**. Spheroid forming cells with the respective isotype IgG1 antibody served as controls **(a-e)**. Images from whole spheroids were taken at various time points after seeding between 2 and 48 h. The time course of the assembly process from one representative spheroid per group is shown here. Images from whole spheroids were taken at a 4-fold magnification; scale bars represent 500 µm. **C)** Change in spheroid size during the assembly process over time represented by the compactness index. *Statistically significant differences ($p < 0.05$) between spheroid forming cells with specific β1-integrin blocking and the isotype control group. Values are expressed as mean with standard deviation (n=4).

4.1.4 Influence of cadherin-binding on the spheroid formation process

Besides cell-surface integrin binding to long chain ECM fibers with multiple RGD motifs like fibronectin, especially homophilic cadherin-cadherin binding between adjacent cells were shown to be responsible for the compaction of cell aggregates at later stages of spheroid formation of various cell types. The requirement for cadherins was described for spheroid formation of several cell types, although a variation of cadherin dependence was reported from cell to cell. Therefore, focus of this part of the investigations concerning ASC spheroid formation was the influence of cadherin-cadherin binding on the ASC assembly process on the non-adherent agarose layer. First the unspecific blocking of cadherin binding between the assembling cells should give initial insights, whether spheroid compaction of ASCs also depends on cell-cell binding via cadherins. For this purpose, Ca^{2+}-dependent cadherins were blocked through the addition of the calcium chelator EGTA to remove extracellular calcium which is an essential factor for cadherin activation. EGTA was added during spheroid assembly in ascending concentrations from 0.1 to 5.0 mM. Assembling spheroids without the addition of the calcium chelator served as control group. The documentation of spheroid morphology at several time points during the assembly process showed a disturbed aggregation of ASCs only for the highest EGTA concentration of 5.0 mM. Lower EGTA concentrations between 0.1 and 1.0 mM had no influence on spheroid formation as no differences in spheroid morphology compared to the control group were observed at any time point. Although an EGTA concentration of 1.0 mM was determined to be sufficient to completely remove the extracellular calcium in the used culture medium, spheroid compaction seemed not to be affected in this group (Figure 4.4 A). The compactness index (CI) illustrates the failed spheroid formation of

ASCs cultured with 5.0 mM EGTA, as the measured values were significantly higher at every time point compared to the control group. The CI of spheroid forming cells with lower EGTA concentrations confirmed the morphological observations that the formation process was not affected in comparison to the control group without addition of a calcium chelator (Figure 4.4 B). As 1.0 mM EGTA should be enough to absorb the available calcium completely, these results suggested that cadherin-cadherin binding plays no decisive role in spheroid compaction, as no activation of the Ca^{2+}-dependent cadherins was possible under this condition. A higher EGTA concentration of 5.0 mM, however, led to a disturbed spheroid formation, so that it should be further investigated, whether this observation was actually due to the blockage of cadherin binding or whether the higher EGTA concentration had further effects on the spheroid forming cells, for example on their viability.

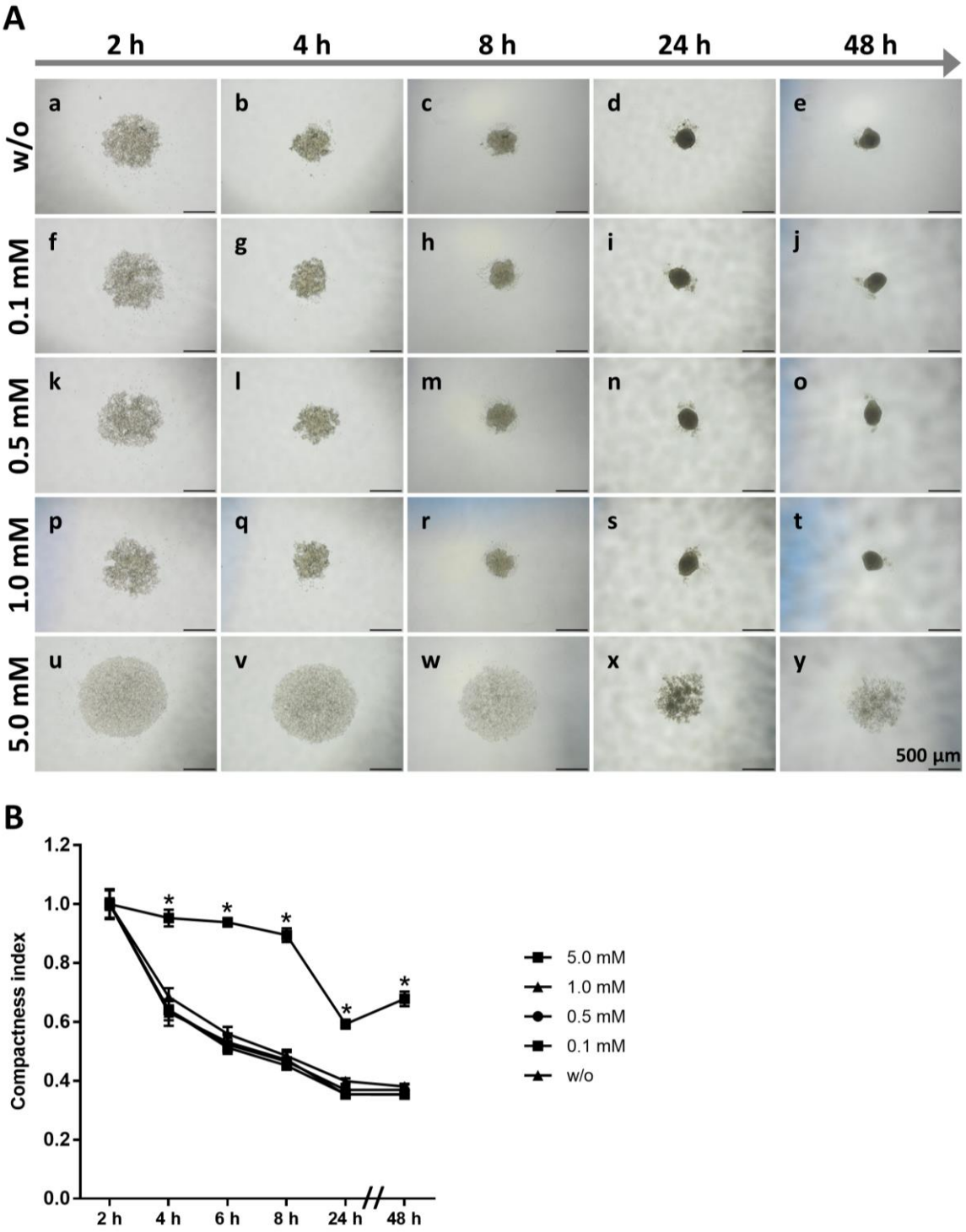

Figure 4.4: Spheroid formation with different EGTA concentrations.

A) Morphology of ASC aggregates during spheroid formation with different concentration of EGTA added to the culture medium. Spheroid forming cells without supplementation of EGTA to the culture medium served as controls **(a-e)**. EGTA was added to the culture medium in different concentrations of 0.1 **(f-j)**, 0.5 **(k-o)**, 1.0 **(p-t)** and 5.0 mM **(u-y)** right before seeding the cells on the agarose layer. Images from whole spheroids were taken at various time points after seeding between 2 and 48 h. The time course of the assembly process from one representative spheroid per group is shown here. Images from whole spheroids were taken at a 4-fold magnification; scale bars represent 500 µm. **B)** Change in spheroid size during the assembly process over time

represented by the compactness index. *Statistically significant differences ($p < 0.05$) between spheroid forming cells with EGTA added to the culture medium and the control group without supplementation. Values are expressed as mean with standard deviation (n=4).

To investigate whether increasing EGTA concentrations affect the viability of the spheroid forming cells, a live/dead assay was performed after 48 h of assembly (Figure 4.5 A). Only a few dead cells were detected in the control group without EGTA and also the addition of 0.1, 0.5 and 1.0 mM EGTA to the culture medium did not affect the cell viability as most of spheroid forming cells were labeled in green. In contrast, the number of dead cells was greatly increased by the addition of 5.0 mM EGTA. This observation was confirmed by determination of the metabolic activity of the cells exposed to varying EGTA concentrations (Figure 4.5 B). Cells exposed up to 1.0 mM EGTA showed no decrease in metabolic activity compared to the untreated control group, whereas incubation with 5.0 mM EGTA reduced metabolic activity to the level of the dead control.

These investigations led to the result, that the highest EGTA concentration of 5.0 mM negatively affected cell viability, which is why the impaired spheroid assembly of these cells could not be traced back to blocked cadherin bonds in this group. Rather, this observation was due to the fact that most of the cells were dead. Altogether based on the given results, interactions between cadherins of adjacent cells may not be responsible for ASC spheroid compaction.

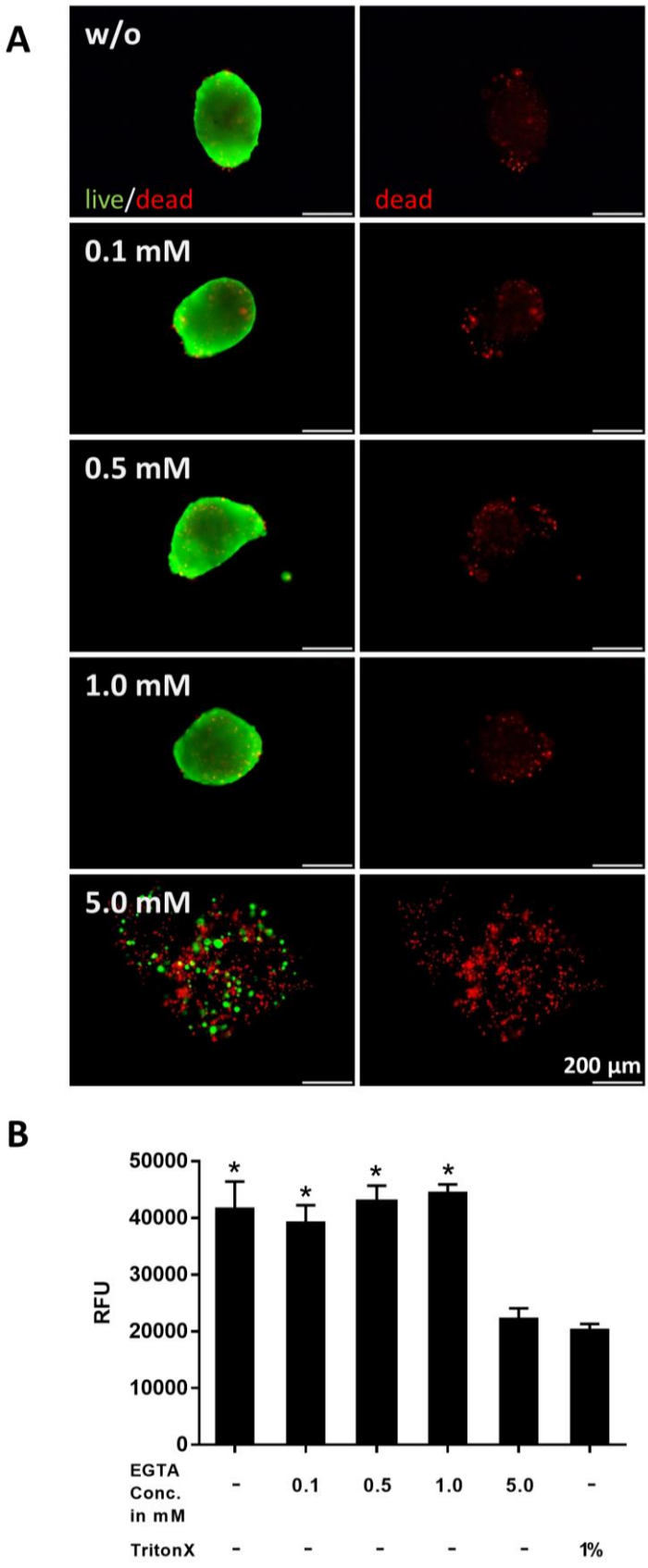

Figure 4.5: Influence of different EGTA concentrations on cell viability.

A) Viability staining of 3D spheroids after 48 h of assembly with different EGTA concentrations (0.1, 0.5, 1.0 and 5.0 mM) added to the culture medium. Spheroids without EGTA supplementation to the culture medium (w/o)

served as controls. Live cells were labeled with calcein acetoxymethyl ester in green and dead cells with ethidium bromide homodimer III (EthD) in red (left column). For a clearer visualization, dead cells of these spheroids were separately shown in the right column. All images were taken in a 10-fold magnification, scale bars represent 200 µm. **B)** Viability of 3D spheroids after 48 h of assembly exposed to resazurin for 4 h. Cells with 1% Triton-X added to the culture medium served as dead control. Relative fluorescence units (RFU) are expressed as mean value with standard deviation of five independent spheroids per group (n=5). *Statistically significant differences ($p < 0.05$) between control spheroids without EGTA supplementation or spheroids with different EGTA concentrations and the dead control.

4.1.5 Spheroid formation with specific blocking of N- and E-cadherin

To further confirm that cadherin binding between adjacent cells has really no pivotal impact on spheroid formation of ASCs, two major cadherins, N- and E-cadherin, were blocked with specific antibodies during the assembly process. Assembling spheroids with a respective isotype antibody added to the culture medium served as control group. By documentation of the spheroid morphology during the assembly process at different time points no difference in spheroid formation and compaction between the N- and E-cadherin blocked ASCs and the control group was obvious, as the accumulating spheroids of each group were comparable in size at every time point (Figure 4.6 A). Furthermore, the progressive cell aggregation and compaction represented by the compactness index confirmed the morphological observations (Figure 4.6 B). The determined indices of the N- and E-cadherin blocked spheroids were not higher at any time point during the formation process, indicating that the spheroids were not affected in their aggregation and compaction through the specific blocking of N- and E-cadherin.

These results confirmed the assumption that cadherins especially the homophilic binding of N- and E-cadherin are not primarily responsible for the spheroid formation and compaction of ASCs on a non-adherent surface like the agarose layer.

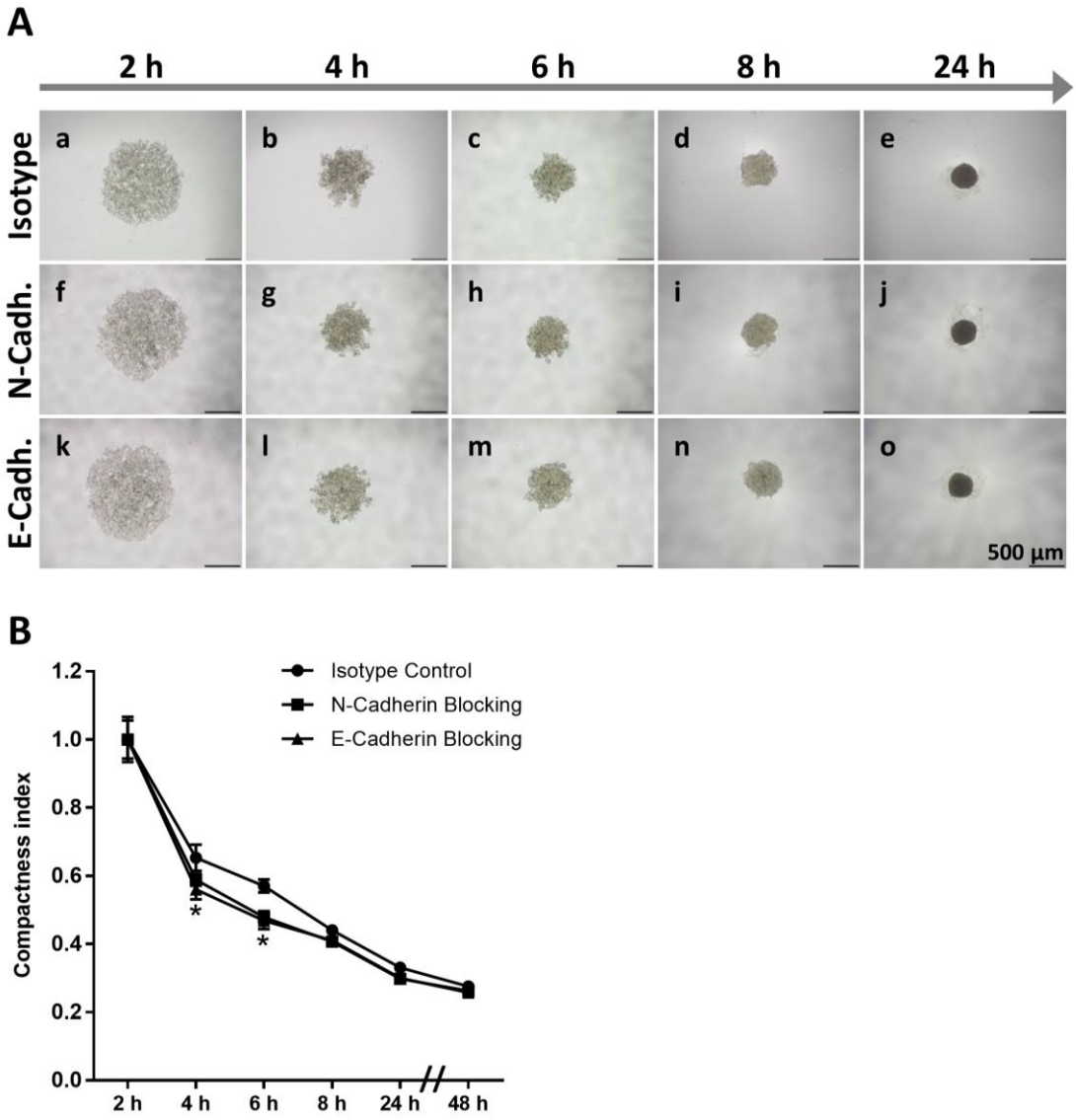

Figure 4.6: Spheroid formation with specific blocking of N- and E-cadherin.

A) Morphology of ASC aggregates during spheroid formation with specific N-cadherin **(f-j)** and E-cadherin **(k-o)** blocking. Spheroid forming cells with the respective isotype IgG1 antibody added to the culture medium served as controls **(a-e)**. Images from whole spheroids were taken at various time points after seeding between 2 and 48 h. The time course of the assembly process from one representative spheroid per group is shown here. Images from whole spheroids were taken at a 4-fold magnification; scale bars represent 500 µm. **C)** Change in spheroid size during the assembly process over time represented by the compactness index. *Statistically significant differences ($p < 0.05$) between spheroid forming cells with specific N- and E-cadherin blocking and the isotype control group. Values are expressed as mean with standard deviation (n=4).

4.1.6 Discussion

Since multicellular 3D spheroids exhibit higher similarity to native tissues in many aspects compared to conventional monolayer culture, they recently gained increasing recognition in biomedical research. This includes among others the application of these cell aggregates as building blocks for tissue engineering approaches (122). Reports on ASC-based spheroids so far have dealt with their therapeutic potency or differentiation capacity. A further characterization of ASC based spheroids concerning mechanisms like spheroid assembly has not been done in these cases. (150,164). For a further extension of spheroid applications in the field of regenerative medicine and adipose tissue engineering, however, an extensive characterization of this spheroid model including the molecular mechanisms contributing to the formation process is of great importance. Based on previous reports, it is essential to characterize the 3D spheroids for each cell type depending on the culture method used for spheroid synthesis, as the process of spheroid formation may vary between them (176). So, the results of this chapter should contribute to a detailed characterization of the ASC spheroid model cultured on a non-adherent surface, which has not been reported in the literature so far.

The generation of viable spheroids, which are easy in handling, scalable and reproducible is one major challenge for their application in the regenerative medicine (151). According to the liquid overlay technique, ASCs were seeded onto a flat 96-well plate coated with agarose as a low-adhesive surface, leading to the formation of one single spheroid in each well. These spheroids consist of the entire amount of the initially seeded cells, as no single cells could be found in the periphery of the finally aggregated spheroids. Therefore, the spheroid size could be determined by the number of seeded cells per well as it was also reported by Zimmermann and Mcdevitt in 2014 (135). Unlike the ASC spheroid formation in microgravity bioreactors or on chitosan membranes, which both result in a heterogeneous population of spheroids with different cell numbers and sizes, the generation of a homogeneous population of ASC aggregates was possible with the method applied here (150,174,176). Thus, the liquid overlay technique in a 96-well plate setup allows a controlled, highly reproducible and scalable method for spheroid generation. Although this method is rather less suitable for high throughput production in tissue engineering applications due to its labour intensity, it is particularly suitable in the area of basic research and fundamental characterization of 3D spheroids.

Initially seeded 5,000 cells per well resulted in compact spheroids with an average size of 320 µm (± 8 µm) within 24 h. The spheroid aggregation of ASCs within 24 h was also described by several other groups (150,151). Microscopic pictures taken at several time points during the

formation process showed, that ASC spheroid formation on the agarose layer starts with an initially loose cell aggregate followed by compaction of the involved cells until the final spheroid size has been reached after 24 h. This observation reflects reports from the literature where the spheroid formation in vitro under low attachment conditions was also described as a process with the formation of a loose cell aggregate through integrin-ECM binding in the beginning followed by the spheroid compaction through enhanced cell to cell connection via homophilic cadherin binding (122,132,177). These reports on spheroid formation cultured in suspension or on non-adherent surfaces are contrasted by the 2D to 3D transition on chitosan membranes (123). Opposed to the described self-aggregation, cells on chitosan membranes first attach and spread before they retract their pseudopodia to form multicellular spheroids (178,179).

The hematoxylin staining of cryosections from assembling spheroids at several time points during their formation demonstrate the development of loose cellular aggregates into compact spheroids. During this process the development of a tightly packed outer cell layer was observed. Lin et al. described the differentiation of cells from the outer layer of compact cell aggregates into smooth, tightly packed, polarized cells, respectively, which acted as a physical barrier preventing small molecules from penetrating inner parts of the spheroid (140). After their final compaction, spheroids are dense cellular structures which are very stable and insensitive to mechanical disruption. Furthermore, it was important to evaluate whether the ASCs, especially in the inner parts of the 3D spheroids, remained viable or not. The Live/Dead assay performed for this purpose, revealed the result that most of the spheroid forming ASCs were viable without the development of a necrotic core in the center. In was reported that dense cellular structures develop hypoxia at distances beyond the diffusion capacity of oxygen, which is typically about 200 µm (174,180). Maybe the gentle agitation of our 3D spheroids during culture helps to overcome this limitation, so that also larger distances are possible before hypoxia and therefore the necrosis of the spheroid core start to develop. Thus, we have succeeded in generating ASC spheroids, which are easy to handle and whose inner parts are still sufficiently supplied with oxygen and nutrients, so that the formation of a necrotic core is avoided.

An extensive characterization of the spheroid model should also include the investigation of the cell surrounding matrix, whose components are secreted by the aggregating cells themselves. This own secreted extracellular matrix, cells are residing and interacting in, distinguishes the spheroid model from other three-dimensional cell culture models with

artificial matrix and thus best reflects the physiological situation in vivo. Nevertheless, the ECM configuration during spheroid assembly has been given so far only little attention, although it is known that not only cell-cell contacts but also cell-ECM interaction mediate 3D cell aggregation. The first detected ECM component at the very beginning of the assembly of ASCs was the non-collagenous ECM protein fibronectin. The cells were already surrounded by fibronectin after 4h of assembly, while the other two investigated major components collagen I and VI could only be detected with increasing compaction in the extracellular space of the 3D spheroids. However, this dynamic expression of the different ECM components in extracellular space was not due to differences in the associated gene expression. Rather, it could be assumed that posttranslational modifications and differences in secretion into the extracellular space were responsible for the dynamic ECM development during spheroid formation. The most prominent ECM component in the early phase of spheroid formation of ASCs, fibronectin, has been described as an important mediator in cell aggregation. In CHO cell lines, the influence of the fibronectin matrix on cellular cohesion was shown specifically via integrins (142,175). These transmembrane cell adhesion proteins act as matrix receptors and tie the fibronectin matrix to the cell´s cytoskeleton. Drastic changes in cell morphology and cytoskeleton arrangement are necessary for cell aggregation, which is why an influence of actin-mediated contractility on hMSC assembly was described in the literature (132). The influence of the early developed fibronectin on the spheroid formation of ASCs was further investigated here, as it was reported to be linked to the actin-skeleton via β1-integrin (132). The interaction of fibronectin and the concomitant developing β1-integrin was blocked with a specific blocking-antibody for the β1-integrin receptor leading to a delayed spheroid assembly within the first 8 hours. This observation partially confirmed the reported three step model of spheroid formation in the literature (140). The initial formation process starts with the loose cell aggregate formation through integrin binding to long chain ECM fibers with multiple RGD motifs, for example fibronectin, what explains a delayed spheroid assembly in the beginning through blocking of the respective receptor. A participation of integrins in the early stages of spheroid formation was also described for hepatoma cells and Casey et al. showed that β1-integrin takes part in the regulation of multicellular spheroid formation as well via blocking and stimulating β1-integrin with specific antibodies (122,163). As the specific blocking of β1-integrin leads to a delayed spheroid formation, fibronectin seems to play a role in the initial cell-aggregation also for ASC spheroid formation. Sottile and Hocking reported, that the extracellular assembly of fibronectin into fibrils is integrin mediated, so that the blocking of integrins maybe leads to a delayed fibronectin assembly in the extracellular environment of the cells, which furthermore

affects the assembly process of the cells (181). After 8 hours, however, ASC spheroids with a blocked β1-integrin receptor made up their retarded initial cell aggregation and ended up with the same compaction and spheroid size like the control spheroids after 24 hours. Although β1-integrin is the classic receptor binding to fibronectin, there are also other integrin subunits like for example β3, which can bind to this ECM molecule, so that the blocked β1-integrin maybe could be replaced by binding of another receptor to fibronectin fibers in order to compensate the delayed cell aggregation from the beginning (182).

After the previously achieved results of the β1-integrin blocking confirmed the importance of integrin-ECM binding in the first part of the spheroid formation also for human ASCs, the influence of cadherin binding in the further compaction of cell aggregates should be also investigated here (122). However, the spheroid compaction by homophilic cadherin-cadherin binding, described as the third part in the above mentioned 3-step model, could not be confirmed for the ASCs cultivated on a non-adherent surface. First, the concentration of free calcium in the cell culture medium was reduced using the calcium chelator EGTA. Calcium is as an essential factor for cadherin activation, so that the reduction of free calcium in the culture medium is one possibility to investigate the influence of cadherins on the spheroid formation of ASCs. However, an inhibitory effect on the spheroid formation could only be observed from an EGTA concentration of 5.0 mM, which was not due to the inhibition of cadherins, but rather to the decline of cell viability. An influence on the aggregation of the ASCs caused by lower EGTA concentrations in the range of 0.1 – 1.0 mM was not observed. This is despite the fact that the calcium present in the culture medium should be calculative completely bound with 1.0 mM EGTA and thus the cadherins should actually be effectively inhibited. On the other hand, there are reports in the literature that describe a clear inhibitory effect on spheroid formation triggered by a reduced extracellular calcium concentration. For example, Yeh et al. already observed a significant reduction of spheroid diameter when adding only 0.5 mM EGTA to the cell culture medium, so that a cadherin dependence of spheroid formation was suspected (176). Mesenchymal stem cells from fat tissue were also used in this study, but cultivation was carried out on a chitosan membrane. It has already been reported, that the assembly process of the cells on chitosan membranes differs significantly from that in a cell suspension or culture on a non-adhesive surface (176). The specific inhibition of N- and E-Cadherin by blocking antibodies also showed that these two cadherins have no influence on the assembly of the ASCs cultivated on agarose layer. Especially for N-Cadherin, this result was particularly comprehensible, as results regarding the gene expression in spheroids (as shown in Chapter 4.4)

demonstrated a reduced expression of the corresponding gene in 3D spheroids. This further indicates that cadherins do not play a pivotal role in the spheroid formation process of human ASCs cultivated on a non-adherent surface. Contrary to previous reports, in which cadherins are significantly involved in the spheroid compaction, it supports the insight that the integrin and cadherin dependence of the assembly process can be different from cell to cell (142–144). The independency of spheroid formation on cadherin interaction was shown, for example, for several tumor cell lines (144).

Other candidates mediating the self-assembly of cells may be connexins, which form gap-junctions between adjacent cells. Bao et al. reported for several tumor cell lines, that gap junction forming connexins, in particular connexin 43, directly connect the cells to each other and therefore contribute to the self-assembly through their adhesive function (141). An increased expression of connexin 26 and 43 could also be demonstrated for the spheroid-forming ASCs (see Chapter 4.4). This could be an indication that these gap junction-forming connexins also participated in the assembly and compaction process of ASCs. Future experiments, such as the blocking of corresponding connexins or the knock-down of respective genes, could contribute to the further elucidation of the molecular mechanisms involved in the spheroid formation of human mesenchymal stem cells isolated from adipose tissue.

Overall, the results of this chapter contribute to a detailed characterization of the 3D spheroid model consisting of human adipose-derived stromal/stem cells. By studying the individual spheroid formation of the ASCs cultured on a non-adherent surface, we were able to describe the initial development of the extracellular matrix and gain some insights into the underlying molecular mechanisms involved in the formation process. This is an important contribution to understand the reasons for the improved regenerative potential of 3D spheroids to further establish them as an approach in regenerative medicine, including tissue engineering.

4.2 Human ASC spheroids possess high adipogenic capacity and acquire an adipose tissue-like ECM pattern

Christiane Hoefner, MSc[1], Christian Muhr, PhD[1], Miriam Wiesner, PhD[1], Katharina Wittmann, PhD[1], Daniel Lukaszyk, MD[1], Katrin Radeloff, MD[2], Marc Winnefeld, PhD[3], Matthias Becker, PhD[4], Torsten Blunk, PhD[1], Petra Bauer-Kreisel, PhD[1]

[1]*Department of Trauma, Hand, Plastic and Reconstructive Surgery, University of Würzburg, Germany*

[2]*Department of Otorhinolaryngology, University of Würzburg, Germany*

[3]*Beiersdorf AG, Hamburg, Germany*

[4]*Institute for Medical Radiation and Cell Research, University of Würzburg, Germany*

submitted to Tissue Engineering Part A, 2019

Multipotent mesenchymal stromal/stem cells residing in the adipose stromal niche are widely used in tissue engineering applications due to their multilineage potential and easy harvest. Adipose-derived stromal cells (ASCs) have extensively been studied for adipose tissue regeneration to overcome the tremendous clinical need for the development of adequate implants to repair soft tissue defects resulting from traumatic injury, tumor resection, and congenital defects (8,9,25,38–40,183). In current ASC research traditional 2D culture is widely used yielding cells separated from their original microenvironment. In addition, for tissue engineering cells expanded in 2D cultures are commonly seeded onto biomaterial-based scaffolds, which in many cases, at least initially, also represent a 2D environment as the cells on scaffold surfaces largely grow in 2D with limited cell-cell contacts (151). As innate properties such as the differentiation capability of ASCs are greatly influenced by their niche with its spatially arranged cell-cell and cell-matrix interactions, cells in a 2D environment may be limited in their regenerative capacity (166,167).

In contrast, the self-assembly and culturing of cells in a 3D context has been shown to create a more in vivo-like microenvironment allowing cells to interact with each other within their secreted extracellular matrix rather than with an artificial surface (162). Culturing and delivery of various cell types as spheroids consequently has been demonstrated to lead to an enhancement of their regenerative potential due to superior differentiation ability, secretion of angiogenic and anti-inflammatory cytokines, and enhanced integration and retention after transplantation in vivo (147,156,161).

ASCs have been shown to aggregate into multicellular 3D spheroids when cultured in suspension or in a non-adhesive environment (151). In this way ASC spheroids potentially form tissue-like structures without the need of an artificial scaffold material and, thus, would be predestined as building blocks in tissue engineering approaches for creation of tissues with proper three-dimensional organization, for example in biofabrication applications (120,133). Through the implementation of tissue-specific precultivation methods, e.g. adipogenic induction, the application of histotypic microtissues is feasible (133). In this context the development of a tissue-specific ECM is an intrinsic feature, as in addition to providing physical support, the ECM actively contributes to the establishment and maintenance of differentiated tissues and is part of the complex communication network of cells in their niche (168). As such the proper development of a tissue-specific ECM must be considered as an important requirement in tissue engineering approaches. However, to date knowledge about ECM composition and development during the adipogenic differentiation process in ASC-derived

spheroids is missing, as the few studies regarding development of ECM during adipogenic differentiation have been done in 2D monolayer culture (59,109,184).

So far ASC-derived spheroids have been rarely investigated for their use in adipose tissue engineering (185,186). In a study conducted by Zhang et al., ASC-derived spheroids, generated in poly(lactid-co-glycolid acid) (PLGA) scaffolds, were shown to trigger adipose tissue formation in vivo. In that study spheroids were cultured in adipogenic induction medium prior to implantation employing a standard long-term induction protocol as it is also often used for 2D cultures (185). This further underlines, in principle, the beneficial effect of adipogenic induction and pre-cultivation of ASCs in vitro for adipose tissue formation in vivo (9).

For the effective application of ASC-derived spheroids as building blocks in adipose tissue engineering, insights into ECM development and efficient adipogenic induction would be conducive. Therefore, in the present study, we investigated the ECM composition of ASC-derived spheroids and the dynamic ECM development during the adipogenic differentiation process. ECM composition of differentiated spheroids was compared to native human fat to demonstrate the resemblance between the ECM of the two tissues. Furthermore, adipogenic induction in 3D spheroids was investigated in comparison to conventional 2D culture. Specifically, different induction protocols were evaluated showing that ASCs in 3D spheroids needed a distinctly shorter adipogenic stimulus to effectively differentiate into adipocytes compared to 2D cultured cells. The results of this study may further the use of ASC-derived spheroids as building blocks for soft tissue engineering.

4.2.1 Formation of ASC-derived spheroids

The self-assembly of ASCs was induced by seeding the cells in agarose-coated well-plates according to the liquid overlay technique. The non-adhesive surface forced the cells to attach to each other resulting in multicellular aggregates. Using an initial cell number of 5,000 cells per well, one single spheroid yielding a densely packed rounded structure with 320 µm (± 8 µm) in size was formed per well. Live/dead staining of fully compacted spheroids (48 h after seeding of the cells) demonstrated the viability of cells within the spheroid (Figure 4.7 A). Thus, the applied technique allows for the generation of viable ASC cell aggregates in a well-defined and highly reproducible manner. To monitor the assembly process, images of assembling spheroids were taken at various time points after seeding (Figure 4.7 B). Two hours after seeding, cells formed a loose aggregate which progressively underwent compaction during the next hours.

The assembly process was completed after 24 h when spheroids reached a round compact shape. This process was reflected by the reduction of the spheroid diameter over time illustrating a sharp decline during the first 8 h after seeding with no further reduction in spheroid diameter after 24 h (Figure 4.7 C). The ECM composition of fully compacted spheroids was examined using immunohistochemical staining (48 h after seeding). In this state spheroids displayed a stromal ECM pattern with fibronectin, Col I and Col VI as major ECM components (Figure 1D). Laminin and Col IV as adipose tissue-specific ECM components were not detectable at this time point, which also represented the time point of adipogenic induction in the following section (Figure 4.7 D).

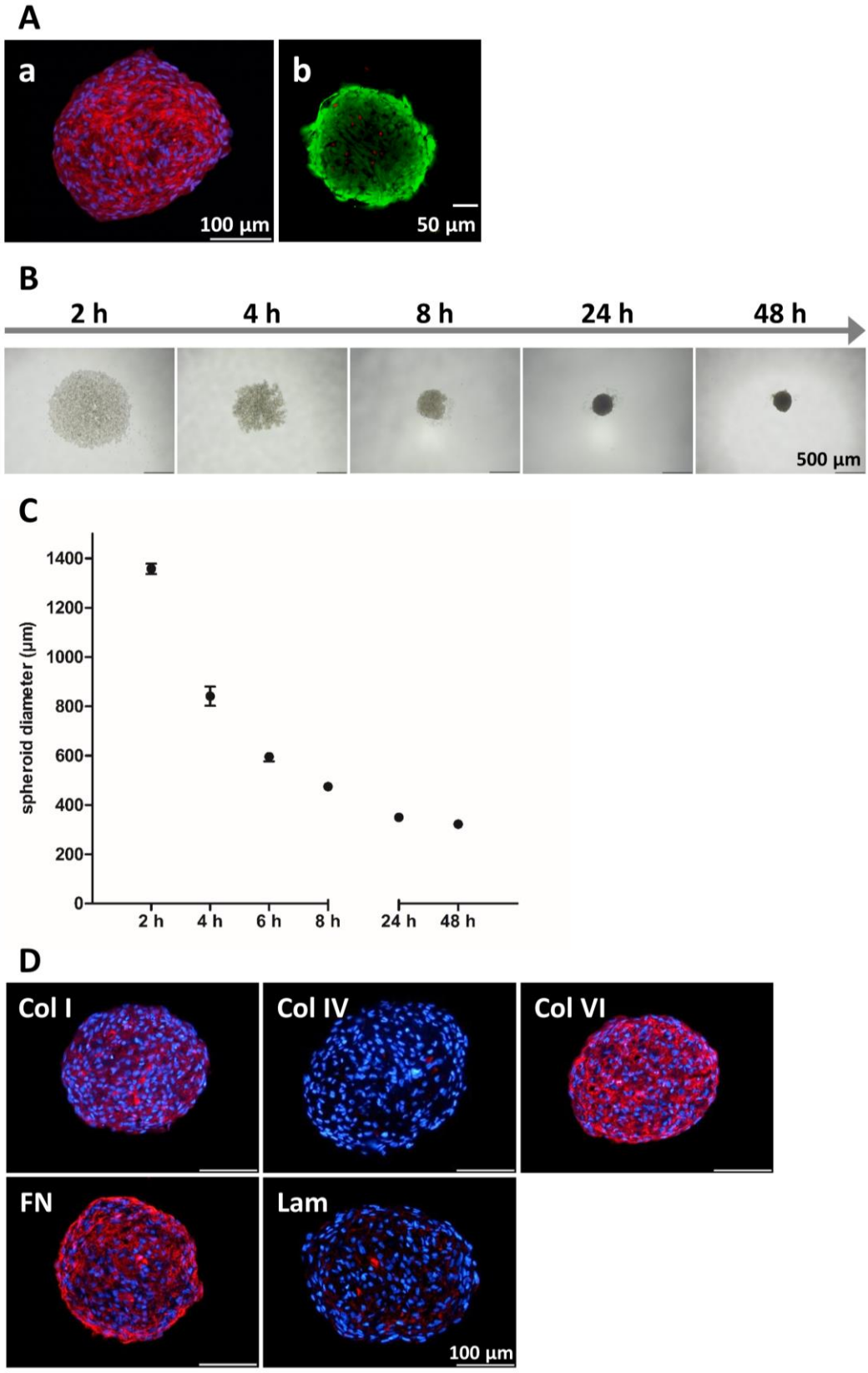

Figure 4.7: Characterization of human ASC spheroids.

A) Morphology of spheroids. a) Phalloidin staining of actin filaments (red), counterstaining of nuclei with DAPI (blue) 48 h after seeding. Scale bar represents 100 µm. b) Confocal microscopic image of live/dead stain at 48h. Living cells were stained with calcein (green) and dead cells were stained with ethidium bromide (red). Scale bar

represents 50 µm. **B)** Assembly of spheroids. 5,000 cells were seeded in agarose-coated 96-wells and observed by phase contrast microscopy at the indicated time points. The time course of the assembly process from one representative spheroid is shown. Scale bars represent 500 µm. **C)** Determination of spheroid diameter during the assembly process. Values are expressed as mean with standard deviation (n=4). **D)** Extracellular matrix characterization of assembled spheroids. Immunofluorescence staining of major ECM components collagen I (Col I), collagen IV (Col IV), collagen VI (Col VI), fibronectin (FN), and laminin (Lam) was performed on 48 h-spheroids. Nuclei were stained blue with DAPI. Scale bars represent 100 µm.

4.2.2 ECM remodeling during adipogenic differentiation and comparison to native human adipose tissue

Next, we analyzed the adipogenic differentiation of ASC and ECM remodeling during the differentiation process in spheroid culture. To this end, spheroids 48 h after seeding were transferred to adipogenic differentiation medium. After 9 days in culture ASCs in 3D spheroids markedly differentiated along the adipogenic lineage as confirmed by Oil Red O staining of accumulated triglycerides. In non-induced spheroids triglyceride accumulation was not detectable (Figure 4.8 A). The extracellular matrix composition of differentiated ASC-derived spheroids and their undifferentiated counterparts was characterized by immunohistochemical staining of major ECM components (Col I, Col IV, Col VI, fibronectin and laminin) and compared to the ECM composition of native human fat tissue (Figure 4.8 B). Spheroids cultured in growth medium (non-induced) retained their ECM composition consisting mainly of fibronectin and Col VI. In contrast, spheroids cultured in adipogenic differentiation medium (induced) developed an ECM pattern with Col IV and laminin as integral parts of the basement membrane surrounding adipocytes, while fibronectin was hardly detectable. Col I and Col VI were found to be expressed more prominently in differentiated spheroids compared to undifferentiated spheroids. The comparison with the ECM pattern of native human adipose tissue revealed a distinct resemblance with the ECM of differentiated spheroids. Col I, Col IV, Col VI and laminin were present in native fat as well as in differentiated ASC-derived spheroids, while fibronectin was barely detectable in both fat tissue and in spheroids. In native fat tissue a net-like structure was apparent representing the ECM network surrounding mature adipocytes. This structure was not as pronounced in the spheroids likely due to the fact that ASCs did not reach their final differentiation stage during the 9 days differentiation period.

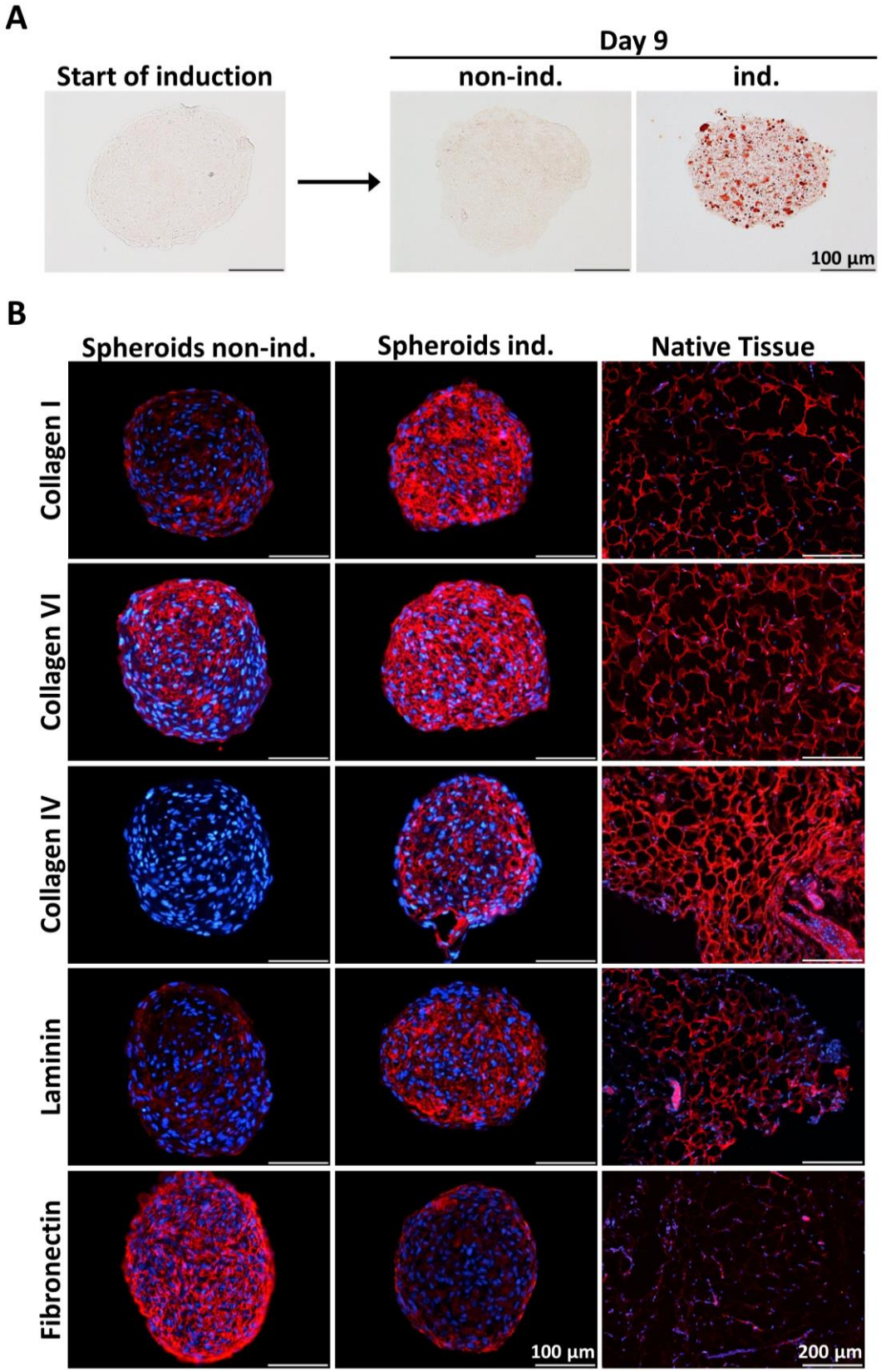

(Figure legend on the next page.)

Figure 4.8: Adipogenic differentiation and ECM development during the differentiation process in ASC-derived spheroids and comparison to human native tissue.
A) Adipogenic differentiation of spheroids. Adipogenic differentiation was induced by transfer to adipogenic culture medium two days after seeding (start of induction). After nine days of induction, adipogenic differentiation was assessed by staining of accumulated triglycerides with Oil Red O. Scale bars represent 100 µm. **B)** Immunohistochemical characterization of major ECM components of adipogenically differentiated spheroids in comparison to native human adipose tissue. Col I, Col VI, Col IV, laminin and fibronectin were immunohistochemically stained on cryosections of non-induced and adipogenically induced spheroids after 9 days (red), counterstaining of nuclei with DAPI (blue). Sections of native human adipose tissue were stained accordingly. Images of spheroids were taken at a 20-fold magnification; scale bars represent 100 µm. Sections of native tissue were imaged at a 10-fold magnification; scale bars represent 200 µm.

In order to depict a chronological sequence of ECM remodeling and adipogenic differentiation in spheroids, accumulating triglycerides and laminin as one major component of the adipose-specific ECM were stained at various time points (d0, d2, d5, d7, d9) during the differentiation process (Figure 4.9). Accumulating triglycerides, as detected by BODIPY staining, became visible not before day 7 with a further increase in staining intensity until day 9. By juxtaposing the laminin deposition at these time points, it became evident that the laminin production clearly preceded the deposition of lipid droplets as a distinct laminin signal could be detected as early as day 2 after adipogenic induction with a further increase in signal intensity during the ongoing differentiation process.

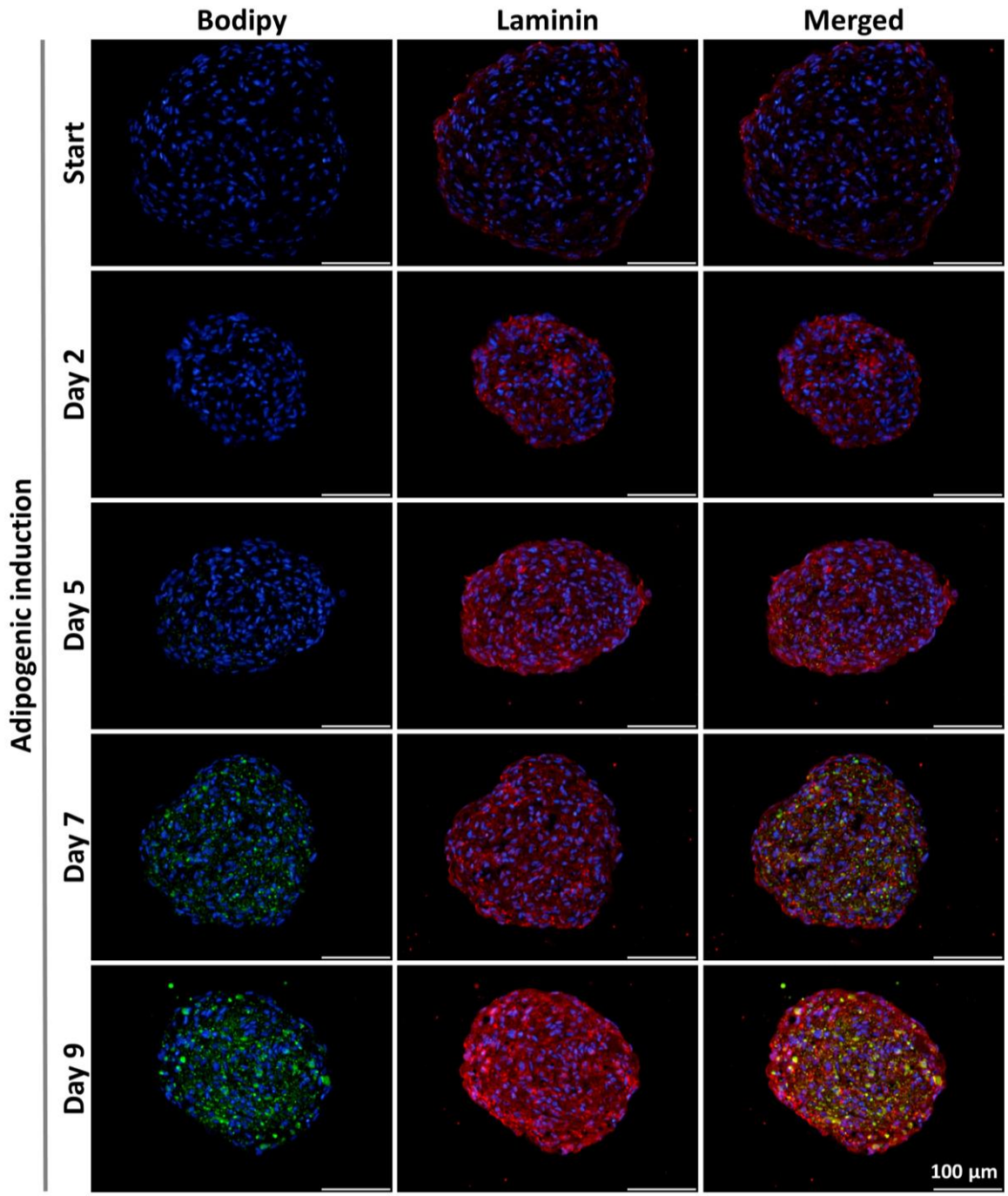

Figure 4.9: Development of laminin during adipogenic differentiation of 3D spheroids.

To visualize progression of adipogenesis accumulating triglycerides were stained with BODIPY (green) at various time points (left column). Laminin deposition was monitored by immunohistochemical staining (red, middle column). Nuclei were counterstained with DAPI (blue). Overlay of lipid and laminin staining (right column). Scale bars represent 100 µm.

4.2.3 Effect of short-term adipogenic induction on adipogenesis in 2D cultures and 3D spheroids

In order to optimize the adipogenic induction protocol for efficient differentiation, i.e. reduction of induction time, spheroids were adipogenically induced using different culture regimes. ASCs in fully compacted spheroids (48 h after seeding) were induced to undergo adipogenesis using a standard induction protocol with permanent application of the adipogenic hormonal cocktail in adipogenic differentiation medium during the complete differentiation period (9 days), and alternatively a short-term induction regime was employed with culture in adipogenic differentiation medium for only 2 days followed by culture in maintenance medium for 7 days (Figure 4.10 A). Adipogenically induced spheroid cultures were compared to induced conventional 2D cultures, and 3D spheroids and 2D monolayers cultured in growth medium during the whole cultivation period served as non-induced controls. Adipogenesis under the different induction conditions was assessed by quantification of accumulated triglycerides at day 9 (Figure 4.10 B). With permanent induction cells in 2D cultures as well as in spheroids differentiated along the adipogenic lineage as shown by significantly elevated triglyceride levels compared to the non-induced controls. ASCs in spheroids displayed a better differentiation capacity reflected by a higher triglyceride content per cell under this condition. With the short-term induction regime, only ASCs cultured as spheroids underwent adipogenesis, whereas for cells in 2D monolayers triglycerides remained at control level. Histological analysis confirmed these results (Figure 4.10 C). Only a minimal number of lipid droplets could be detected in cells that were cultured in monolayers, whereas in short-term induced spheroids triglyceride accumulation was comparable to the accumulation observed in cells cultured in adipogenic differentiation medium for 9 days. To investigate whether the depicted differences in adipogenic capacity between 2D and 3D cultures were also reflected on gene expression level, qRT-PCR was performed to analyse the expression of PPARγ, a master regulator of adipogenesis, and aP2, a marker gene of terminal adipogenic differentiation. In spheroids, expression of PPARγ was greatly increased either by short-term or permanent induction, whereas in 2D monolayers PPARγ expression was significantly reduced under short-term induction conditions. A similar expression pattern was observed for the expression of aP2.

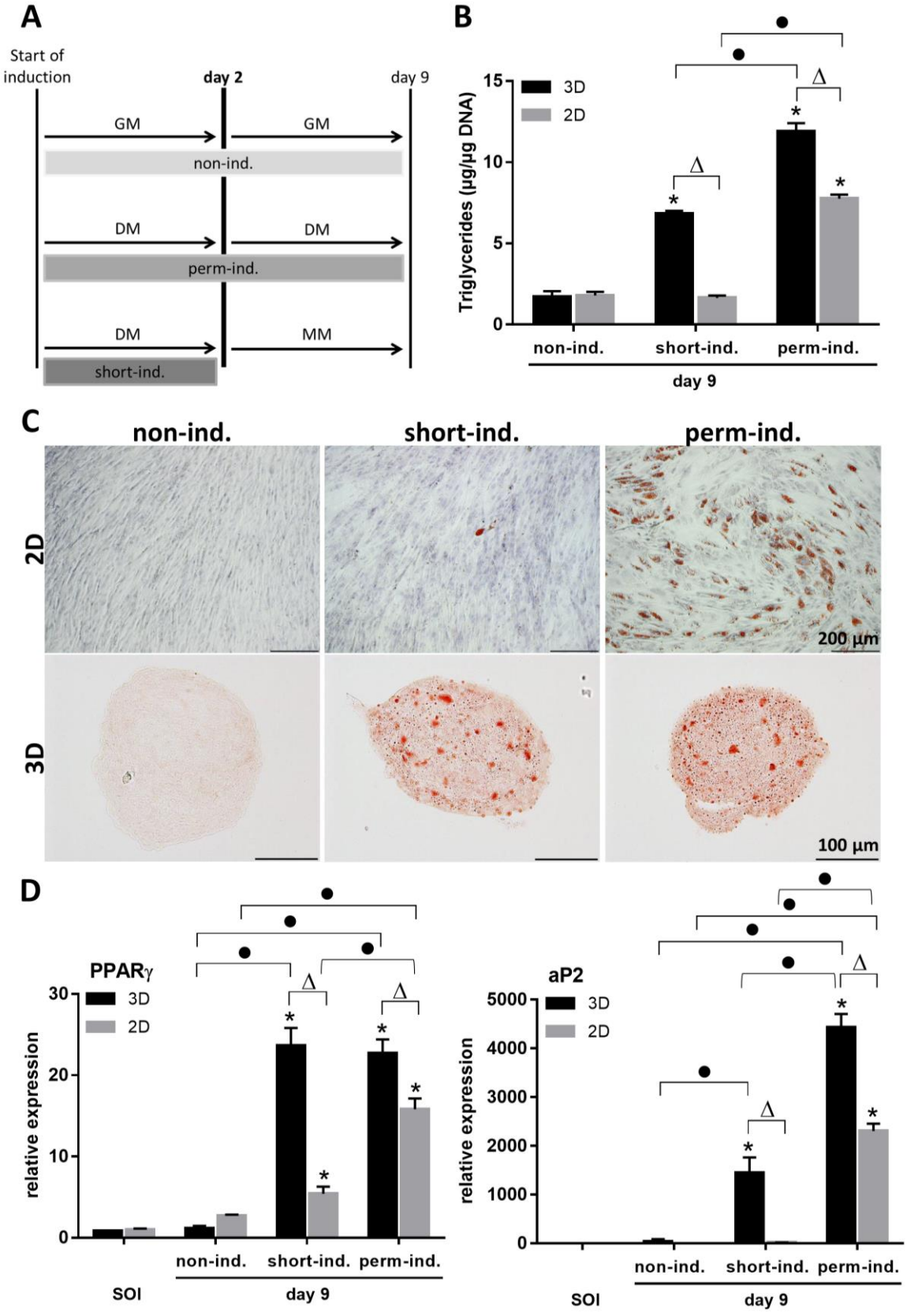

(Figure legend on the next page.)

Figure 4.10: Characterization of adipogenic differentiation of ASCs in 2D monolayer and 3D spheroid culture with different induction protocols (permanent and short-term induction).
A) Experimental setup: Adipogenic differentiation was induced two days after cell seeding (start of induction). For permanent induction (perm-ind.) cells were continuously treated with differentiation medium (DM) for nine days. For short-term induction (short-ind.) cells were treated with DM for two days, followed by maintenance medium (MM) until the end of the experiment. Non-induced controls (non-ind.) were cultured in growth medium (GM) during the whole culture time. **B)** Triglyceride content of ASCs under 2D and 3D culture conditions after nine days of short-term vs. permanent induction. Non-induced 2D monolayers and 3D spheroids served as controls. Triglyceride content was normalized to the DNA content of the respective samples. Values are expressed as mean with standard deviation (n=3). Statistically significant differences ($p < 0.05$) to the non-induced control group (non-ind., 3D and 2D culture, respectively) are indicated by *, between 2D and 3D culture under the same induction condition by Δ, and significant differences between permanent and short-term induction within a culture condition group are indicated by ●. **C)** Histological staining (Oil Red O) of accumulated triglycerides in 2D monolayers and 3D spheroids treated with permanent or short-term induction. Non-induced monolayers and spheroids served as controls. Images from 2D monolayers were taken at a 10-fold magnification; scale bars represent 200 µm. Cryosections of 3D spheroids were imaged with a 20-fold magnification; scale bars represent 100 µm. **D)** The expression of the adipogenic marker genes PPARγ and aP2 was determined by qRT-PCR for cells of 2D monolayers and 3D spheroids. Gene expression was normalized to EF1α; the obtained values were further normalized to 2D monolayer at the start of induction. Values are expressed as mean with standard deviation (n=3). Statistically significant differences ($p < 0.05$) to the start of induction (SOI, 3D and 2D culture, respectively) are indicated by *, between 2D and 3D culture under the same induction condition by Δ, and significant differences between the different induction conditions at day 9 within a culture condition group are indicated by ●.

Overall, these results demonstrated that ASCs cultured as 3D spheroids required a shorter stimulus to undergo adipogenic differentiation and possess higher differentiation potential compared to ASCs in conventional 2D monolayer culture.

4.2.4 Adipogenic differentiation of ASC-derived spheroids after early and late onset of induction

In order to further improve the precultivation regime for the application of spheroids in adipose tissue engineering, we varied the time point for adipogenic induction. For this purpose, cell aggregates were induced during the assembly process (7 hours after seeding) or after final compaction (2 days after seeding), with either the short-term induction or the permanent induction regime. The application of the adipogenic hormonal cocktail during assembly did not impact the compaction process of the spheroids (Figure 4.11).

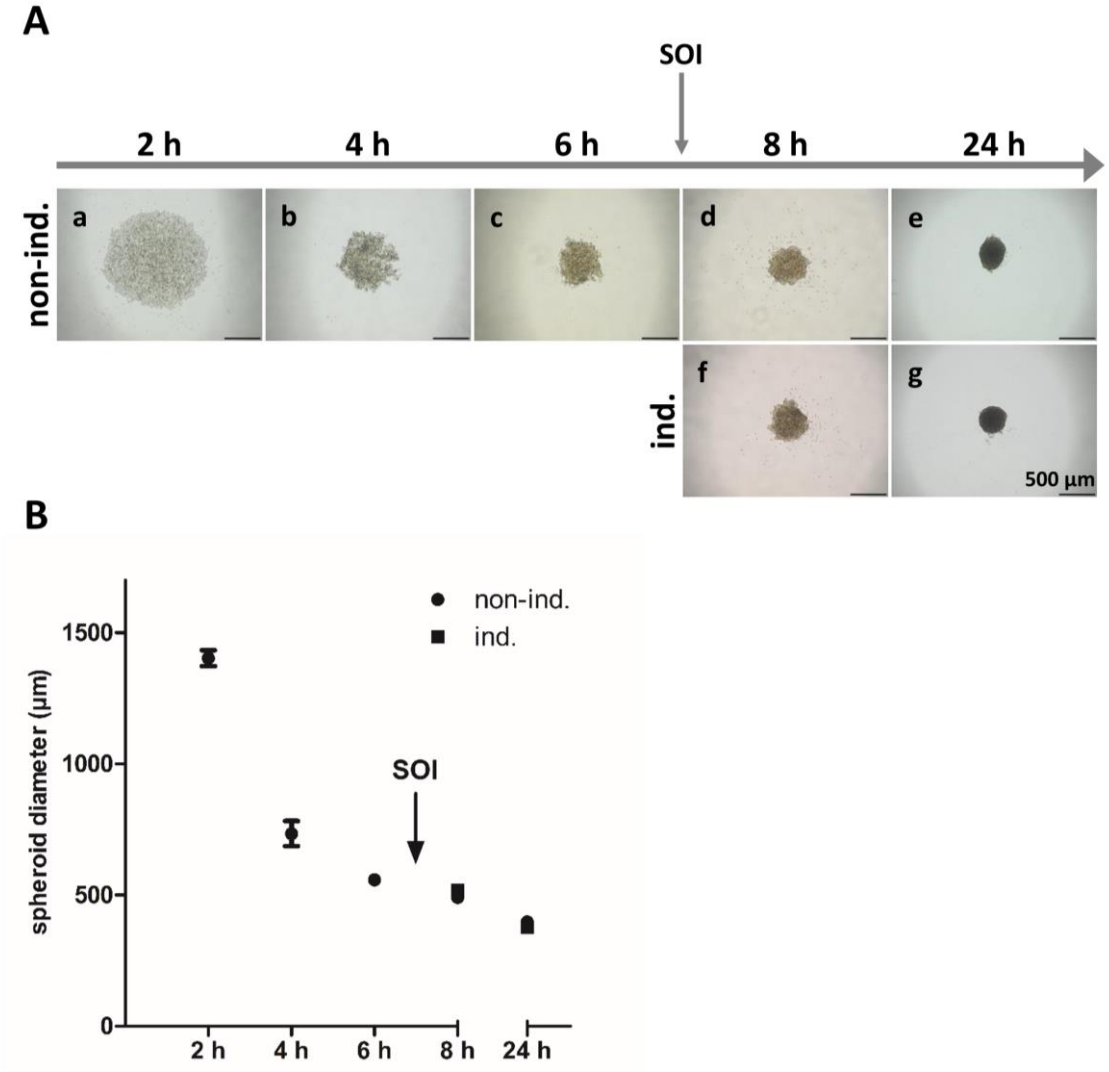

Figure 4.11: Spheroid formation with adipogenic induction during the assembly process.
A) Morphology of ASC aggregates during spheroid formation. Light microscopy images were taken at various time points after seeding (between 2 and 24 h). Spheroids were adipogenically induced at 7h after seeding (SOI) by adding adipogenic inducers to the culture medium of 3D spheroids (ind.). Spheroids cultured in growth medium served as controls (non-ind.). Images were taken at a 4-fold magnification; scale bars represent 500 µm. **B)** Assessment of decreasing spheroid diameter during assembly in induced vs non-induced spheroids. Values are expressed as mean with standard deviation (n=4).

Histological staining of accumulated triglycerides with Oil Red O indicated differentiation along the adipogenic lineage of ASC-derived spheroids both under short-term and permanent induction regardless of the time point of induction (Figure 4.12 A). The quantification of accumulated triglycerides confirmed the histological observations and indicated that the differentiation capability of ASC-derived spheroids induced during assembly (after 7 h) was even significantly enhanced compared to the induction of fully compacted spheroids (induced after 2 days) (Figure 4.12 B).

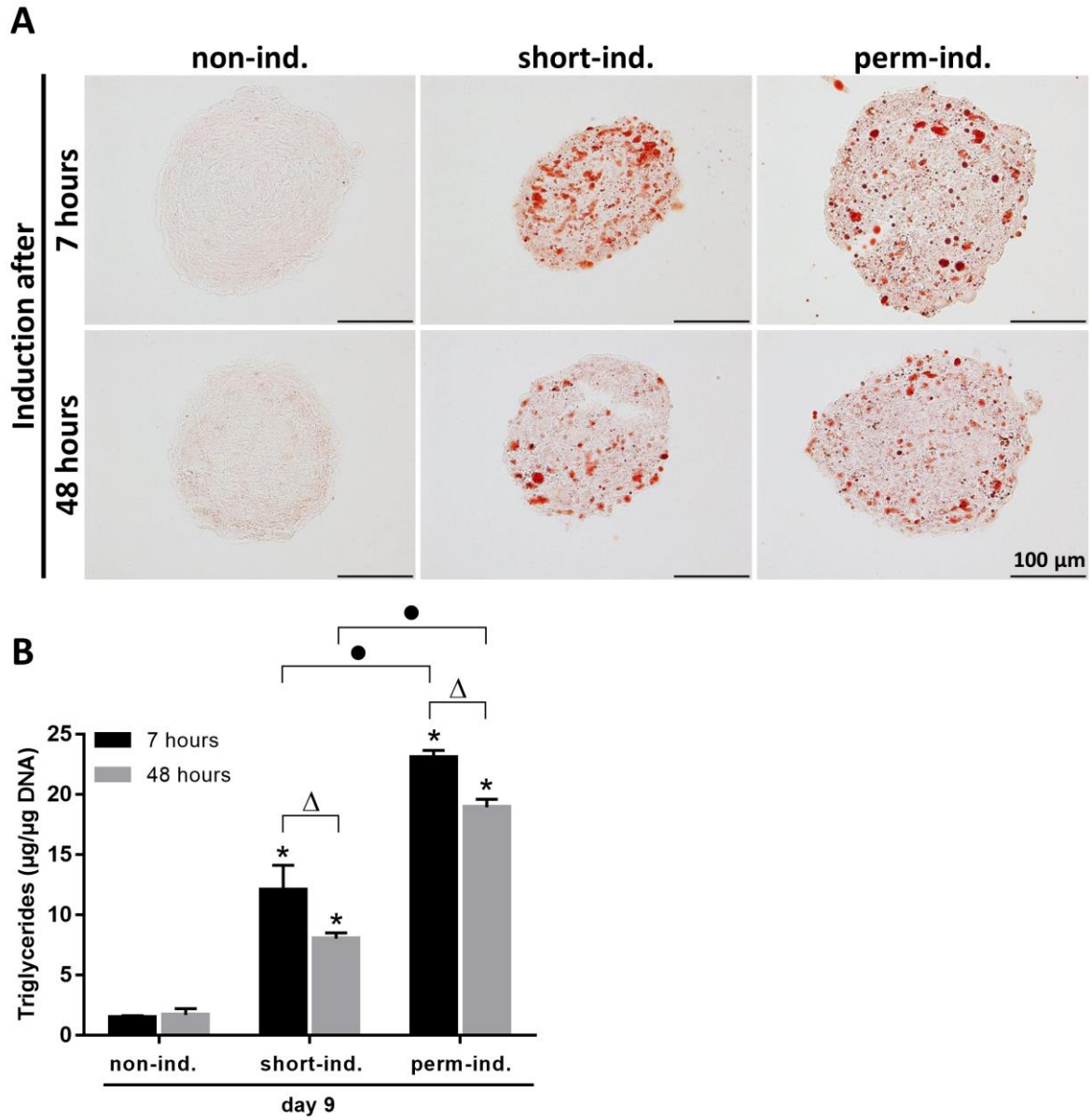

Figure 4.12: Adipogenic differentiation of 3D spheroids with different starting time points of induction. Spheroids were induced after final assembly and compaction (48 hours after seeding) or during the assembly process (7 hours after seeding) and treated with short-term or permanent induction. **A)** Histological analysis of adipogenic differentiation was performed after nine days of induction. Cryosections of short-term induced and permanent induced 3D spheroids were stained with Oil Red O to visualize accumulated triglycerides. Non-induced spheroids served as control. Scale bars represent 100 µm. **B)** Quantitative analysis of triglyceride content after induction at different stages of assembly (7h, 48h). Analysis was performed at day 9. Spheroids were induced according to the short-term and permanent induction protocol. Non-induced samples served as control. Triglyceride contents were normalized to the DNA content of the respective samples. Data represents mean with standard deviation (n=3). Statistically significant differences ($p < 0.05$) to the non-induced control group are indicated by *, between groups with different starting point of induction under the same induction condition by Δ, and significant differences between permanent and short-term induction are indicated by ●.

4.2.5 Discussion

Spheroids generated from adipose stromal/stem cells appear eminently suited as building blocks for adipose tissue engineering as they are based on a readily available cell source and can be implanted as microtissues with cells residing and interacting within their endogenous ECM, which in general has been reported to enhance cell survival, cell retention and functional performance after transplantation (123,125,187). However, with regard to adipose tissue engineering ASC spheroids have been rarely investigated and the in-depth characterization of these 3D microtissues in this context is missing so far. Thus, in this study we specifically addressed the ECM composition and remodeling in ASC spheroids, investigated different culture regimes for effective adipogenic induction, and demonstrated the suitability of these cell aggregates to build adipogenic microtissues upon a short adipogenic stimulus.

For spheroid production, the liquid overlay technique (188,189) was used to generate spheroids of reproducible size and shape. According to the specific demands on the extracellular environment of differentiating cells, their ECM constantly undergoes dynamic changes and therefore has been supposed to play also a critical role for the differentiation process itself (60,105). To date the composition and remodeling of the ECM during the adipogenic differentiation process has been investigated in 2D cultures for bone marrow-derived MSCs, 3T3-L1 preadipocytes, and bovine intramuscular preadipocytes (59,109,184,190,191). We have now sought for the first time to elucidate the ECM composition and development in ASC spheroids, which as 3D culture displays the ECM in a more in vivo-like setting compared to conventional 2D culture. In finally compacted, undifferentiated spheroids, fibronectin and collagen I and VI were found to be the most prominent ECM components, thus in these undifferentiated cellular aggregates the ECM displayed a stromal character, while adipose-specific components like laminin or collagen IV were hardly detectable.

Upon hormonal induction, ASC spheroids were shown to differentiate effectively along the adipogenic lineage within nine days. During adipogenesis, ECM remodeling was evident with the development of typical features of an adipose-specific extracellular matrix with collagen IV and laminin being abundantly present as major parts of the adipocyte basement membrane (79,104). Also, for collagen I and VI an increased signal was shown in differentiated 3D spheroids compared to their undifferentiated counterparts. This is in accordance with studies in 2D cultures reporting an increase of collagen VI during the differentiation process of hMSCs (109,184). Collagen VI is a non-fibrillar collagen, distributed widely in tissues, that forms thin

microfilaments and binds to various other ECM components, including collagens I, II and IV, and FN (104). Collagen I as part of the supporting ECM framework was previously described in adipogenically differentiated hMSCs (59). In the present study, fibronectin, which represented an integral part of the ECM in undifferentiated spheroids, was only marginally expressed in differentiated spheroids. This data is consistent with studies using 3T3 preadipocytes that reported a degradation of fibronectin during adipogenesis in 2D cultures of these cells (108).

In order to prove the resemblance of the generated adipogenic 3D microtissues to human native fat, a comparison regarding the expression of the investigated ECM components was conducted using human abdominal fat tissue samples. A distinct match in the ECM composition between native tissue samples and spheroid-based microtissues was evident with collagen I, IV, VI, and laminin expression verified both in native tissue and in vitro generated microtissues. As in native human fat tissue, fibronectin was only marginally part of the ECM in differentiated spheroids. Overall these findings underlined the similarity of native fat tissue and in vitro fabricated adipogenic microtissues with regard to the tissue-specific ECM composition.

In an attempt to delineate the time course of ECM remodeling during adipogenesis laminin deposition as a key component of the adipose ECM was investigated. Laminin is an integral part of the basement membrane surrounding differentiated adipocytes (107). In the spheroids, laminin deposition was evident in the course of adipogenesis with increasing signal intensity. Interestingly, onset of laminin production was observed at very early time points in the differentiation process (2 days after induction) and preceded the generation of lipid droplets. Laminin has been reported to promote adipogenic differentiation in 2D culture on laminin-coated substrata as shown with a MSC cell line (D1-Cells) and primary porcine preadipocytes (192,193). Laminin alpha 4 null mice exhibited a decreased capacity for adipose tissue expansion and weight gain underlining the role of laminin in adipose tissue development and function (194). Immunohistochemical studies in pig embryos demonstrated an association of laminin expression with the earliest phases of adipocyte development during embryogenesis indicating a role of laminin in the very early stage of the adipogenic differentiation process (195). Thus, the observed deposition of laminin at the onset of the differentiation process in the ASC spheroids may trigger and sustain adipogenesis and contribute to the superior differentiation capability of spheroids.

For the use of the ASC spheroids as building blocks for adipose tissue engineering applications, an efficient adipogenic induction leading to effective differentiation is desirable.

Well in line with other studies on adipogenic differentiation of ASC spheroids (150,164,196), we observed an enhanced differentiation capability of our spheroids, as cells in spheroids revealed a significantly elevated triglyceride storage and expression level of two major adipogenic marker genes compared to cells in 2D monolayer. Besides the enhanced triglyceride storage in spheroids under permanent induction, we demonstrated that applying a short-term induction protocol with addition of the adipogenic hormonal cocktail for only two days led to effective differentiation in the spheroid culture. 2D cultured cells failed to differentiate under these conditions. Thus, in the 3D setting with cells embedded within their own matrix, less (shorter) stimulus was required to trigger and sustain the adipogenic differentiation cascade compared to conventional 2D culture.

To date, there is no evidence about the precise mechanism that drives the enhanced differentiation in 3D culture. As discussed above, the demonstrated early expression of laminin in the spheroids may contribute to the sustainment of adipogenesis upon a short induction stimulus. Another factor contributing to the superior differentiation capability may be the high cell density in spheroids. Gap junction-mediated intercellular communication, which is favored in high density cultures, was shown to positively impact adipogenesis in ASCs (197). Furthermore, the morphology of cells and mechanophysical properties of spheroids appear to be favorable for adipogenic differentiation as cells in spheroids exhibit a small, rounded phenotype and are embedded in an environment of neighboring cells and ECM, which has been reported to be characterised by a low elastic modulus of less than 0.1 kPa, two factors also known to positively influence adipogenic differentiation of cells (123,198,199).

In order to determine the optimal time point for an efficient induction, spheroids were adipogenically induced during the assembly (after 7 hours) before reaching their final size and after full compaction (after 2 days). Interestingly, the differentiation of spheroids induced during assembly was improved over spheroids induced after compaction. As after 7 hours of spheroid assembly, the compaction process has not been finished, a higher permeability for the hormonal inducers may be likely. Using a low-molecular weight fluorescent dye, Lin et al. demonstrated that the penetration of small molecules to the core of cell aggregates was only possible during early stages of assembly (140). Overall, priming of the cells towards the adipogenic lineage by adipogenic precultivation has been shown to be advantageous for fat formation in vivo (185,200). As ASC spheroids require only a short induction period combined with a feasible early induction onset (7 h after seeding), with the use of spheroids in a clinical

setting the cost-intensive in vitro precultivation time span necessary to trigger adipogenic differentiation in vivo may be minimized.

In conclusion, during adipogenic conversion the ECM of ASC spheroids was observed to be remodeled from a stromal to an adipose-specific pattern with the ECM remodeling starting at very early time points and preceding the accumulation of lipid droplets. The observed resemblance of the ECM composition to native fat tissue may provide a valuable 3D model to further characterize the functional relationship between ECM composition and cellular behavior in a more in vivo-like context, which could also be beneficial in studies regarding obesity research. For adipose tissue engineering approaches, ASC spheroids appear to be predestined candidates as prefabricated, material-free modules with cells in their own tissue-specific matrix. The superior differentiation capability and the need for only a short induction stimulus renders them attractive for potential clinical application. Further research should include the combination of ASC spheroids with delivery vehicles such as hydrogels or specifically designed scaffolds. Recent biofabrication concepts including the automated assembly of preformed micro-tissues within a 3D plotted polymer scaffold (201) or the seeding of thin-fiber melt electrowritten scaffolds with cellular spheroids generating sheet-like structures (202) may be applied to adipose tissue engineering.

4.3 The influence of laminin α4 synthesis on the differentiation capability of ASCs

For a long time, the extracellular matrix (ECM) was thought to act only as a scaffold with the main function of sustaining tissue and organ structure. In recent years, however, it was recognized that the ECM plays also a functional role in numerous cellular processes (61). As part of the complex communication network of cells in their tissue-specific environment, the ECM greatly influences their innate properties including cell proliferation, survival, differentiation and morphogenesis (166,167). Therefore, the development of a tissue-specific ECM is an intrinsic feature which must be considered as an important requirement in tissue engineering approaches. As already shown in chapter 4.2 of this thesis, the 3D spheroid ASC differentiation system meets this requirement, because the ECM that is formed under these conditions resembles in its composition and structure the ECM of native fat tissue.

The differentiation of preadipocytes into mature, lipid-laden adipocytes is accompanied by drastic morphological changes from a fibroblastic spindle-like to a spherical cell shape. This morphological change is accompanied by several changes to the expression of individual ECM components and structural changes of the ECM. Thus, the development of the ECM from a fibrillar to a laminar structure takes place during adipogenic differentiation including a strong upregulation of major basement membrane components (79). Laminin and type IV collagen represent the major part of the basal lamina, which surrounds each adipocyte in a dense sheet-like structure which protects the surrounded adipocytes from mechanical stress and disruption. Therefore the basement membrane is considered to be a requirement for the survival of mature adipocytes (107). Due to their drastic morphological alteration, differentiating cells have to remodel their surrounding ECM during adipogenesis, while the ECM components, in turn, also influence the differentiating cells via interaction with cellular receptors (9,54,58). The data presented in the previous chapter shows that laminin is deposited in the extracellular space during an early stage of adipogenesis. Based on the data from chapter 4.2, which described a superior differentiation capability and the sustainment of adipogenesis upon a short induction stimulus for ASCs of 3D spheroids, one can hypothesize that the early expression of laminin may contribute to this fact. Since to date there is no evidence about the precise mechanism that drives the enhanced differentiation in 3D culture this hypothesis was examined in more detail below.

In order to further confirm the hypothesis that the early expression of laminin contributes to the improved differentiation capability of ASCs in the 3D context, first the composition of

the ECM with respect to laminin isoforms was analyzed in differentiating 2D and 3D spheroid cultures. As the literature describes an pro-adipogenic mode of action for laminin (192), a second set of experiments addressed whether this also applies to ASCs in 2D and 3D differentiation cultures and whether laminin expression by ASCs is a requirement for adipogenesis under these culture conditions. Therefore, a shRNA targeting approach was used to investigate the effect laminin knockdown (KD) in ASCs on their adipogenic differentiation.

Laminin is a heterotrimeric glycoprotein and exists in numerous isoforms according to the composition of the three different polypeptide chains, referred to as α, β and γ (112,203). So far, five α, three β and three γ chains have been identified in vertebrates, which can be assembled into at least 18 different laminin αβγ heterotrimers (92). The expression of the alpha chain is an important determinant of the tissue specificity of the laminin isoforms. Accordingly, laminins containing the α4 chain are specific for cells of mesenchymal origin (100). This includes also laminin-8, which belongs to the main constituents of the ECM in white adipose tissue (101). In addition, the alpha chain of the heterotrimeric glycoprotein is the largest isoform and it is responsible for the interaction with cellular receptors such as integrins and dystroglycans. These interactions in turn influence various cellular processes such as proliferation, differentiation, adhesion, and migration (98). For these reasons, the laminin α4 chain encoding gene *LAMA4* was knocked down by shRNA-mediated gene silencing. After conformation of a stable *LAMA4* KD, the effect of the KD on the adipogenic differentiation of the cells was analyzed. The overall aim of the work presented in this chapter was to contribute to a better understanding of how extracellular components such as laminin are involved in differentiation and therefore start to understand the precise mechanism that drives the enhanced adipogenesis under 3D culture conditions.

4.3.1 Early and sustained deposition of laminin in the ECM of differentiating 3D spheroids

In order to clarify the expression of laminin in 3D spheroids in comparison to conventional 2D monolayers during the course of differentiation, ASCs of both culture conditions were differentiated along the adipogenic lineage using the permanent and short-term induction protocol described in chapter 4.2. Non-induced ASCs, cultured in growth medium served as controls. The laminin deposition in the extracellular space of ASCs in 2D monolayers and 3D spheroids was analyzed by immunohistological staining of ASC cultures before adipogenic differentiation (SOI) as well as after two and nine days of differentiation. Please note that after

two days of induction no short-term treated cells were assessed since all treatment-protocols include culture of cells in adipogenic differentiation medium up to this time point.

Before starting culture of cells in adipogenic differentiation medium no laminin was detected in the ECM of 2D monolayer cultures and in the ECM of 3D spheroid cultures. After nine days of differentiation in the presence of adipogenic differentiation medium (perm-ind.) both in the ECM of 2D monolayers and in the ECM of 3D spheroids a strong increase in the laminin signal was detected (Figure 4.13). In the control cells that were treated with growth medium for nine days a faint laminin signal was detected in 3D spheroids, while in the respective 2D monolayer control cultures no laminin in the extracellular space was detected. In the ECM of short-term induced monolayers laminin was only barely detectable and surrounded only a few cells, while in 3D spheroids a strong laminin signal was observed throughout the spheroid. One further difference between the laminin development in 3D spheroids and 2D monolayers was observed much earlier in the differentiation process. While in the ECM of 2D monolayers no laminin was detectable at all after two days of induction, a strong laminin accumulation in the respective 3D spheroids was already observed in this early stage of adipogenic differentiation (highlighted with the red box in Figure 4.13). The early expression of laminin in the extracellular space of 3D spheroids may contribute to the sustained adipogenic differentiation of these cultures after short-term induction.

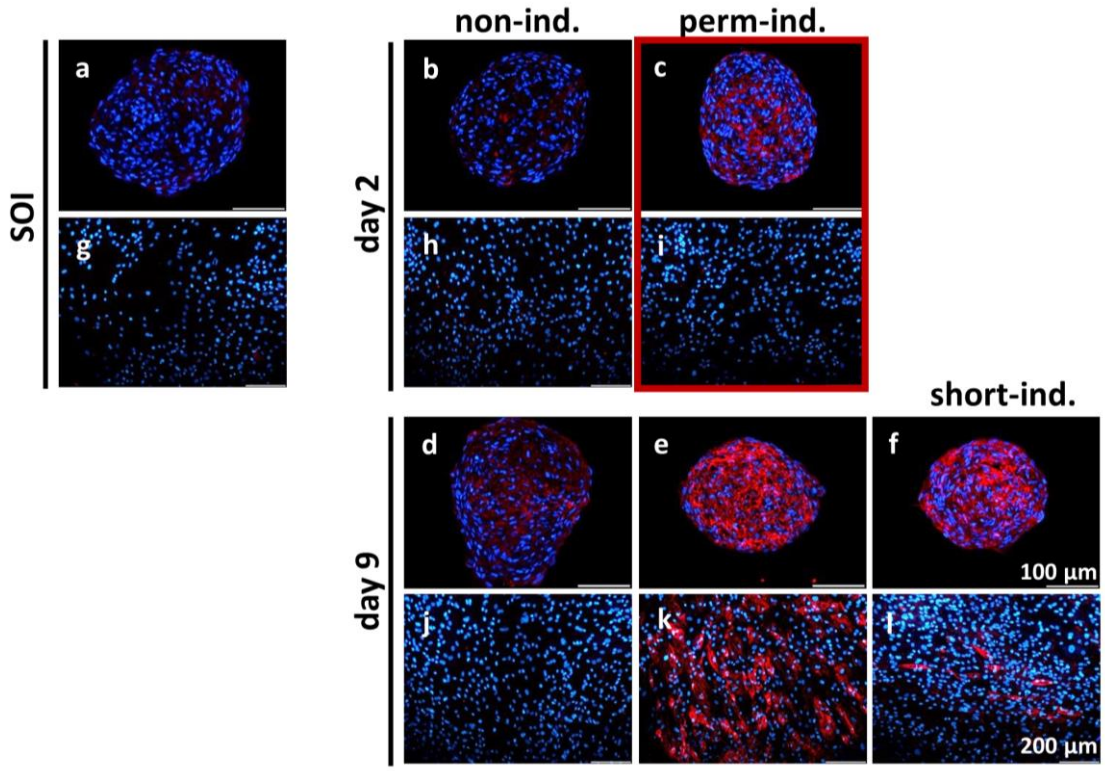

Figure 4.13: Deposition of extracellular laminin at different time points of adipogenic differentiation in ASC 3D spheroids and 2D monolayer cultures.

Overlay fluorescence images of laminin (red) and 4´,6-diamidino-2-phenylindole (DAPI) nuclear counterstain (blue) from 8 µm cryosections of 3D spheroids (a-f) and 2D monolayers (g-l). Immunostaining was performed on ASC cultures that were differentiated following the two different induction protocols described in chapter 4.2: permanent induction (perm-ind.) and short-term induction (short-ind.). Extracellular laminin was stained in fixed cultures at the start of induction (SOI), as well as after two and nine days of differentiation. 3D spheroids an 2D monolayers which were cultured in basal medium during the whole experiment served as controls (non-ind.). Images from 2D monolayers were taken at a 10-fold magnification; scale bars represent 200 µm. Cryosections of 3D spheroids were imaged with a 20-fold magnification; scale bars represent 100 µm.

4.3.2 shRNA-mediated knockdown of the laminin α 4 encoding gene *LAMA4*

To analyze the influence of laminin on the adipogenic differentiation of ASCs, the expression of the laminin α4 chain as essential component of the adipose-tissue specific laminin-8 heterotrimer, was knocked down by shRNA-mediated gene silencing. To this end ASCs were transduced with three different retroviral vectors (A, B, C) which each coded for a different *LAMA4*-specific shRNA. These different shRNAs were designed to target multiple splice variants in the *LAMA4* gene transcript. Transduction with a vector coding for a non-specific scrambled 29mer sequence served as control.

Puromycin selection of transduced cells was used to select for stably expressing cells. To verify the knockdown efficiency, relative expression of the target gene was determined by qRT-PCR from total RNA that was prepared from ASCs transduced with the target specific shRNAs and control vector. Expression levels of the shRNA transduced cells are presented relative to the the expression levels of scrambled control vector transduced cells (Figure 4.14). The data show that expression of all three *LAMA4*-specific shRNA vectors A, B and C led to a knockdown of the target gene. With a knockdown efficiency of around 70%, the greatest silencing effect was achieved with construct A. For the target specific constructs B and C, the knock down efficiency reached almost 50%. To proof specificity of the *LAMA4*-specific shRNA vectors, the relative expression of *LAMA4*-related genes laminin β1 (*LAMB1*) and laminin γ1 (*LAMC1*), was assessed. The data presented in Figure 4.14 show that the expression of these two genes in the transduced cells remained unaffected, the specificity of the three target specific shRNA constructs A, B and C was therefore confirmed.

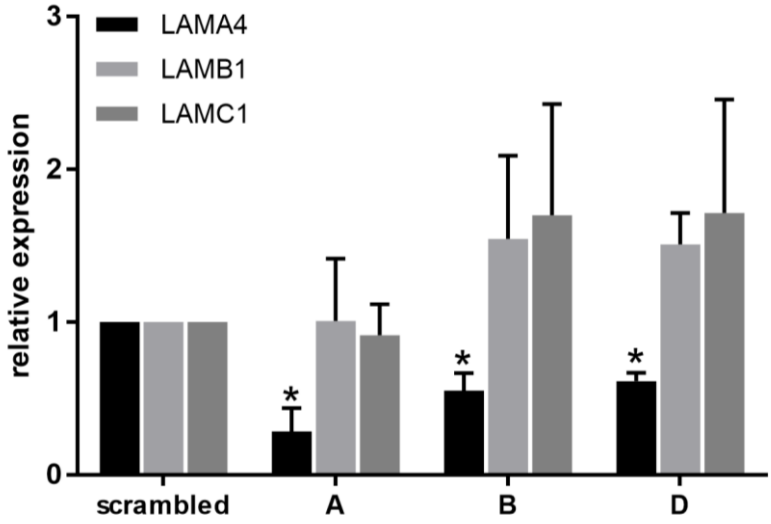

Figure 4.14: shRNA-mediated gene silencing of *LAMA4*.

Relative expression of LAMA4, LAMB1 and LAMC1 in ASCs transduced with three different LAMA4-specific retroviral shRNA vectors A, B and C. Total RNA was prepared seven days after retroviral transduction of ASCs. Gene expression was normalized to EF1α as housekeeping gene. Expression levels were expressed relative to that of cells transduced with the sample control vector. Values are expressed as mean with standard deviation (n=3). *Statistically significant differences ($p < 0.05$) between ASCs transduced with LAMA4-specific shRNA constructs and the scrambled control.

4.3.3 Effect of *LAMA4* knockdown on the adipogenic differentiation of ASCs

After an efficient knockdown with *LAMA4*-specific shRNA constructs was confirmed, the influence of *LAMA4* silencing, on the adipogenic differentiation of ASCs was analyzed. Therefore, ASCs transduced with the three *LAMA4*-specific shRNA vectors as well as with the scrambled control vector were differentiated by culturing the cells in adipogenic differentiation medium for 14 days. Non-induced cells cultured in growth medium served as controls. For the qualitative evaluation of the adipogenic differentiation of ASCs with a *LAMA4* knockdown, cells in 3D spheroid and in 2D monolayer cultures were compared. The qualitative results of the Oil Red O staining for accumulated triglycerides are shown in Figure 4.15 A. Both under 2D and 3D culture conditions, ASCs with a shRNA-mediated *LAMA4* knockdown differentiated at least as well as the respective scrambled control. No differences in the adipogenic differentiation efficiency were observed between 3D spheroids and 2D monolayers, which was also not to be expected under permanent induction conditions. Accumulating triglycerides were not observed in the non-induced controls (data not shown). Due to the limited number of transduced ASCs, a simultaneous examination of the adipogenic differentiation under short-term induction conditions could not be performed.

The low yield of transduced cells was also the reason why further quantitative evaluation of the differentiation capability was restricted to 2D monolayer cultures. For the 2D monolayer culture the results of the histological examination via Oil Red O staining were also confirmed by the quantitative analysis of the accumulated triglycerides (Figure 4.15 B). Furthermore, the relative expression of two major adipogenic marker genes *PPARγ* and *CEBPα* (Figure 4.15 C) were determined by qRT-PCR and confirmed the results obtained from histology and triglyceride accumulation analyses of 2D monolayers. Taken together, these results indicate that the knockdown of *LAMA4* expression alone has no adverse effect on the adipogenic differentiation of the ASCs.

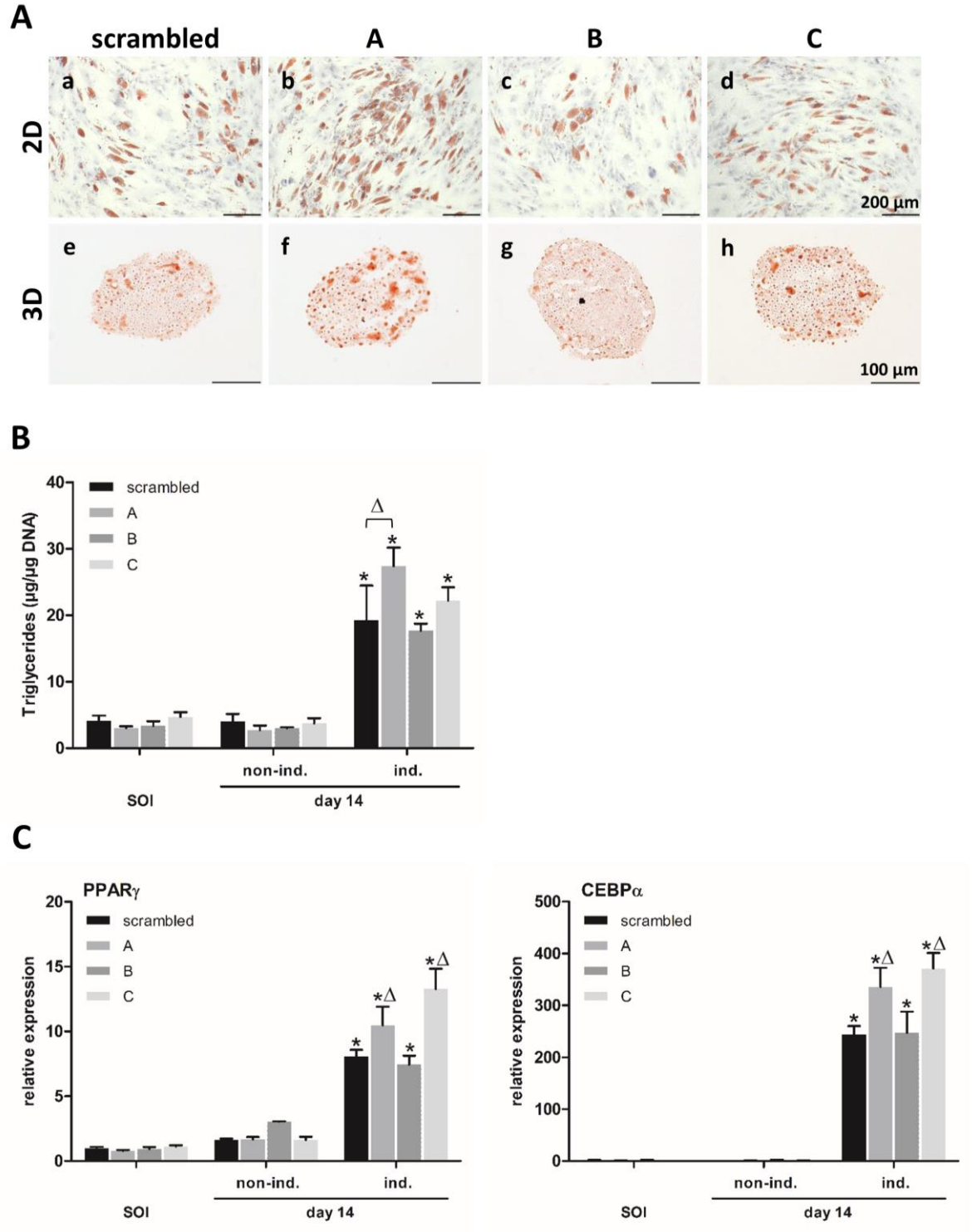

Figure 4.15: Influence of the *LAMA4* knockdown on the adipogenic differentiation.

Adipogenic differentiation was induced two days after seeding the cells either as 2D monolayers or 3D spheroids (Start of induction; SOI). For *LAMA4* knockdown ASCs were transduced with three vectors (A, B or C) coding for the different *LAMA4* –specific shRNAs and one scramble control vector. Transduced cells under both culture conditions were continuously cultured with adipogenic differentiation medium containing puromycin as antibiotic selection marker for transduced cells, according to the permanent induction protocol described in chapter 4.2, until harvest after 14 days. **A)** Histological analysis of accumulating triglycerides by Oil Red O staining of

differentiating 2D monolayers and 8 µm cryosections of 3D spheroids, respectively. Images from 2D monolayers were taken at a 10-fold magnification; scale bars represent 200 µm. Cryosections of 3D spheroids were imaged with a 20-fold magnification; scale bars represent 100 µm. **B)** Triglyceride content of transduced ASCs under 2D culture conditions. Quantitative analysis of adipogenic differentiation was performed after 14 days of culture in differentiation medium. Non-induced 2D monolayers served as controls. Triglyceride content was normalized to the DNA content of the respective samples. Data represents mean with standard deviation (n=3). *Statistically significant differences ($p < 0.05$) between induced 2D monolayers and the respective non-induced control as well as the 2D monolayer at the start of induction (SOI). Δ Statistically significant differences between induced 2D monolayers transduced with one of the three LAMA4- specific shRNAs or the scramble control. **C)** The expression of two adipogenic marker genes PPARγ and CEBPα was determined by qRT-PCR for cells of 2D monolayer cultures. Gene expression was normalized to EF1α as a housekeeping gene; the obtained values were further normalized to 2D monolayers transduced with the scrambled control vector at the start of induction (SOI). Values are expressed as mean with standard deviation (n=3). *Statistically significant differences ($p < 0.05$) between differentiating 2D monolayers and the respective non-differentiating control as well as the 2D monolayer at the start of induction. Δ Statistically significant differences between induced 2D monolayers transduced with one of the three target specific shRNAs and the induced scramble control.

4.3.4 Verification of *LAMA4* knockdown stability during adipogenic differentiation

Since the data of the previous section show that the knockdown of *LAMA4* expression had no adverse effect on the adipogenic differentiation capability of the cells, one could assume that despite the addition of puromycin for the selection of transduced cells, the knockdown did not remain stable during the 14-days differentiation period. To verify the stability of the knockdown during the time course of adipogenic differentiation, the relative expression of *LAMA4* was analyzed after 14 days of culture in adipogenic differentiation medium by qRT-PCR. For this purpose, total RNA was harvested from the transduced 2D monolayers directly before the start of adipogenic induction, as well as after 14 days of differentiation. The respective non-induced monolayers from each group served as controls. As shown in Figure 4.16, *LAMA4* expression was reduced during adipogenic differentiation in cells that expressed any of the three target-specific shRNA constructs. Thus, the knockdown remained stable also during the differentiation process. Only for ASCs transduced with construct B a slight increase in *LAMA4* expression was observed in the respective non-induced control at day 14 compared to the start of the experiment.

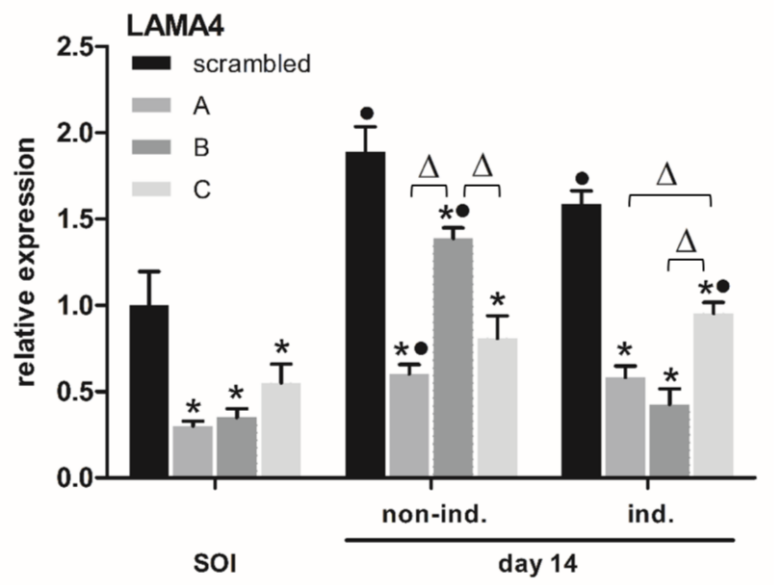

Figure 4.16: shRNA-mediated gene silencing of *LAMA4* during adipogenic differentiation.
Relative expression of LAMA4 in ASC 2D monolayers transduced with three different *LAMA4*-specific shRNA constructs A, B or C during 14 days of adipogenic differentiation. Total RNA was harvested right before the start of induction (SOI) as well as after 14 days of adipogenic differentiation. Non-induced 2D monolayers transduced with the respective shRNA constructs, cultured in growth medium during the whole experiment, served as controls. Gene expression was normalized to EF1α as housekeeping gene. Expression levels were expressed relative to that of cells transduced with the sample control vector at the start of induction (SOI). Values are expressed as mean with standard deviation (n=3). Statistically significant differences ($p < 0.05$) between the target specific shRNA constructs and the scrambled control at the SOI as well as under the same induction condition after 14 days are indicated by *. ● indicates statistically significant differences ($p < 0.05$) within one group of shRNA construct between 14 days of culture (non-ind. and ind., respectively) and the SOI. Statistically significant differences ($p < 0.05$) between the different target-specific shRNA constructs under the same induction condition are indicated by Δ.

4.3.5 Effects of the shRNA-mediated *LAMA4* gene knockdown on protein level

After it was shown that the *LAMA4* gene expression knockdown was stable during 14 days of adipogenic differentiation, it was further investigated in a first approach whether this gene silencing effect also has an impact on protein expression of total laminin. The aim was to examine whether a reduced expression of the α4 laminin encoding gene also results in a reduced expression of total laminin on protein level. For this purpose, the extracellular laminin was immunohistologically analyzed after 14 days of adipogenic differentiation for the transduced ASCs cultured as 3D spheroids (Figure 4.17). A strong laminin signal was detected in the ECM of differentiated spheroids transduced with the *LAMA4* specific shRNA constructs A and C,

which was comparable to that of the scrambled control spheroids. In the spheroids consisting of differentiated ASCs transduced with construct B, the detected laminin signal was slightly increased compared to the respective non-induced control, but it was markedly reduced in comparison to the differentiated ASC-based spheroids transduced with construct A and C, as well as the scrambled control. However, the reduced laminin level in construct B spheroids was not accompanied by a simultaneous reduction of the adipogenic differentiation capacity of the 3D-cultured cells, since both the qualitative and quantitative determination of the stored triglycerides presented in the previous section showed that also ASCs transduced with construct B efficiently differentiated along the adipogenic lineage.

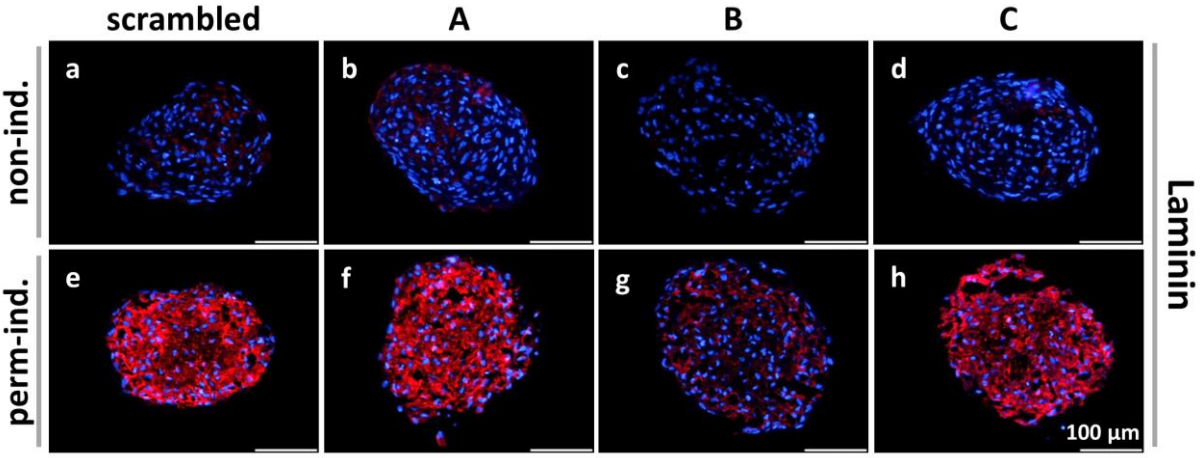

Figure 4.17: Effects of the shRNA-mediated *LAMA4* gene silencing on protein level.
Overlay fluorescence images of laminin (red) and 4´,6-diamidino-2-phenylindole (DAPI) nuclear counterstain (blue) 8 µm cryosections of 3D spheroids consisting of ASCs transduced with one of three *LAMA4*-specific shRNA-constructs A, B, C or the scrambled vector as control. Immunostaining of total laminin was performed after 14 days of adipogenic differentiation following the permanent induction protocol. 3D spheroids from the respective group which were cultured in growth medium during the whole experiment served as controls (non-ind.). Cryosections of 3D spheroids were imaged with a 20-fold magnification; scale bars represent 100 µm.

These results led to the assumption that a decreased expression of the gene encoding the α4 chain of laminin has no effect on total laminin protein expression. Only for cells that were transduced with shRNA vector B, somewhat reduced total laminin protein levels were observed. Further work is needed to further analyze the effect of reduced *LAMA4* gene expression on total laminin protein expression. This includes the specific detection of the α4 chain of the laminin heterotrimer on protein level as well as the quantification of the synthesized laminin, for example by Western blot analyses.

4.3.6 Discussion

As a necessity for the viability of mature adipocytes, the laminin-rich basement membrane develops during the differentiation along the adipogenic lineage. This basement membrane not only forms a structural supporting framework to which adipocytes adhere, but it also affects adipocyte properties (60,79,115). In order to contribute to a better understanding of how specifically laminin, influences cellular processes including differentiation, laminin expression and its influence on adipogenic differentiation of ASCs was examined in more detail in this part of the thesis. From the observations of the previous chapter the hypothesis emerged, that early expression of laminin contributes to the improved adipogenic differentiation capability of the ASC 3D spheroid cultures, and that laminin deposition in general is a prerequisite for the adipogenic differentiation of ASCs, independent of the culture method. To explore this hypothesis further, the focus was first on the deposition of laminin during the ASC differentiation in 2D monolayer or 3D spheroid cultures.

The immunohistological analyses showed that both under 2D and 3D culture conditions, the laminin in the extracellular matrix of cells was highly enriched after nine days of adipogenic differentiation. This observation coincides with reports from the literature, where laminin was also only detectable in the extracellular matrix of differentiated cells, while the laminin detection failed for undifferentiated MSCs (204). In the present work, an interesting difference between 2D and 3D cultured ASCs was observed at an early stage of adipogenesis. While laminin could already be detected in 3D spheroids after two days of induction, no laminin was observed in 2D monolayers at this time point. This observation supports the hypothesis postulated in the previous chapter, that the early deposition of laminin within the ECM could be a necessity for the sustained ASC differentiation in 3D spheroid cultures after short-term induction. An adipogenesis-promoting effect has also already been described for laminin in the literature (192).

To contribute to a better understanding of whether and how laminin actually influences the process of adipogenic differentiation, a shRNA targeting approach was used to knock down the expression of laminin in ASCs. As already mentioned, numerous α, β and γ chains exist in vertebrates, which are assembled in 18 different laminin heterotrimers (92). The tissue specificity of the laminin isoforms is mainly determined by the expression of the alpha chain. Thus, it is reported that the α4 chain is characteristic for cells of mesenchymal origin (100). Together with β1 and γ1, the α4 chain forms the laminin isoform 8 which belongs to the main constituents of the ECM of white adipose tissue (101). Niimi et al. reported that laminin-8 is

the only isoform expressed during adipogenesis of 3T3-L1 cells (205). Furthermore, it is known that the synthesis of the laminin α chain is the rate-limiting step in the assembly of several types of laminin (206,207). Li et al. showed with their results that this is also the case for the α4 chain during the process of synthesis and deposition into the extracellular space of laminin-8 (208). Thus, the α chain is mainly responsible for the self-assembly and the integration of the laminin heterotrimer into the extracellular matrix. The interaction of the extracellular laminin with cell surface receptors such as integrins, takes also place via the alpha chain, through which laminin can influence numerous cellular processes (92,98,209). Therefore, it was assumed that a knockdown of the laminin α4 chain should be the most efficient in order to impede or interfere with the expression and deposition of laminin in transduced cells.

The RNAi mediated knockdown of the laminin α4 chain was assayed with three different shRNA constructs specific for three different *LAMA4* sequences. *LAMA4* expression was found to be markedly reduced upon expression of the different shRNAs in ASCs. Through qRT-PCR analyses the knockdown specificity was confirmed since neither the β1 nor the γ1 chain of the laminin-8 heterotrimer was affected by the perfomed shRNA-mediated KD. To the best our knowledge, this was the first time that the influence of laminin on the adipogenic differentiation behavior of ASCs was investigated through the knockdown of a specific alpha chain of the laminin-heterotrimer. In previous studies described in the literature, regarding the role of this non-collagenous basement membrane protein in the process of adipogenic differentiation, laminin was provided as an extracellular matrix substrate to the cells, either under 2D or 3D culture conditions (192,210,211).

The histological evaluation of the differentiation experiment showed that ASCs with reduced *LAMA4* expression did not exhibit reduced adipogenic differentiation. Further quantitative analyses confirmed the result of this histological evaluation. A direct correlation between *LAMA4* gene expression level and the adipogenic differentiation of the ASCs could therefore not be identified. Thus, a reduction in the *LAMA4* expression alone did not entail a negative impact on the differentiation behavior of the cells. In the literature, however, there have been reports of in vivo experiments in which laminin α4 deficient mice showed a decreased adipose tissue expansion and further exhibited reduced weight gain in response to a high-fat diet (194,212). At the same time there are reports in the literature, where the addition of laminin as an extracellular matrix substrate resulted in an improved adipogenesis of the cells. For example, Chaubey and Burg showed in 2008 that cultivating mouse bone marrow stem cells on a laminin coated surface promotes the triglyceride accumulation upon adipogenic

differentiation (192). Lee and Abdeen observed an improved adipogenic differentiation of human bone marrow derived MSCs cultured on an artificial laminin surface (211). Not only in 2D monolayers, but also in 3D culture conditions similar results were achieved. For example, Hsueh and Chen used alginate-beads modified with laminin as carrier for mouse 3T3-L1 preadipocyte cells and observed a significantly improved adipogenic differentiation compared to the use of unmodified cell-carriers (210).

One possible explanation for the lack of influence of the *LAMA4* knockdown on adipogenic differentiation in the experiment described here, could be that the knockdown was not stable during adipogenesis. However, this was excluded through the gene expression analysis of *LAMA4* during adipogenic differentiation, by demonstrating that the expression was also significantly reduced for all three target-specific shRNA constructs during the experiment compared to the scrambled control group. Furthermore, the *LAMA4* gene expression did not change during adipogenic differentiation. This goes along with reports from the literature describing that intracellular laminin synthesis does not change during adipogenesis, whereas the extracellular laminin increases during differentiation (191). However, also conflicting observations of increased laminin α4-, β1- and γ1-mRNA expression during the adipogenic differentiation of bone marrow derived MSCs are existing (213).

In a first attempt to examine the association between the reduced *LAMA4* gene expression and the actual amount of total laminin protein in the ECM, it was shown that only ASCs transduced with construct B showed less of the total laminin in the ECM of the differentiated cells. Neither for construct A, nor for construct C the detected total laminin signal in the extracellular matrix of differentiated cells differed from the scrambled control. Therefore, a decreased expression of the gene *LAMA4* encoding for the α4 chain of laminin was not consistently reflected in total laminin expression on protein level. This also made it impossible to assess the influence of the *LAMA4* gene expression on ASCs adipogenic differentiation. One possible explanation for this observation could be, that cells store laminin α4 chain Protein in the cytoplasm and that the final synthesis of the heterotrimeric laminin molecule and the subsequent secretion into the extracellular space takes place only after the adipogenic stimulus. In this case, the reduction of the corresponding *LAMA4* mRNA level would not affect the adipogenic differentiation. Furthermore, it is conceivable that the α4 chain could be replaced by another of the five known α chains (92). The latter assumption could be studied in follow-up experiments in which the mRNA synthesis of all laminin α chains, α1-5, is tested by expression analyses after a target specific *LAMA4* knockdown.

As it could be shown in this study, the shRNA-mediated knockdown of *LAMA4* expression did not correlate consistently with the total laminin expression on protein level in the extracellular space. Since there are many different isoforms of laminin, it may not have been the right approach to investigate the general influence of laminin on cellular processes in ASCs, including their adipogenic differentiation by knocking down one specific alpha chain of the laminin heterotrimer, even if this chain is described as the major component of white adipose tissue. The transduction of the ASCs with the shRNA construct B at least gave an indication that there seems to be no connection between reduced laminin expression in the ECM and the adipogenic differentiation of the cells. However, further experiments are required to confirm this evidence. In a follow-up study, the role of laminin might be analyzed by inhibiting the interaction of laminin with the ASCs and thus preventing cellular processes from being influenced by extracellular laminin. This could be achieved, for example, by blocking specific integrins or the respective epitopes on the laminin α chains with suitable antibodies.

In summary, we succeeded in achieving a stable knockdown of the expression of the laminin α4 encoding gene *LAMA4*, which also remained stable during the differentiation of ASCs. However, there was no consistent link between reduced gene expression and total laminin expression on protein level. Therefore, it was not possible to assess the influence of total laminin on adipogenic differentiation of ASCs, with this approach.

4.4 ASCs cultured as 3D spheroids – gene expression, secretory properties, and cell junctions

The resemblance to the ECM composition of native adipose tissue together with the superior differentiation capability, both described in chapter 2 of this thesis, makes 3D spheroids consisting of ASCs highly feasible building blocks for adipose tissue engineering applications. Studies on exploring the therapeutic benefits of mesenchymal stromal/stem cells (MSCs) in the last years, however, showed that enhanced tissue repair is not only attributable to the engraftment and differentiation to replace injured cells, but also to paracrine secretions or cell-to-cell contacts that modulate inflammatory or immune reactions (147).

MSCs have multifaceted therapeutic capabilities, which are not restricted to their potential to differentiate along mesenchymal lineages, but also to their ability to secrete a large number of cytokines with angiogenic, anti-apoptotic and also anti-inflammatory as well as immunomodulatory properties (145,214,215). By now the anti-inflammatory and immunomodulatory potential of MSCs is well documented, however, the knowledge of MSC behavior and capabilities is mostly based on studies using conventional 2D monolayer culture (216,217). Though, in the last years, three-dimensional culture conditions such as spheroid culture have been shown to enhance the therapeutic efficiency of MSCs compared to monolayer culture (146). First observations made by Lee et al. in 2009 demonstrate that lung MSC micro-emboli of myocardial infarcted mice produce TNFα-stimulated gene/protein-6 (TSG6) (218). This anti-inflammatory factor, however, was not found in conventional 2D monolayer culture of MSCs. Furthermore, Bartosh et al. showed that MSC spheroids in hanging drop culture also produce significantly higher TSG6 than respective monolayer cultures. Additionally, higher expression of a set of anti-inflammatory and anti-apoptotic proteins as well as anti-cancer proteins were found in the MSC spheroids (147).

This impact of three-dimensional cell culture conditions on the therapeutic capabilities of MSCs may contribute to the benefit of using multicellular 3D spheroids in the field regenerative medicine and cellular therapies (216). By far, most of 3D spheroid studies regarding the improvement of their therapeutic efficiency, especially the secretion of relevant cytokines, were done with human MSCs derived from the bone marrow. Investigations on the paracrine secretion using adipose derived mesenchymal stromal/stem cells (ASCs) in a three-dimensional environment are scarce. To overcome this gap and to further implement ASC 3D spheroids as a promising approach in cellular therapies and regenerative medicine, investigations on their gene expression and secretory properties are indispensable. For this purpose, the expression of

various genes encoding a set of anti-inflammatory and anti-apoptotic as well as anti-cancer proteins was analyzed and compared between ASCs of 2D and 3D culture conditions. Furthermore, the actual secretion of one of the major anti-inflammatory mediators, prostaglandin E2 (PGE2), was also investigated on secretion level.

The observed enhancement in their therapeutic efficiency when ASCs are cultivated as 3D spheroids compared to 2D monolayers is easy to understand, because 3D spheroid culture is much more closer to the physiological conditions in vivo, however, the exact mechanism of action remain to be defined (219). It exists the assumption that the paracrine effects of MSCs have a relationship with niche-specific settings, including intensive cell-ECM as well as cell-cell interactions. This complex communication network together with several biochemical and mechanical cues are critical for a normal cell physiology (119). Especially cell junctions further play an important role in this system, so that the expression of their related genes was investigated in the second part of this chapter. Cell junctions are subcellular macromolecular structures which connect cells to each other as well as to the extracellular matrix. Including focal adhesions, tight junctions, gap junctions, adherens junctions, desmosomes and hemidesmosomes, cell junctions are involved in many different cellular processes. Besides cell and metabolite transport across epithelial layers, development and differentiation, also the immune response is partially regulated by cell junctions (220–222). Since in 2D monolayers, cell to plastic interaction prevail rather than the more physiological cell-cell and cell-ECM interaction in 3D spheroids, the investigation of cell junctions seems to be a suitable aspect for further investigations to explain why the observed differences between ASCs under 2D and 3D culture conditions occur. These examinations not only contribute to the further characterization of the ASC 3D spheroids, but also to their further implementation as promising approach in cell therapy and regenerative medicine.

4.4.1 Changes in the expression of genes encoding secreted factors of ASCs cultured as 3D spheroids

Expression analyses with special interest on genes encoding either secretion factors involved in the inflammation response, or anticancer proteins were performed comparing 2D monolayer and 3D spheroid culture conditions. The start of the experiment was defined as the time at which passage 5 ASCs were seeded either on agarose-coated 96-well plates (5,000 cells per well) for assembling into spheroids, or on 24-well tissue culture plates (25,000 cells/cm^2) for conventional 2D monolayer culture. After 72 h of culture 2D monolayers and 3D spheroids

were harvested and mRNA was isolated for the following gene expression analyses. Real time PCR assays (Figure 4.18) demonstrated marked increases in the expression of genes, encoding factors involved in the inflammation response, in ASCs cultured as 3D spheroids compared to conventional 2D monolayer culture. For example, the expression of cyclooxygenase-2 (COX2), an essential enzyme in the synthesis of prostaglandin E2 (PGE2), one potential anti-inflammatory factor, was highly elevated in ASCs of 3D spheroids after 72 h of culture. The expression in 2D monolayers remained unchanged compared to the start of the experiment, where nearly no expression of *COX2* could be measured. A similar picture also emerged for the expression analyses of genes encoding the anti-inflammatory TNFα-stimulated gene/protein-6 (*TSG6*), the anti-inflammatory cytokine IL10 (*IL10*), as well as for the expression of *STC1*, encoding the glycoprotein stanniocalcin-1, which has both anti-inflammatory and anti-apoptotic properties. Furthermore, the expression of genes for three anti-cancer proteins was investigated, including the tumor suppressor protein IL24 (*IL24*), the TNFα related apoptosis inducing ligand (*TRAIL*), a protein with selectivity for killing certain cancer cells as well as CD82, a surface protein associated with the suppression of metastases. The results for all of them were comparable to those of the previously investigated anti-inflammatory protein encoding genes. Thus, for all genes examined here an increased expression was observed exclusively for ASCs cultivated as 3D spheroids.

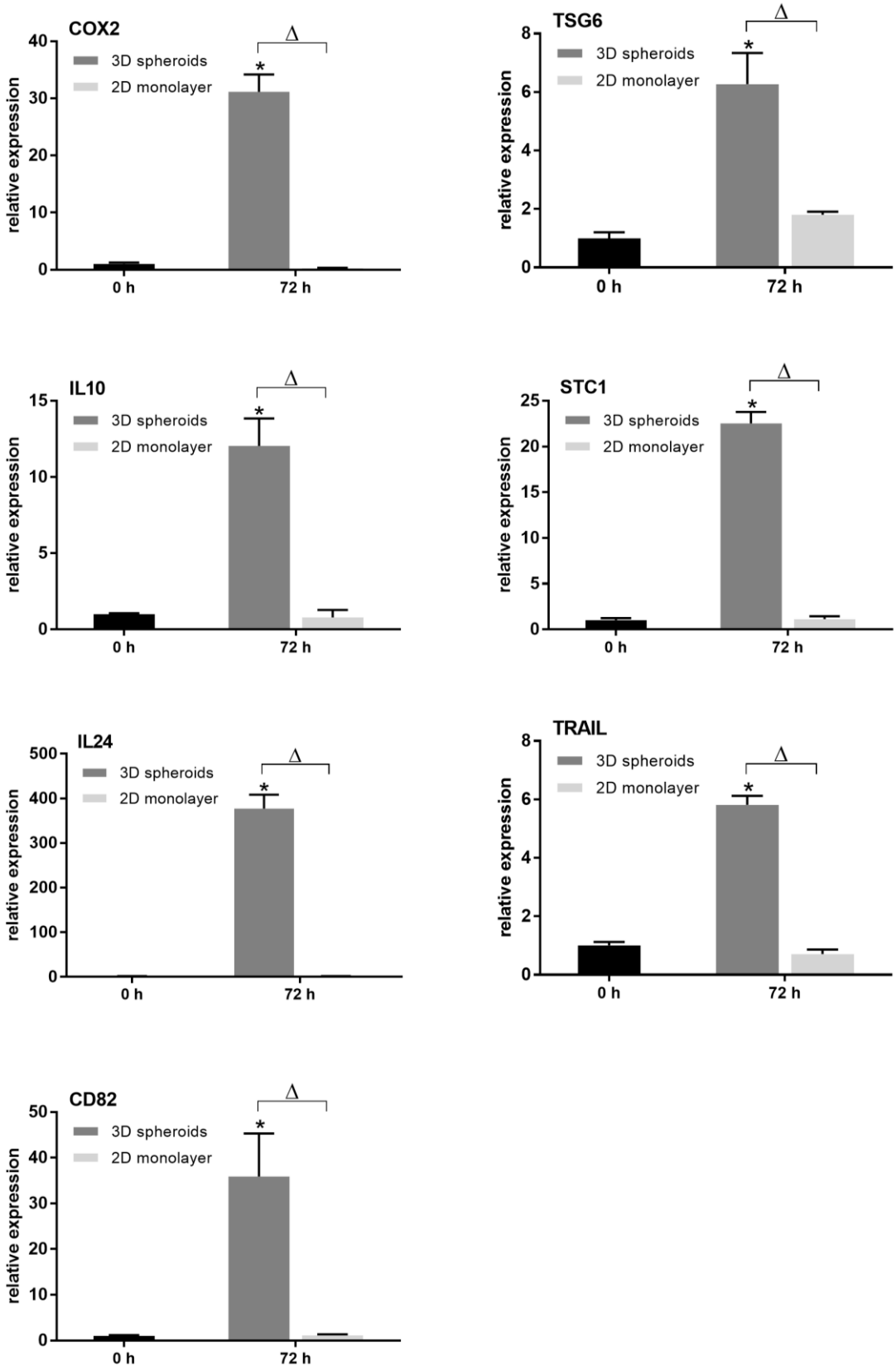

(Figure legend on the next page.)

Figure 4.18: Expression of immunomodulatory and cancer-related genes concerning the potential therapeutic properties of ASCs cultured under 2D and 3D culture conditions.
Relative expression of *COX2, TSG6, IL10, STC1, IL24, TRAIL* and *CD82* mRNA was determined by qRT-PCR. Total RNA for expression analysis was harvested prior to seeding the cells for the further treatment under 2D and 3D culture conditions (0 h), as well as 72 h after culturing the cells as 2D monolayers and 3D spheroids, respectively. Gene expression was normalized to *EF1α* as housekeeping gene. Expression levels were expressed relative to the start of the experiment. Values are expressed as mean with standard deviation (n=3). *Statistically significant differences ($p < 0.05$) between ASCs cultured for 72 h as 2D monolayers or 3D spheroids, respectively, and the starting point of seeding the cells. Δ Statistically significant differences between different culture conditions.

4.4.2 PGE2 secretion of 3D spheroids and spheroid derived ASCs

The actual secretion of the anti-inflammatory factor PGE2 into the extracellular space was further investigated. For the quantitative detection of PGE2 in cell culture supernatants, an ELISA-assay was conducted. Human ASCs were cultured for three days under 2D and 3D culture conditions. To exclude a density effect, cells for the 2D culture were seeded at a very high density of 200,000 cells/cm^2. 3D spheroids of two different sizes were generated. One group of spheroids consisted as usual of 5,000 cells each. The other group consisted of spheroids with a fivefold cell count of 25,000 cells each. After three days of culture, medium was harvested, and the secreted PGE2 was measured (Figure 4.19). The measured PGE2 amount was normalized to the DNA content. While no secreted PGE2 could be measured in the supernatant of 2D monolayers, a considerable amount was detected in the culture medium of the 3D spheroids. During three days of culture, cells of 3D spheroids released about 20-30 ng/µg DNA PGE2 into the culture medium. The different spheroid size seemed not to have an influence on the PGE2 secretion, as the secreted amount normalized to DNA was nearly the same for spheroids consisting of 5,000 and 25,000 cells. As the ASCs of 2D monolayers were seeded at a very high density, it can be partly excluded that the secretion of PGE2 by cells cultured as 3D spheroids is due to a density effect.

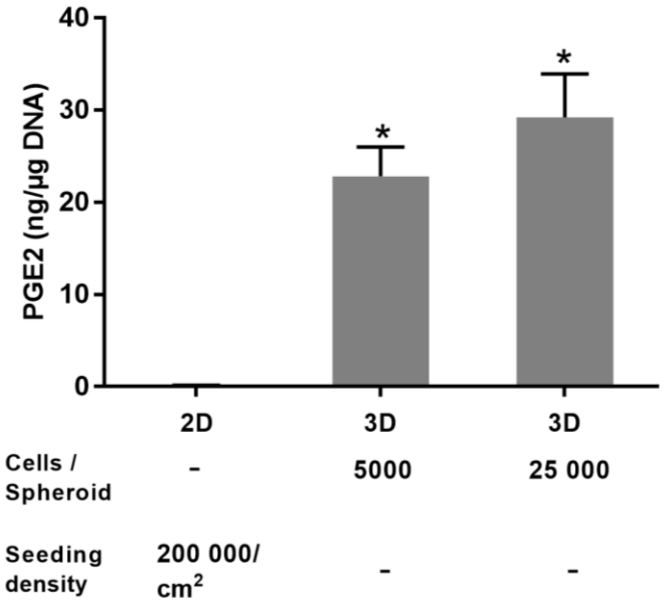

Figure 4.19: PGE2 secretion of ASCs cultured under 2D and 3D culture conditions.

For the measurement of PGE2 production, cells were cultured either in 2D monolayers with a high cell density of 200,000 cells/cm^2 or in 3D spheroids consisting of 5,000 or 25,000 cells, respectively. After 72 h of culture, cell culture medium was harvested and analyzed with respect to the secreted amount of PGE2. Measured PGE2 values were normalized to the DNA content of the respective samples. Data represents mean with standard deviation (n=3). *Statistically significant differences ($p < 0.05$) between 3D spheroids with different cell numbers per cell aggregate and the high density 2D monolayers.

Further it was investigated whether ASCs of 3D spheroids retain their anti-inflammatory capability to secrete PGE2 even when they were dissociated into single cells and cultured again under 2D culture conditions. For this purpose, ASCs were cultured as 3D spheroids for three days, before they were dissociated via trypsinization. The spheroid derived cells (SDC) were immediately reseeded into 24-well plates for culture under 2D conditions for another three days. The start of this experiment was defined as the time of reseeding the SDC under 2D culture conditions. For comparison, ASCs expanded in tissue culture flasks, were simultaneously seeded either into 24-well plates for 2D conditions or into agarose coated 96-well plates for 3D spheroid culture. After 72 h of culture supernatants were harvested and the secreted amount of PGE2 was quantified using an ELISA-assay (Figure 4.20 A). The detected amount of the anti-inflammatory factor was also normalized to the DNA content. No secretion of PGE2 could be measured for conventional 2D monolayers. For 3D spheroids, a considerable amount of secreted PGE2 was detected in the supernatant. While the spheroids secreted an amount of approx. 20 ng/µg DNA, the quantity of PGE2 in the culture medium of 2D monolayers, consisting of spheroid derived cells was comparatively low at 3 ng/µg DNA.

The result of PGE2 quantification should be confirmed by further expression analysis of COX2, the responsible enzyme for PGE2 secretion, via qRT-PCR (Figure 4.20 B). Therefore, mRNA was harvested directly at the starting point of the experiment, as well as after three days of culture under the respective culture conditions. Two different groups had to be distinguished at the experiment start: single cells originating from 3D spheroids (SDC) and cells expanded in the tissue culture flask. After three days of culture under different conditions mRNA was harvested from the following groups: 2D monolayers, consisting of cells which have not been cultivated as 3D spheroids before (2D monolayer), 2D monolayers, consisting of spheroid derived cells (SDC) and ASCs cultivated as 3D spheroids during the three-day experiment. Directly after dissociation of the 3D spheroids, SDC showed a highly increased *COX2* expression, which was nearly 80-times higher than in the cells, cultured under 2D conditions before. However, when further cultured as monolayer for three days, the *COX2* expression in SDC was significantly decreased to the level of cells originating from conventional 2D monolayers. Only ASCs cultured as 3D spheroids within these three days showed a significant increase in their *COX2* expression, which is about 30-times higher at the end of the experiment compared to the initial point, right before seeding the cells for spheroid synthesis. For 2D monolayers, consisting of cells, which have never been cultured as 3D spheroids before, no change in the *COX2* expression within the three days of culture could be observed.

Although the *COX2* gene was highly expressed immediately after dissociation of the spheroids, as described above, the expression obviously was downregulated very fast in 2D culture resulting in low levels of secreted PGE2 in 2D culture of SDC. This suggests that ASCs of 3D spheroids are unable to maintain the secretion of the anti-inflammatory factor PGE2, once they are re-cultured under 2D conditions.

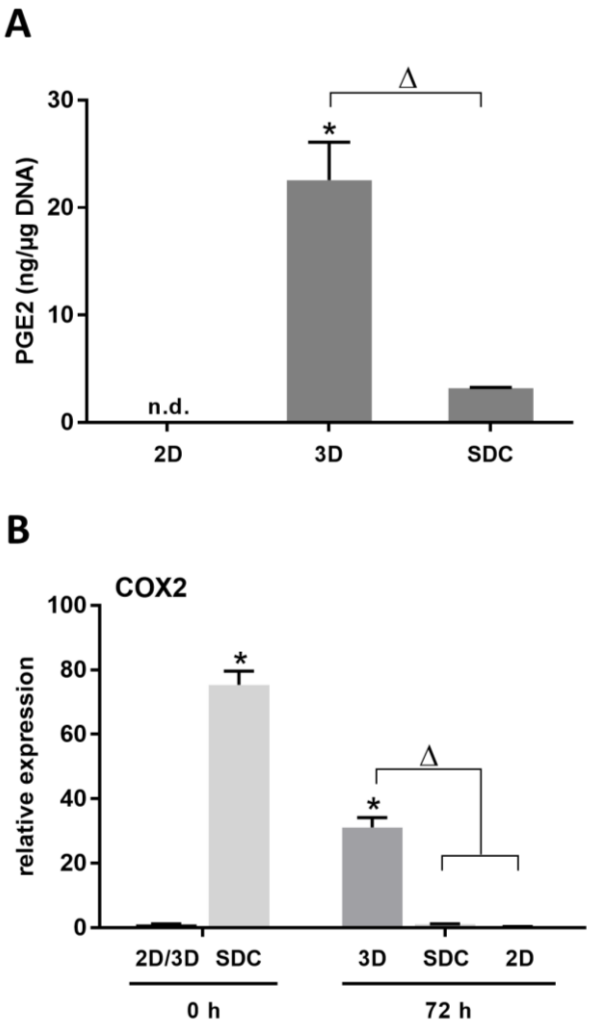

Figure 4.20: PGE2 secretion of spheroid derived ASCs and relative COX2 expression.

A) Measurement of the secreted amount of PGE2 in the cell culture medium of 3D spheroids, as well as 2D monolayers consisting of conventionally cultured ASCs and SDC after 72 h of culture. Measured PGE2 values were normalized to the DNA content of the respective samples. Data represents mean with standard deviation (n=3). *Statistically significant differences ($p < 0.05$) between 3D spheroids and 2D monolayers from conventionally cultured ASCs, Δ Statistically significant differences between 3D spheroids and 2D monolayers from SDC**. B)** Relative expression of *COX2* was determined by qRT-PCR. Total RNA for expression analysis was harvested from cells prior to seeding the cells as well as directly after dissociation of spheroids for generating spheroid derived cells (SDC) (0 h). SDC were further cultured under 2D culture conditions for 72 h. 3D spheroids and 2D monolayers consisting of non-spheroid derived cells were cultured, respectively. After 72 h total RNA from cells of the three groups was harvested. Gene expression was normalized to *EF1α* as housekeeping gene. Expression levels were expressed relative to basic levels before seeding (0 h). Values are expressed as mean with standard deviation (n=3). *Statistically significant differences ($p < 0.05$) between SDC or 3D spheroids and ASCs before seeding. Δ Statistically significant difference between 72 h old 3D spheroids and 2D monolayers consisting either of conventionally cultured ASCs or SDC, respectively.

4.4.3 PCR array for expression analysis of cell junction related genes

Furthermore, the expression of cell junction related genes was analyzed, compared between ASCs cultivated as 2D monolayers and 3D spheroids. For this purpose, passage 5 ASCs were cultured either as 2D monolayers (25,000 cells/cm^2) or as 3D spheroids (5,000 cells/spheroid) for three days. Subsequently, the mRNA was harvested and the expression of 84 cell junction related genes were investigated using the RT^2 Profiler PCR Array from Qiagen. In Table 4.1 all genes which were increased in ASCs of 3D spheroids compared to 2D monolayers are listed. The most prominent one was the gene encoding for the gap junction protein β2 (also known as connexin 26), which expression in 3D spheroids was 13-times higher compared to 2D monolayers. In second place, with a 7-fold higher expression in 3D spheroids, was the gene encoding the junctional adhesion molecule 2, followed by integrin α2 and β3, which expression was about 5-times higher in 3D spheroids. The other listed genes were also higher expressed in ASCs cultured under 3D conditions, but their expression was only about 2-3-fold increased in comparison to 2D monolayers. In Table 4.2, genes are listed which were downregulated in 3D spheroids compared to 2D monolayers. The cell junction related gene with the lowest expression in 3D spheroids was the gene encoding for N-cadherin with a 9-fold lower expression compared to 2D monolayers. All the other downregulated genes in this table were about 4-fold (Claudin-11) or less downregulated.

The expression of the underlined genes was verified by quantitative RT-PCR using 3D spheroids (5,000 cells/spheroid) and 2D monolayers with a cell density of 25,000 cells/cm^2 and 200,000 cells/cm^2. This additional high-density 2D culture (2D_HD) was included in the experimental set-up to investigate the effect of cell density in 2D culture in comparison to the effect of dimensionality (2D vs. 3D).

Table 4.1: List of upregulated genes in ASCs of 3D spheroids compared to cells from 2D monolayers after 72 h of culture.

Gene Symbol	Gene Name	Fold Regulation
GJB2	Gap junction protein, β2	13.42
JAM2	Junctional adhesion molecule 2	7.29
ITGA2	Integrin α2	5.86
ITGB3	Integrin β3	5.34
TJP2	Tight junction protein 2	3.15
NOTCH3	Notch 3	3.14
NOTCH4	Notch 4	2.87
ICAM1	Intercellular adhesion molecule 1	2.74
GJA1	Gap junction protein, α1	2.65

Table 4.2: List of downregulated genes in ASCs of 3D spheroids compared to cells from 2D monolayers after 72 h of culture.

Gene Symbol	Gene Name	Fold Regulation
CDH2	N-Cadherin	-9.32
CLDN11	Claudin 11	-4.91
ITGA3	Integrin α3	-3.58
ITGA4	Integrin α4	-2.87
ITGA7	Integrin α7	-2.35
ICAM2	Intercellular adhesion molecule 2	-2.09
PVRL2	Poliovirus receptor-related 2	-2.08

In Figure 4.21 the results of the qRT-PCR expression analysis for the selected overexpressed genes are shown. A significant upregulation of the five genes under investigation in spheroids compared to 2D monolayers was shown, which was in accordance with the gene array results, albeit with a lower level of upregulation for single genes. The gene encoding the gap junction protein, β2 (*GJB2*), also known as connexin 26, for example, was 13-times higher expressed in 3D spheroids analyzed with the PCR Array, while the qRT-PCR experiment only showed a five-fold increase in expression compared to 2D monolayers. This was also the case for the genes encoding the tight junction protein 2 (*TJP2*) and Notch 3. In contrast, the measured value for the fold regulation of the junctional adhesion molecule 2 (*JAM2*) and the gap junction

protein, α1 (*GJA1*), also known as connexin 43, was nearly the same for the previous PCR-array and the qRT-PCR experiment described here. The last two genes mentioned above were also significantly overexpressed in the high-density culture (2D_HD) compared to the conventional 2D monolayer culture. Only *GJA1* and *TJP2* were significantly upregulated in the 3D spheroid culture compared to the high-density monolayers (2D_HD). With regard to TJP2, the encoding gene was even significantly downregulated in the high-density culture (2D_HD) compared to the conventional 2D culture, as well as to the 3D spheroids. For the other genes examined here it made no difference whether the cells were cultured in a high-density 2D culture or under three-dimensional conditions.

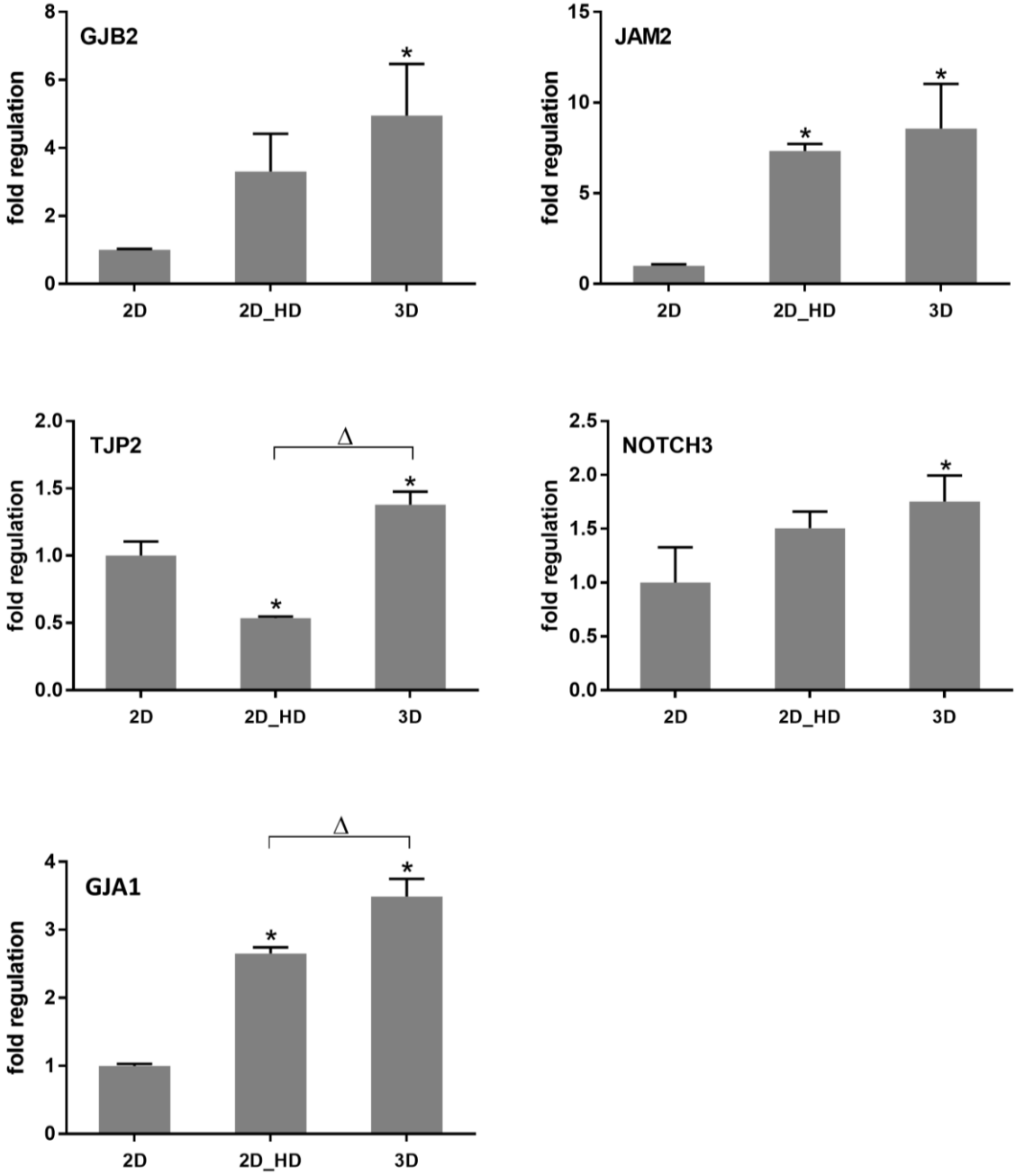

Figure 4.21: Verification of the PCR array hits for upregulated genes in ASCs of 3D spheroids.

Fold regulation of gene expression of *GJB2*, *JAM2*, *TJP2*, *NOTCH3* and *GJB1* was determined by qRT-PCR. ASCs were either cultured in 2D monolayers with two different seeding densities, 25,000 cells/cm^2 (2D) and 200,000 cells/cm2 (2D_HD), or in 3D spheroids with 5,000 cells per cell aggregate. Total RNA for expression analysis was harvested after 72 h of culture. Gene expression was normalized to *HPRT1* as housekeeping gene. Fold regulation was expressed relative to 2D monolayers with 25,000 cell/cm^2 (2D). Values are expressed as mean with standard deviation (n=3). *Statistically significant differences ($p < 0.05$) between 2D monolayers with the high cell density (2D_HD) as well as 3D spheroids and 2D monolayers with only 25,000 cells/cm^2. Δ Statistically significant differences between 3D spheroids and high density 2D monolayers.

The results of the qRT-PCR expression analysis for two genes showing downregulation, N-cadherin (*CDH2*) and claudin 11 (*CLDN11*), in 3D spheroids are depicted in Figure 4.22. The results for the underexpressed genes obtained from the previous PCR array were also confirmed by the qRT-PCR experiment. Both N-cadherin and claudin 11 were significantly downregulated in ASCs of 3D spheroids compared to 2D monolayers. However, N-cadherin was also expressed significantly lower in the ASCs of the high-density culture (2D_HD) than in the ASCs of the 2D monolayer culture with the conventional seeding density used in this work, even though the effect was more pronounced in the 3D spheroids. For claudin 11, the culture of ASCs under high-density conditions seemed not to have an influence on the expression of the respective gene, as hardly any difference could be observed between ASCs of normal and high-density 2D monolayers.

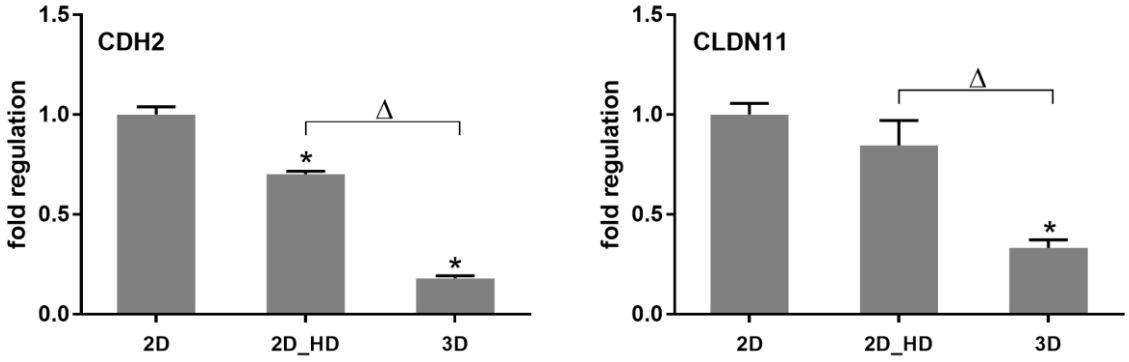

Figure 4.22: Verification of the PCR array hits for downregulated genes in ASCs of 3D spheroids.
Fold regulation of gene expression of *CDH2* and *CLDN11* was determined by qRT-PCR. ASCs were either cultured in 2D monolayers with two different seeding densities, 25,000 cells/cm^2 (2D) and 200,000 cells/cm^2 (2D_HD), or in 3D spheroids with 5,000 cells per cell aggregate. Total RNA for expression analysis was harvested after 72 h of culture. Gene expression was normalized to *HPRT1* as housekeeping gene. Fold regulation was expressed relative to 2D monolayers with 25,000 cell/cm^2 (2D). Values are expressed as mean with standard deviation (n=3). *Statistically significant differences ($p < 0.05$) between 2D monolayers with the high cell density (2D_HD) as well as 3D spheroids and 2D monolayers with only 25,000 cells/cm^2. Δ Statistically significant differences between 3D spheroids and high density 2D monolayers.

4.4.4 Discussion

In general, 3D multicellular spheroids of mesenchymal stromal/stem cells are nowadays regarded to have beneficial therapeutic properties compared to cells cultured in conventional 2D monolayers (179). Their enhanced differentiation capability along the mesenchymal lineages is not the only characteristic improving their regenerative potential, but also

immunomodulatory and anti-inflammatory properties contribute (146). Since the first observation from Lee et al. of TSG-6 producing lung MSC micro-emboli of myocardial infarcted mice in 2009, the number of studies demonstrating an improved paracrine secretion of MSCs cultured in a 3D environment increased (218). The secretion factors documented in this context range from factors with anti-inflammatory and anti-apoptotic to anti-carcinogenic properties, leading to a further enhancement of the therapeutic potential of MSC 3D spheroids (148). Previous studies demonstrating an improved secretory potential of 3D spheroids have been carried out almost exclusively with bone marrow derived MSCs. Investigations on MSCs isolated from adipose tissue concerning this issue are so still scarce. The easy accessibility of their tissue of origin, as well as their high abundancy inside, however, makes them highly advantageous over BMSCs (41–43). Thus, in this study we investigated the therapeutic efficiency and regenerative potential of ASC spheroids with regard to their gene expression and secretory properties in order to further establish them as promising approach for cellular therapies and in the field of regenerative medicine.

Expression analysis of genes encoding a set of secreted factors with anti-inflammatory and anti-cancerogenic potential in ASC spheroids compared with conventional 2D monolayers showed a marked increase in the expression of all investigated genes within three days of culture, solely in cells cultured under three dimensional conditions. Part of this investigation were three anti-cancer protein related genes (*TRAIL*, *IL24* and *CD82*). The expression of all these three genes increased within three days of three-dimensional culture of ASCs, however, in their two-dimensional counterpart no upregulation in the expression of the respective genes was observed. In 2014 Yeh et al. published their results from mRNA microarrays comparing MSCs from human umbilical cord blood under 2D and 3D culture conditions, where they also documented an upregulation of genes associated with anti-tumor properties in MSCs of 3D spheroids (179). One of these upregulated genes was also interleukin 24 (*IL24*) which is a member of the IL 10 family of cytokines. It is of growing interest because it is considered to be a tumor suppressor which selectively induces apoptosis in cancer cells while leaving normal cells unaffected (161). In addition to IL24, Bartosh et al. reported an upregulation of the two anti-cancer protein related genes *TRAIL* and *CD82* for BMSC spheroids, just as it was observed for ASC spheroids in the present study. The apoptosis inducer TRAIL is also reported to be selective for killing certain cancer cells and CD82 known as a suppressor protein for metastasis (147,223). These observations make spheroids additionally interesting and suitable for the therapy of some types of cancer, especially for those which are additionally sensitive to anti-

inflammatory factors (147). For the ASC spheroids investigated in this study, this is another property that further advances their application in the field of regenerative medicine especially at defect sites resulting from tumor resections.

Besides the genes encoding for the above mentioned anticancer proteins, those for secreted factors involved in the inflammation response (*TSG6*, *STC1* and *COX2*) were also upregulated in the ASC spheroids. An increase in the expression within three days of culture, however, was not observed for the respective 2D monolayer cultures. Besides the upregulation of genes associated with anti-cancer proteins, Yeh et al. were also able to prove this for genes associated with anti-inflammatory properties of MSCs in their mRNA microarray study (179). Bartosh et al. used a hanging drop culture to generate spheroids of bone marrow derived MSCs and revealed an increased expression of secretion factors with anti-inflammatory properties as well. One of these factors was the TNF-stimulated gene 6 protein (TSG-6), which was reported to be expressed and secreted at very high levels from the BMSC spheroids compared with the monolayer culture (147). As already mentioned above, TSG-6 was the first anti-inflammatory factor which was observed to be produced by lung MSC micro emboli of myocardial infarcted mice in vivo. However, Bartosh et al. demonstrated with their results, that MSCs are not only able to secrete such factors in vivo, but also possess this property in vitro if cultured in a 3D environment to provide more physiological conditions. Besides *TSG6*, genes encoding two further inflammation-modulating factors, stanniocalcin 1 (*STC-1*) and cyclooxygenase 2 (*COX2*), were shown to be upregulated in 3D spheroids of BMSCs.

The present study revealed the result that ASCs assembled into multicellular 3D spheroids have an increased expression of genes associated with anti-cancer as well as anti-inflammatory proteins, compared to cells from 2D monolayers. This has also been reported for MSCs originated from other tissues. Thus, this leads to the conclusion, that MSCs isolated from different tissues have very similar secretory properties regarding factors involved in the inflammation response or anti-cancer proteins when they are cultured as 3D spheroids.

To show the improved paracrine secretion of three-dimensionally cultured ASCs not only on gene expression but also on secretion level, we focused on prostaglandin E2 (PGE2) as one major anti-inflammatory secretion factor involved in the inflammation response. The expression of COX2, which is a key enzyme in the synthesis of PGE2 (148), was already shown in the section above to be highly elevated in ASC spheroids. This observation was confirmed by measuring the actual amount of PGE2 released into the culture medium. While ASCs cultured as 3D spheroids released a measurable amount of PGE2 over a period of three days,

no PGE2 was detectable in the supernatant of 2D monolayers. Also the high density 2D culture (200,000 cells/cm^2), which better reflects the cell density in the spheroid and thus more closely approximates that of native tissues, did not lead to PGE2 secretion of the ASCs under 2D culture conditions. It seems like dimensionality and the way how cells interact with each other and with their surrounding matrix affect their secretory properties more than the cell density. In order to investigate whether ASCs can maintain their improved secretory capabilities once cultured under 3D conditions, 3D spheroids were dissociated, and spheroid derived cells were cultured again under 2D conditions. This led to the result that ASCs originating from the 3D spheroids were not able to secrete PGE2 anymore seeded back on a plastic surface, supporting the above-mentioned assumption that dimensionality is an influential factor in cell behavior. Similar results have also been described in the literature for the two secretion factors, TSG-6 and STC-1, which are also involved in the inflammation response. Their high expression level was maintained for one day after the MSCs were dissociated from the spheroids, before it subsequently decreased again under 2D culture conditions (147). Also, Ylöstalo et al. showed during their exploration of the anti-inflammatory properties of BMSC spheroids, that one major factor involved in the inflammation response secreted by the cells was PGE2. Furthermore, they reported that BMSC spheroids promoted the transition of macrophages from a primarily proinflammatory M1 to a more anti-inflammatory M2 phenotype through interaction of the secreted PGE2 with the EP4 receptor of stimulated macrophages (148). Locally secreted PGE2 is therefore reported to be one of the most potent activators of anti-inflammatory M2 macrophages and thus contributes to the promotion of inflammation resolution (177).

The increase in the expression of secretion factors involved for example in the inflammation response does not only occur at the transcriptional level of ASC spheroids. Investigations on PGE2, as a representative example of the secretion factors investigated on gene expression level above, confirmed that these factors can also be detected at the secretion level and are actually secreted by the ASC spheroids into the culture medium. However, in future studies, this should be also experimentally examined for the other secretion factors and anticancer proteins, which were already investigated on the gene expression level. This finding of the increased immunoregulatory effects of ASCs cultivated as 3D spheroids further elevates their therapeutic and regenerative potential.

The improved therapeutic potential of 3D spheroids has already been shown in vivo applications for BMSCs. In a zymosan induced mouse model for peritonitis the injection of MSC spheroids into the peritoneum suppressed the inflammation much more effectively than

the injection of MSCs cultured as 2D monolayers. Although MSCs, injected as single cells, also aggregate and form spheroids in vivo accompanied by an increase in the expression of potentially therapeutic genes, MSCs cultured and injected directly as spheroids are more effective (147). These observations led to the assumption, also described in the literature, that MSCs express the corresponding genes in 3D spheroids already at the time of injection and thus avoid the lag period which is required to upregulate the expression of the genes in cells cultured as monolayers before (147). During this time many of the injected single cells can undergo necrosis and apoptosis, which is why their effectiveness and therapeutic potential are significantly lower compared to the injected MSC spheroids (218). The preincubation of MSCs as spheroids can thus serve as an induction of their secretory potential so that the cells already possess their complete therapeutic properties at the time of in vivo application. Another type of preconditioning was described in chapter 2 regarding the use of ASC spheroids for adipose tissue engineering. The preincubation of the 3D spheroids with a hormonal cocktail should direct the cells along the adipogenic lineage prior to in vivo application in order to enhance their therapeutic potential to restore soft tissue defects. However, ASCs used in the present study for the investigation of their secretory properties were undifferentiated, as it was reported that the differentiation of MSCs leads to a decrease of their immunomodulatory properties (216). This goes along with the observation from Ylöstalo et al. that the inhibition of COX2 through indomethacin, which is part of the adipogenic induction cocktail, abolished the secretion of PGE2 by the MSC spheroids (148). As a possible therapeutic approach, a combination of differentiated and undifferentiated spheroids would therefore be conceivable. Thus, the secretory potential of the undifferentiated spheroids, as well as the property of differentiating spheroids to restore tissue defects can be combined and therefore, the entire therapeutic potential of ASC spheroids can be optimally exploited.

Molecular forces responsible for the increased expression of anti-inflammatory and anti-tumorigenic genes in cells assembled into spheroids are not yet fully understood and remain still unclear. Among others, contact-dependent signalling pathways could be involved as the cells of 3D spheroids are in close association with each other, so that signal cues can be transmitted more effectively than in 2D monolayer cultures, where only a small part of the cell is in contact with its cellular neighbours (147). Therefore, a PCR array was used to screen the expression of cell junction related genes in ASCs assembled into 3D spheroids compared to cells cultured as 2D monolayers, in order to obtain initial indications of differences in gene expression that might be responsible for the beneficial properties of 3D cultured cells. Since

this was the first time to the best of our knowledge that genes related to cell junctions were examined in ASC 3D spheroids, this is another contribution to a broad characterization of these spheroids, which is indispensable regarding their further implementation in the field of regenerative medicine.

The two approaches most frequently discussed in the literature with regard to signalling pathways involved in the increased expression of potentially therapeutic genes in BMSC spheroids are upregulated genes for the stress activated IL1 signalling and the contact dependent signalling pathway for Notch. According to the latter, also in ASC spheroids two Notch related genes, *NOTCH3* and *NOTCH4*, were found to be upregulated, of which it is described in the literature that they might drive the expression of *COX2* and might be therefore involved in PGE2 secretion (177).

Furthermore, among the upregulated genes in ASCs cultured in a 3D environment, were two genes (*GJB2* and *GJA1*) encoding for two building block proteins of gap junctions, connexin 26 (Cx26) and connexin 43 (Cx43). Gap junction channels are constructed of two apposed integral membrane hexamers of connexin proteins arranged around a central pore, which enables the direct cytoplasmic exchange of ions and low molecular weight metabolites between adjacent cells. To date, 21 different connexins are known in humans, with connexin 43 representing the most abundant isoform in human tissue (224,225). Also for ASCs the presence of Cx43-containing gap junctions has already been reported (197). Connexin 26 is mostly reported in connection with cochlear fibrocytes in the inner ear, where deficient Cx26-mediated gap junctions are the most frequent cause of hearing loss. There are no reports of Cx26 expression in ASCs so far, however there are indications in the literature that transplanted bone marrow-derived MSCs have the capacity to repair injured cochlear fibrocytes and lead to a significant improvement of hearing recovery in a rat model through repair of the interrupted gap junction network mediated by Cx26 expression (226,227).

The intercellular communication through connexin-mediated gap junctions is the most direct way of cell-cell signalling and plays an essential role in several cellular processes. Besides their role in tissue development and coordinated cellular activity, gap junctions also serve as modulators of cellular differentiation and in various parts of the immune system their presence and functional role has been reported (228). Thus, the expression of connexin 43 (Cx43) in lymphocytes was described, where the blockage of the direct intercellular communication via gap junctions led to the disruption of immunoglobulin release and cytokine production (229). This demonstrates the importance of direct cell-cell communication for the

anti-inflammatory secretion and could be an indication that also in ASC spheroids gap junctional intercellular communication could be involved in the improved secretory properties. In the qRT-PCR experiment for verification of the PCR array hits, a density dependence of the expression of both connexin-encoding genes could be observed in the 2D monolayer cultures. This means that also in high density 2D monolayer cultures a slight increase in the expression of *GJB2* and *GJA1* could be detected, what has already been observed for connexin 43 in previous experiments by our group (197). This indicates that an increased expression of these two connexin-mediated genes alone is not decisive for an increased secretion potential of the ASCs, since despite a high cell density a detection of PGE2 in the culture medium of 2D monolayers was not possible. In order to investigate the specific influence of connexin 26 and 43-mediated gap junctions on the behavior of ASCs in 3D spheroids, either knockdown experiments of the related genes or a specific blocking by inhibitors of the respective gap junctions would be conceivable in future investigations.

Some further upregulated genes in ASCs assembled into 3D spheroids are encoding for tight junction proteins. Tight junctions are the most junctional multi-protein complexes in certain epithelial and endothelial cells, contributing to their barrier function through regulating the permeability between adjacent cells. This tight junction forming proteins can be sub-divided into the integral membrane and cytoplasmic proteins. The latter also includes the tight junction or zonula occludens protein-2 (ZO-2) encoded by the *TJP2* gene, which expression is upregulated in ASCs of 3D spheroids. These zonula occludens proteins link the membrane proteins to the actin cytoskeleton and are therefore critical to junction assembly and permeability, because it has been reported that in the absence of ZO-1 and ZO-2 cells fail to form tight junctions (230). Interestingly, *TJP2* was the only upregulated gene among the examined genes which is not density dependent and therefore an elevated expression could not be observed also in high density monolayer cultures but exclusively in assembled 3D spheroids. In addition, this finding coincides with the observations in chapter one of this thesis, where the outer cells of the spheroid develop into a densely packed cell layer. Tight junctions therefore may be involved in creating a barrier against the 3D spheroids surrounding environment, as it was also described by Lin et al. to prevent small molecules from entering the interior of the spheroids (140,231). However, the cytoplasmic tight junction proteins are not alone involved in the barrier formation. To seal the paracellular space between adjacent cells, tight junctions also include integral membrane proteins such as the junctional adhesion molecules (JAM) (232,233). The JAM-family encompasses three classical members JAM A, B and C, whereby

the expression of the JAM B encoding gene (*JAM2*) was also elevated in the spheroid forming ASCs. Junctional adhesion molecules are reported to be expressed by a large variety of cell types and tissues, including epithelial and endothelial cells, but also leukocytes and fibroblasts. But specifically enriched at the tight junctions of these cells, JAMs are not only involved in the formation of a physical barrier, but also in a variety of other biological processes, including those of inflammation (232,234). Here in particular, their involvement in leukocyte recruitment as a result of anti-inflammatory signals is described. It is therefore possible that the increased expression of the junctional adhesion molecule related gene in the ASCs is a further contribution to the anti-inflammatory effect of assembled 3D spheroids, in addition to the secretion of corresponding cytokines. In the function of junctional adhesion molecules, their interaction with integrins also seems to play an important role. The heterophilic interaction with this cell-matrix mediating transmembrane molecules is reported to be necessary for the leukocyte recruitment during inflammation regarding their migration through tissues to reach the site of inflammation (234). The binding between junctional adhesion molecules and integrins is likely to be highly specific, which would explain an upregulation of the expression of respective integrins in the ASC spheroids (Integrin α2 and β3), with a concomitant decrease in integrin related gene expression, which are maybe of lesser importance for the molecular processes and functions of the 3D spheroids (Integrin α3, α4 and α7). In addition to the integrins, also cadherins belong to the cell adhesion molecules. Through calcium dependent homophilic interactions they are also responsible for the formation of intercellular connections known as adherens junctions (235). In the ASCs assembled into 3D spheroids, the low expression of one cadherin related gene, *CDH2*, was particularly noticeable in comparison to the conventional 2D monolayers. N-cadherin, encoded by the *CDH2* gene, is one of the most well studied cadherins and is mostly expressed in neuronal cells, however there are suggestions in the literature that this cadherin may also be important in mediating the anti-inflammatory effects of MSCs (235). However, this does not correspond with the observed improved anti-inflammatory effect of the 3D spheroids and the simultaneous decrease of *CDH2* expression in the corresponding ASCs. Instead, this observation supports one possible explanation for the improved adipogenic differentiation of ASC 3D spheroids, as N-cadherin was reported to be decreased during adipogenic differentiation of preadipocytes (236).

In summary, it was shown in this chapter that besides enhanced differentiation capabilities also a modulated gene expression ranging from anti-inflammatory and anti-apoptotic up to anti-carcinogenic factors, contributes to an increased therapeutic potential of ASCs assembled into

3D spheroids. This opens up new, versatile possibilities for the use of ASC 3D spheroids, which concurs to further advance their implementation in cellular therapies and regenerative medicine.

In the second part of this chapter, a first comprehensive study of cell junction related gene expression contributed to a further characterization of the 3D spheroid model consisting of ASCs. Thereby, differences in gene expression between ASCs cultivated as 3D spheroids or under conventional 2D conditions could be detected. This may form the basis for further investigations in this field. Further knockout or specific blocking experiments can now help to uncover contact dependent molecular forces involved, which help to fully elucidate and understand the beneficial properties of 3D spheroids.

5 Conclusion and Outlook

The ability to differentiate into mesenchymal lineages, as well as immunomodulatory, anti-inflammatory, anti-apoptotic, and angiogenic properties give ASCs great therapeutic potential. Through their culture as multicellular, three-dimensional spheroids this potential can even be enhanced. Accordingly, 3D spheroids are not only promising candidates for the application in regenerative medicine and inflammatory disease therapy, but also for the use as building blocks in tissue engineering approaches. Due to the resemblance to physiological cell-cell and cell-matrix interactions, 3D spheroids gain higher similarity to real tissues, what makes them a valuable tool in the development of bioactive constructs equivalent to native tissues in terms of its cellular and extracellular structure. Especially, to overcome the still tremendous clinical need for adequate implants to repair soft tissue defects, 3D spheroids consisting of ASCs are a promising approach in adipose tissue engineering. Nevertheless, studies on the use of ASC-based spheroids as building blocks for fat tissue reconstruction have so far been very rare. In order to optimally exploit their therapeutic potential to further their use in regenerative medicine, including adipose tissue engineering approaches, a 3D spheroid model consisting of ASCs was characterized extensively in this work. This included not only the elucidation of the structural features, but also the differentiation capacity, gene expression, and secretory properties. In addition, the elucidation of underlying mechanisms contributing to the improved therapeutic efficiency was addressed.

First, it was important to gain a comprehensive understanding of the spheroid formation process itself and the mechanisms contributing to it. For this purpose, the individual spheroid formation of ASCs was monitored using the liquid overlay technique in a 96-well plate setup. With this method applied here, the generation of ASC-based spheroids was possible in a well-controlled, reproducible, and scalable manner. A broad characterization of the spheroid model also entailed the investigation of the extracellular matrix development during spheroid assembly. It is known that not only cell-cell, but also cell-ECM interactions are involved in the formation process of spheroids. The non-collagenous ECM protein fibronectin was shown to be prominent already in a very early phase of spheroid formation, while collagen I and VI only appeared with progressive compaction in the ECM of the cell aggregates. The fact that fibronectin actually had an influence on the initial cell aggregation could be shown by the specific blocking of the β1-integrin receptor. The disturbed interaction of the cells with the surrounding fibronectin led to a delayed spheroid formation and thus confirmed the

participation of cell-ECM interactions in the spheroid formation of ASCs. An influence of cell-cell interactions via cadherins on the compaction of spheroids, however, could not be confirmed for ASCs. Neither unspecific blocking of cadherins through the reduction of extracellular calcium, nor the specific antibody blocking of N- and E-cadherin showed an effect on spheroid formation. There were indications of other candidates mediating self-assembly through cell-cell interactions, for example the gap junction-forming connexins. Future experiments may include blocking of respective connexins or the knockdown of the encoding genes to contribute to the further elucidation of the molecular mechanisms involved in the spheroid formation process of ASCs. In summary, we were able to describe the formation of spheroids from an initially loose cell aggregate to compact spheroids together with the development of respective extracellular matrix components. Furthermore, first insights into the underlying mechanisms involved in the formation process were gained with this study.

ASCs as self-assembled 3D spheroids with cells residing and interacting within their own secreted ECM appear attractive as building blocks for adipose tissue engineering. As the development of a tissue-specific ECM must be considered as an important requirement in tissue engineering approaches, investigations on the dynamic ECM development during adipogenesis of ASC spheroids were performed. Undifferentiated spheroids displayed a stromal ECM pattern with fibronectin and type VI collagen as main components. In the course of adipogenic differentiation, a dynamic shift of the ECM composition towards an adipogenic phenotype with laminin, collagen I, IV and VI as major parts of the ECM framework was observed, representing a distinct resemblance to the ECM composition of native adipose tissue. Furthermore, the differentiation capacity of ASCs cultured as 3D spheroids was examined in comparison to their 2D counterparts. A superior differentiation capability of spheroids compared to 2D cultured cells was shown with spheroids needing a distinctly shorter adipogenic stimulus to sustain adipogenesis, which was demonstrated on the cellular and molecular level with regard to triglyceride content and adipogenic marker gene expression. In summary, ASC spheroids could efficiently be differentiated upon a short inductive stimulus and represent adipose-like microtissues, which make them a promising approach as building blocks in adipose tissue engineering. Further research should include the combination of ASC spheroids with delivery vehicles such as hydrogels or specifically designed scaffolds to promote their potential in clinical applications.

The dynamic development of the ECM composition is not only the consequence of morphological changes during the differentiation process, but in turn influence differentiating

cells via interaction with cellular receptors. Laminin as a major component of the basement membrane was detected in the ECM of 3D spheroids after two days of induction, while no laminin was detected in the 2D monolayers at this early time point of differentiation. This led to the assumption that the early presence of laminin within the ECM could be a necessity for the progressing differentiation in 3D spheroids after a short induction stimulus, while ASCs of 2D monolayers failed to differentiate after this early withdrawal of hormonal inducers. Thus, the influence of laminin on the adipogenic differentiation process was investigated by a shRNA-mediated knockdown of the laminin expression. As essential component of the adipose tissue specific laminin-8 heterotrimer, the respective gene encoding for the laminin α4 chain (*LAMA4*) was chosen as target for the shRNA-mediated gene silencing. Through qRT-PCR analyses a specific knockdown of *LAMA4* could be demonstrated which also remained stable during adipogenic differentiation. With regard to triglyceride content and adipogenic marker gene expression, the reduction in *LAMA4* gene expression was not accompanied by a reduced adipogenic differentiation capability. As the reduced gene expression of *LAMA4* was not reflected in the total laminin deposition on protein level, the influence of laminin on the adipogenic differentiation process could not be assessed with this approach. Further investigations would be necessary to investigate the actual involvement of laminin in cellular processes, for example through the inhibition of cell-laminin interactions via blocking of respective cellular receptors.

Not only an improved differentiation capability, but also anti-inflammatory, and immunomodulatory properties via paracrine secretion contribute to an enhanced therapeutic potential of mesenchymal stem cells in a 3D environment. For ASC-based spheroids, however, investigations on respective gene expression and their secretory properties were so far missing. To overcome this gap and to evaluate gene expression of ASCs in a 3D spheroid culture system compared to conventional 2D monolayers, mRNA expression analyses of various genes encoding a set of anti-inflammatory, anti-apoptotic, and anti-cancer proteins were performed. All factors investigated were significantly elevated in the ASCs of 3D spheroids compared to the respective 2D monolayer culture, confirming the enhanced secretory potential of cells in a 3D environment. One of the highly expressed factors in ASCs cultured as 3D spheroids was COX2 (cyclooxygenase-2), which is a key enzyme in the synthesis of prostaglandin E2, one major anti-inflammatory secretion factor involved in the inflammation response. For this factor the improved paracrine secretion of ASCs in a 3D environment could also be confirmed through measurement of the actual secreted amount of PGE2 using a specific enzyme-linked

immunosorbent assay (ELISA). In order to investigate the actual anti-inflammatory effect of ASC spheroids, future studies may include the examination of the influence of 3D spheroid conditioned media on proinflammatory M1 macrophages.

The identification of the underlying mechanisms and the driving forces for the increased beneficial properties of cells in a 3D environment is still pending. Niche-specific settings, including cell-cell and cell-ECM interactions together with the involved cellular junctions are considered to be involved in paracrine effects and differentiation capacity. Cell junctions therefore play certainly also an important role in the 3D culture context and influence cellular processes. To further investigate the involvement of cell junctions in 3D spheroids, a PCR-array for screening cell junction-related genes in ASCs cultured under 2D and 3D conditions was performed. Distinct differences in the expression of cell junction-related genes between 3D spheroids and 2D monolayers could be detected. These results may form a basis for further investigations deciphering cell-cell interactions contributing to cellular processes (e.g. differentiation, secretion), which are improved in the 3D context of spheroids. Further knockdown or specific blocking experiments can now help to uncover contact dependent molecular mechanisms involved to define the decisive forces for the improved beneficial properties of ASC spheroids more precisely.

Taken together, the results of this thesis contribute to a broad characterization of the spheroid model consisting of ASCs. The findings gained about their structural features, adipogenic differentiation capacity, gene expression, and secretory properties help to further implement ASC-based spheroids as a promising approach in regenerative medicine and adipose tissue engineering. First investigations on cell junctions revealed distinct differences between ASCs cultured under 2D and 3D conditions, which now form the basis for further research to clarify the underlying mechanisms of their enhanced therapeutic efficiency and subsequently make optimal use of it in the application of ASC-based spheroids.

References

1. Patrick CW. Tissue engineering strategies for adipose tissue repair. The Anatomical Record. *263*, 361–6, 2001.
2. Cannon B, Nedergaard J. Brown adipose tissue: function and physiological significance. Physiological Reviews. *84*, 277–359, 2004.
3. Choi JH, Gimble JM, Lee K, Marra KG, Rubin JP, Yoo JJ, Vunjak-Novakovic G, Kaplan DL. Adipose tissue engineering for soft tissue regeneration. Tissue Engineering. Part B, Reviews. *16*, 413–26, 2010.
4. Gomillion CT, Burg KJL. Stem cells and adipose tissue engineering. Biomaterials. *27*, 6052–63, 2006.
5. Frühbeck G. Overview of adipose tissue and its role in obesity and metabolic disorders. Methods in Molecular Biology. *456*, 1–22, 2008.
6. Kahn CR. Medicine. Can we nip obesity in its vascular bud? Science. *322*, 542–3, 2008.
7. Gesta S, Tseng Y-H, Kahn CR. Developmental Origin of Fat: Tracking Obesity to Its Source. Cell. *131*, 242–56, 2007.
8. Gimble JM, Bunnell BA, Frazier T, Rowan B, Shah F, Thomas-Porch C, Wu X. Adipose-derived stromal/stem cells: a primer. Organogenesis. *9*, 3–10, 2013.
9. Bauer-Kreisel P, Goepferich A, Blunk T. Cell-delivery therapeutics for adipose tissue regeneration. Advanced Drug Delivery Reviews. *62*, 798–813, 2010.
10. Trayhurn P. Adipocyte biology. Obesity Reviews : An Official Journal of the International Association for the Study of Obesity. *8 Suppl 1*, 41–4, 2007.
11. Chun T-H, Hotary KB, Sabeh F, Saltiel AR, Allen ED, Weiss SJ. A pericellular collagenase directs the 3-dimensional development of white adipose tissue. Cell. *125*, 577–91, 2006.
12. Guerre-Millo M. Adipose tissue hormones. Journal of Endocrinological Investigation. *25*, 855–61, 2002.
13. Hausman DB, DiGirolamo M, Bartness TJ, Hausman GJ, Martin RJ. The biology of white adipocyte proliferation. Obesity Reviews : An Official Journal of the International Association for the Study of Obesity. *2*, 239–54, 2001.
14. Flynn L, Semple JL, Woodhouse KA. Decellularized placental matrices for adipose tissue engineering. Journal of Biomedical Materials Research. Part A. *79*, 359–69, 2006.
15. Mahoney CM, Imbarlina C, Yates CC, Marra KG. Current Therapeutic Strategies for Adipose Tissue Defects/Repair Using Engineered Biomaterials and Biomolecule Formulations. Frontiers in Pharmacology. *9*, 507, 2018.
16. Miller AM, Steiner CA, Barrett ML, Fingar KR, Elixhauser A. Breast Reconstruction Surgery for Mastectomy in Hospital Inpatient and Ambulatory Settings, 2009–2014: Statistical Brief #228. Healthc. Cost Util. Proj. Stat. Briefs. 2017.
17. Tachi M, Yamada A. Choice of flaps for breast reconstruction. International Journal of Clinical Oncology. *10*, 289–97, 2005.
18. Rocco N, Gloria A, De Santis R, Catanuto G, Nava MB, Accurso A. Improving Outcomes In Breast Reconstruction: From Implant-Based Techniques Towards Tissue Regeneration. Procedia CIRP. *49*, 183–7, 2016.

19. Monfort A, Izeta A. Strategies for Human Adipose Tissue Repair and Regeneration. Journal of Cosmetics, Dermatological Sciences and Applications. *2*, 93–107, 2012.

20. Hong SJ, Lee JH, Hong SM, Park CH. Enhancing the viability of fat grafts using new transfer medium containing insulin and β-fibroblast growth factor in autologous fat transplantation. Journal of Plastic, Reconstructive & Aesthetic Surgery. *63*, 1202–8, 2010.

21. Patrick CW. Breast Tissue Engineering. Annual Review of Biomedical Engineering. *6*, 109–30, 2004.

22. Griffith LG. Emerging design principles in biomaterials and scaffolds for tissue engineering. Annals of the New York Academy of Sciences. *961*, 83–95, 2002.

23. Fuchs JR, Nasseri BA, Vacanti JP. Tissue engineering: a 21st century solution to surgical reconstruction. The Annals of Thoracic Surgery. *72*, 577–91, 2001.

24. Beahm EK, Walton RL, Patrick CW. Progress in adipose tissue construct development. Clinics in Plastic Surgery. *30*, 547–58, 2003.

25. Gomillion CT, Burg KJL. Stem cells and adipose tissue engineering. Biomaterials. *27*, 6052–63, 2006.

26. Hemmrich K, von Heimburg D, Rendchen R, Di Bartolo C, Milella E, Pallua N. Implantation of preadipocyte-loaded hyaluronic acid-based scaffolds into nude mice to evaluate potential for soft tissue engineering. Biomaterials. *26*, 7025–37, 2005.

27. De Ugarte DA, Ashjian PH, Elbarbary A, Hedrick MH. Future of fat as raw material for tissue regeneration. Annals of Plastic Surgery. *50*, 215–9, 2003.

28. Ailhaud G, Grimaldi P, Négrel R. Cellular and molecular aspects of adipose tissue development. Annual Review of Nutrition. *12*, 207–33, 1992.

29. Rodriguez A-M, Elabd C, Delteil F, Astier J, Vernochet C, Saint-Marc P, Guesnet J, Guezennec A, Amri E-Z, Dani C, Ailhaud G. Adipocyte differentiation of multipotent cells established from human adipose tissue. Biochemical and Biophysical Research Communications. *315*, 255–63, 2004.

30. Dani C. Embryonic Stem Cell-Derived Adipogenesis. Cells Tissues Organs. *165*, 173–80, 1999.

31. Kang X, Xie Y, Powell HM, James Lee L, Belury MA, Lannutti JJ, Kniss DA. Adipogenesis of murine embryonic stem cells in a three-dimensional culture system using electrospun polymer scaffolds. Biomaterials. *28*, 450–8, 2007.

32. Hillel AT, Varghese S, Petsche J, Shamblott MJ, Elisseeff JH. Embryonic germ cells are capable of adipogenic differentiation in vitro and in vivo. Tissue Engineering. Part A. *15*, 479–86, 2009.

33. Gimble JM, Katz AJ, Bunnell BA. Adipose-derived stem cells for regenerative medicine. Circulation Research. *100*, 1249–60, 2007.

34. Brown BN, Barnes CA, Kasick RT, Michel R, Gilbert TW, Beer-Stolz D, Castner DG, Ratner BD, Badylak SF. Surface characterization of extracellular matrix scaffolds. Biomaterials. *31*, 428–37, 2010.

35. Bencherif SA, Sands RW, Bhatta D, Arany P, Verbeke CS, Edwards DA, Mooney DJ. Injectable preformed scaffolds with shape-memory properties. Proceedings of the National Academy of Sciences. *109*, 19590–5, 2012.

36. Londono R, Badylak SF. Biologic Scaffolds for Regenerative Medicine: Mechanisms of In vivo Remodeling. Annals of Biomedical Engineering. *43*, 577–92, 2015.

37. Place ES, George JH, Williams CK, Stevens MM. Synthetic polymer scaffolds for tissue engineering. Chemical Society Reviews. *38*, 1139–51, 2009.

38. Brett E, Chung N, Leavitt WT, Momeni A, Longaker MT, Wan DC. A Review of Cell-Based Strategies for Soft Tissue Reconstruction. Tissue Engineering. Part B, Reviews. *23*, 336–46, 2017.

39. Bunnell BA, Flaat M, Gagliardi C, Patel B, Ripoll C. Adipose-derived stem cells: Isolation, expansion and differentiation. Methods. *45*, 115–20, 2008.

40. Philips BJ, Marra KG, Rubin JP. Healing of grafted adipose tissue: current clinical applications of adipose-derived stem cells for breast and face reconstruction. Wound Repair and Regeneration : Official Publication of the Wound Healing Society [and] the European Tissue Repair Society. *22*, 11–3, 2014.

41. Baer PC. Adipose-derived mesenchymal stromal/stem cells: An update on their phenotype in vivo and in vitro. World Journal of Stem Cells. *6*, 256–65, 2014.

42. Lindroos B, Suuronen R, Miettinen S. The Potential of Adipose Stem Cells in Regenerative Medicine. Stem Cell Reviews and Reports. *7*, 269–91, 2011.

43. Fraser JK, Wulur I, Alfonso Z, Hedrick MH. Fat tissue: an underappreciated source of stem cells for biotechnology. Trends in Biotechnology. *24*, 150–4, 2006.

44. Zuk PA, Zhu M, Ashjian P, De Ugarte DA, Huang JI, Mizuno H, Alfonso ZC, Fraser JK, Benhaim P, Hedrick MH. Human adipose tissue is a source of multipotent stem cells. Molecular Biology of the Cell. *13*, 4279–95, 2002.

45. Rosen ED, MacDougald OA. Adipocyte differentiation from the inside out. Nature Reviews Molecular Cell Biology. *7*, 885–96, 2006.

46. Green H, Kehinde O. An established preadipose cell line and its differentiation in culture II. Factors affecting the adipose conversion. Cell. *5*, 19–27, 1975.

47. Guo L, Li X, Tang Q-Q. Transcriptional regulation of adipocyte differentiation: a central role for CCAAT/enhancer-binding protein (C/EBP) β. The Journal of Biological Chemistry. *290*, 755–61, 2015.

48. Haslam DW, James WPT. Obesity. Lancet. *366*, 1197–209, 2005.

49. Entenmann G, Hauner H. Relationship between replication and differentiation in cultured human adipocyte precursor cells. American Journal of Physiology-Cell Physiology. *270*, C1011–6, 1996.

50. Tang Q-Q, Otto TC, Lane MD. Mitotic clonal expansion: A synchronous process required for adipogenesis. Proceedings of the National Academy of Sciences. *100*, 44–9, 2003.

51. Farmer SR. Transcriptional control of adipocyte formation. Cell Metabolism. *4*, 263–73, 2006.

52. Ntambi JM, Young-Cheul K. Adipocyte Differentiation and Gene Expression. The Journal of Nutrition. *130*, 3122–6, 2000.

53. Zhang Y, Khan D, Delling J, Tobiasch E. Mechanisms underlying the osteo- and adipo-differentiation of human mesenchymal stem cells. TheScientificWorldJournal. *2012*, 793823, 2012.

54. Gregoire FM, Smas CM, Sul HS. Understanding adipocyte differentiation. Physiological Reviews. *78*, 783–809, 1998.

55. Tang QQ, Lane MD. Adipogenesis: from stem cell to adipocyte. Annual Review of Biochemistry. *81*, 715–36, 2012.

56. Widberg CH, Newell FS, Bachmann AW, Ramnoruth SN, Spelta MC, Whitehead JP, Hutley LJ, Prins JB. Fibroblast growth factor receptor 1 is a key regulator of early adipogenic events in human preadipocytes. American Journal of Physiology - Endocrinology and Metabolism. *296*, 121–31, 2009.

57. Lu Q, Li M, Zou Y, Cao T. Delivery of basic fibroblast growth factors from heparinized decellularized adipose tissue stimulates potent de novo adipogenesis. Journal of Controlled Release. *174*, 43–50, 2014.

58. Hynes RO. The extracellular matrix: not just pretty fibrils. Science. *326*, 1216–9, 2009.

59. Ullah M, Sittinger M, Ringe J. Extracellular matrix of adipogenically differentiated mesenchymal stem cells reveals a network of collagen filaments, mostly interwoven by hexagonal structural units. Matrix Biology. *32*, 452–65, 2013.

60. Gattazzo F, Urciuolo A, Bonaldo P. Extracellular matrix: a dynamic microenvironment for stem cell niche. Biochimica et Biophysica Acta. *1840*, 2506–19, 2014.

61. Daley WP, Peters SB, Larsen M. Extracellular matrix dynamics in development and regenerative medicine. Journal of Cell Science. *121*, 255–64, 2008.

62. Discher DE, Mooney DJ, Zandstra PW. Growth factors, matrices, and forces combine and control stem cells. Science. *324*, 1673–7, 2009.

63. Peerani R, Zandstra PW. Enabling stem cell therapies through synthetic stem cell-niche engineering. The Journal of Clinical Investigation. *120*, 60–70, 2010.

64. Pera MF, Tam PPL. Extrinsic regulation of pluripotent stem cells. Nature. *465*, 713–20, 2010.

65. Watt FM, Fujiwara H. Cell-extracellular matrix interactions in normal and diseased skin. Cold Spring Harbor Perspectives in Biology. *3*, 1–14, 2011.

66. Nakayama KH, Batchelder CA, Lee CI, Tarantal AF. Decellularized rhesus monkey kidney as a three-dimensional scaffold for renal tissue engineering. Tissue Engineering. Part A. *16*, 2207–16, 2010.

67. Soto-Gutierrez A, Yagi H, Uygun BE, Navarro-Alvarez N, Uygun K, Kobayashi N, Yang Y-G, Yarmush ML. Cell delivery: from cell transplantation to organ engineering. Cell Transplantation. *19*, 655–65, 2010.

68. Song JJ, Ott HC. Organ engineering based on decellularized matrix scaffolds. Trends in Molecular Medicine. *17*, 424–32, 2011.

69. Watt FM, Huck WTS. Role of the extracellular matrix in regulating stem cell fate. Nature Reviews Molecular Cell Biology. *14*, 467–73, 2013.

70. Ozbek S, Balasubramanian PG, Chiquet-Ehrismann R, Tucker RP, Adams JC. The evolution of extracellular matrix. Molecular Biology of the Cell. *21*, 4300–5, 2010.

71. Legate KR, Wickström SA, Fässler R. Genetic and cell biological analysis of integrin outside-in signaling. Genes & Development. *23*, 397–418, 2009.

72. Lu P, Weaver VM, Werb Z. The extracellular matrix: a dynamic niche in cancer

progression. The Journal of Cell Biology. *196*, 395–406, 2012.

73. Reilly GC, Engler AJ. Intrinsic extracellular matrix properties regulate stem cell differentiation. Journal of Biomechanics. *43*, 55–62, 2010.

74. Mammoto T, Ingber DE. Mechanical control of tissue and organ development. Development. *137*, 1407–20, 2010.

75. Moore SW, Roca-Cusachs P, Sheetz MP. Stretchy Proteins on Stretchy Substrates: The Important Elements of Integrin-Mediated Rigidity Sensing. Developmental Cell. *19*, 194–206, 2010.

76. DuFort CC, Paszek MJ, Weaver VM. Balancing forces: architectural control of mechanotransduction. Nature Reviews Molecular Cell Biology. *12*, 308–19, 2011.

77. Gattazzo F, Urciuolo A, Bonaldo P. Extracellular matrix: a dynamic microenvironment for stem cell niche. Biochimica et Biophysica Acta. *1840*, 2506–19, 2014.

78. Schwarzbauer J. Basement membranes: Putting up the barriers. Current Biology : CB. *9*, R242-4, 1999.

79. Mariman ECM, Wang P. Adipocyte extracellular matrix composition, dynamics and role in obesity. Cellular and Molecular Life Sciences. *67*, 1277–92, 2010.

80. Badylak SF. Regenerative medicine and developmental biology: The role of the extracellular matrix. Anatomical Record - Part B New Anatomist. *287*, 36–41, 2005.

81. Rozario T, DeSimone DW. The extracellular matrix in development and morphogenesis: a dynamic view. Developmental Biology. *341*, 126–40, 2010.

82. Ricard-Blum S. The collagen family. Cold Spring Harbor Perspectives in Biology. *3*, a004978, 2011.

83. Gordon MK, Hahn RA. Collagens. Cell and Tissue Research. *339*, 247–57, 2010.

84. Khoshnoodi J, Cartailler J-P, Alvares K, Veis A, Hudson BG. Molecular Recognition in the Assembly of Collagens: Terminal Noncollagenous Domains Are Key Recognition Modules in the Formation of Triple Helical Protomers. Journal of Biological Chemistry. *281*, 38117–21, 2006.

85. Bella J, Liu J, Kramer R, Brodsky B, Berman HM. Conformational Effects of Gly–X–Gly Interruptions in the Collagen Triple Helix. Journal of Molecular Biology. *362*, 298–311, 2006.

86. Shaw LM, Olsen BR. FACIT collagens: diverse molecular bridges in extracellular matrices. Trends in Biochemical Sciences. *16*, 191–4, 1991.

87. Kadler KE, Baldock C, Bella J, Boot-Handford RP. Collagens at a glance. Journal of Cell Science. *120*, 1955–8, 2007.

88. Myllyharju J, Kivirikko KI. Collagens, modifying enzymes and their mutations in humans, flies and worms. Trends in Genetics. *20*, 33–43, 2004.

89. Khan T, Muise ES, Iyengar P, Wang Z V., Chandalia M, Abate N, Zhang BB, Bonaldo P, Chua S, Scherer PE. Metabolic Dysregulation and Adipose Tissue Fibrosis: Role of Collagen VI. Molecular and Cellular Biology. *29*, 1575–91, 2009.

90. Ibrahimi A, Bonino F, Bardon S, Ailhaud G, Dani C. Essential role of collagens for terminal differentiation of preadipocytes. Biochemical and Biophysical Research Communications. *187*, 1314–22, 1992.

91. Kivirikko KI, Myllylä R, Pihlajaniemi T. Protein hydroxylation: prolyl 4-hydroxylase, an enzyme with four cosubstrates and a multifunctional subunit. FASEB Journal : Official Publication of the Federation of American Societies for Experimental Biology. *3*, 1609–17, 1989.

92. Senyürek I, Kempf WE, Klein G, Maurer A, Kalbacher H, Schäfer L, Wanke I, Christ C, Stevanovic S, Schaller M, Rousselle P, Garbe C, Biedermann T, Schittek B. Processing of laminin α chains generates peptides involved in wound healing and host defense. Journal of Innate Immunity. *6*, 467–84, 2014.

93. Hohenester E. Structural biology of laminins. Essays in Biochemistry. *63*, 285–95, 2019.

94. Aumailley M, Bruckner-Tuderman L, Carter WG, Deutzmann R, Edgar D, Ekblom P, Engel J, Engvall E, Hohenester E, Jones JCR, Kleinman HK, Marinkovich MP, Martin GR, Mayer U, Meneguzzi G, Miner JH, Miyazaki K, Patarroyo M, Paulsson M, et al. A simplified laminin nomenclature. Matrix Biology : Journal of the International Society for Matrix Biology. *24*, 326–32, 2005.

95. Morita A, Sugimoto E, Kitagawa Y. Post-translational assembly and glycosylation of laminin subunits in parietal endoderm-like F9 cells. Biochemical Journal. *229*, 259–64, 1985.

96. Schneider H, Mühle C, Pacho F. Biological function of laminin-5 and pathogenic impact of its deficiency. European Journal of Cell Biology. *86*, 701–17, 2007.

97. Yurchenco PD, Quan Y, Colognato H, Mathus T, Harrison D, Yamada Y, O'Rear JJ. The chain of laminin-1 is independently secreted and drives secretion of its - and -chain partners. Proceedings of the National Academy of Sciences. *94*, 10189–94, 1997.

98. Tzu J, Marinkovich MP. Bridging structure with function: structural, regulatory, and developmental role of laminins. The International Journal of Biochemistry & Cell Biology. *40*, 199–214, 2008.

99. Givant-Horwitz V, Davidson B, Reich R. Laminin-induced signaling in tumor cells. Cancer Letters. *223*, 1–10, 2005.

100. Wondimu Z, Geberhiwot T, Ingerpuu S, Juronen E, Xie X, Lindbom L, Doi M, Kortesmaa J, Thyboll J, Tryggvason K, Fadeel B, Patarroyo M. An endothelial laminin isoform, laminin 8 (alpha4beta1gamma1), is secreted by blood neutrophils, promotes neutrophil migration and extravasation, and protects neutrophils from apoptosis. Blood. *104*, 1859–66, 2004.

101. Nie J, Sage EH. SPARC functions as an inhibitor of adipogenesis. Journal of Cell Communication and Signaling. *3*, 247–54, 2009.

102. Nie J, Sage EH. SPARC Inhibits Adipogenesis by Its Enhancement of β-Catenin Signaling. Journal of Biological Chemistry. *284*, 1279–90, 2009.

103. Pankov R, Yamada KM. Fibronectin at a glance. Journal of Cell Science. *115*, 3861–3, 2002.

104. Huang G, Greenspan DS. ECM roles in the function of metabolic tissues. Trends in Endocrinology and Metabolism: TEM. *23*, 16–22, 2012.

105. Divoux A, Clément K. Architecture and the extracellular matrix: the still unappreciated components of the adipose tissue. Obesity Reviews : An Official Journal of the International Association for the Study of Obesity. *12*, e494-503, 2011.

106. Napolitano L. The differentiation of white adipose cells. An electron microscope study.

The Journal of Cell Biology. *18*, 663–79, 1963.

107. Pierleoni C, Verdenelli F, Castellucci M, Cinti S. Fibronectins and basal lamina molecules expression in human subcutaneous white adipose tissue. European Journal of Histochemistry : EJH. *42*, 183–8, 1998.

108. Antras J, Hilliou F, Redziniak G, Pairault J. Decreased biosynthesis of actin and cellular fibronectin during adipose conversion of 3T3-F442A cells. Reorganization of the cytoarchitecture and extracellular matrix fibronectin. Biology of the Cell. *66*, 247–54, 1989.

109. Sillat T, Saat R, Pöllänen R, Hukkanen M, Takagi M, Konttinen YT. Basement membrane collagen type IV expression by human mesenchymal stem cells during adipogenic differentiation. Journal of Cellular and Molecular Medicine. *16*, 1485–95, 2012.

110. Kubo Y, Kaidzu S, Nakajima I, Takenouchi K, Nakamura F. Organization of extracellular matrix components during differentiation of adipocytes in long-term culture. In Vitro Cellular & Developmental Biology. Animal. *36*, 38–44, 2000.

111. Cheng Y-S, Champliaud M-F, Burgeson RE, Marinkovich MP, Yurchenco PD. Self-assembly of Laminin Isoforms. Journal of Biological Chemistry. *272*, 31525–32, 1997.

112. Timpl R, Brown JC. Supramolecular assembly of basement membranes. BioEssays. *18*, 123–32, 1996.

113. Nakajima I, Muroya S, Tanabe R, Chikuni K. Extracellular matrix development during differentiation into adipocytes with a unique increase in type V and VI collagen. Biology of the Cell. *94*, 197–203, 2002.

114. Taleb S, Cancello R, Clément K, Lacasa D. Cathepsin S Promotes Human Preadipocyte Differentiation: Possible Involvement of Fibronectin Degradation. Endocrinology. *147*, 4950–9, 2006.

115. O'Connor KC, Song H, Rosenzweig N, Jansen DA. Extracellular matrix substrata alter adipocyte yield and lipogenesis in primary cultures of stromal-vascular cells from human adipose. Biotechnology Letters. *25*, 1967–72, 2003.

116. Spiegelman BM, Ginty CA. Fibronectin Modulation of Cell Shape and Lipogenic Gene Expression in 3T3-Adipocytes. Cell Copyright. *35*, 657–66, 1963.

117. Rodríguez Fernández JL, Ben-Ze'ev A. Regulation of fibronectin, integrin and cytoskeleton expression in differentiating adipocytes: inhibition by extracellular matrix and polylysine. Differentiation. *42*, 65–74, 1989.

118. Croissandeau G, Chrétien M, Mbikay M. Involvement of matrix metalloproteinases in the adipose conversion of 3T3-L1 preadipocytes. The Biochemical Journal. *364*, 739–46, 2002.

119. Achilli T-M, Meyer J, Morgan JR. Advances in the formation, use and understanding of multi-cellular spheroids. Expert Opinion on Biological Therapy. *12*, 1347–60, 2012.

120. Fennema E, Rivron N, Rouwkema J, van Blitterswijk C, de Boer J. Spheroid culture as a tool for creating 3D complex tissues. Trends in Biotechnology. *31*, 108–15, 2013.

121. Kleinman HK, Philp D, Hoffman MP. Role of the extracellular matrix in morphogenesis. Current Opinion in Biotechnology. *14*, 526–32, 2003.

122. Lin RZ, Chang HY. Recent advances in three-dimensional multicellular spheroid culture

for biomedical research. Biotechnology Journal. *3*, 1172–84, 2008.

123. Cesarz Z, Tamama K. Spheroid Culture of Mesenchymal Stem Cells. Stem Cells International. *2016*, 9176357, 2016.

124. Mueller-Klieser W. Multicellular spheroids. A review on cellular aggregates in cancer research. Journal of Cancer Research and Clinical Oncology. *113*, 101–22, 1987.

125. Sart S, Tsai A-C, Li Y, Ma T. Three-Dimensional Aggregates of Mesenchymal Stem Cells: Cellular Mechanisms, Biological Properties, and Applications. Tissue Engineering Part B: Reviews. *20*, 365–80, 2014.

126. Sasai Y. Cytosystems dynamics in self-organization of tissue architecture. Nature. *493*, 318–26, 2013.

127. Sasai Y. Next-Generation Regenerative Medicine: Organogenesis from Stem Cells in 3D Culture. Cell Stem Cell. *12*, 520–30, 2013.

128. Holtfreter J. A study of the mechanics of gastrulation. Part I. Journal of Experimental Zoology. *94*, 261–318, 1943.

129. Moscona A, Moscona H. The dissociation and aggregation of cells from organ rudiments of the early chick embryo. Journal of Anatomy. *86*, 287–301, 1952.

130. Pedersen JA, Swartz MA. Mechanobiology in the Third Dimension. Annals of Biomedical Engineering. *33*, 1469–90, 2005.

131. Pampaloni F, Reynaud EG, Stelzer EHK. The third dimension bridges the gap between cell culture and live tissue. Nature Reviews Molecular Cell Biology. *8*, 839–45, 2007.

132. Tsai A-C, Liu Y, Yuan X, Ma T. Compaction, Fusion, and Functional Activation of Three-Dimensional Human Mesenchymal Stem Cell Aggregate. Tissue Engineering Part A. *21*, 1705–19, 2015.

133. Laschke MW, Menger MD. Life is 3D: Boosting Spheroid Function for Tissue Engineering. Trends in Biotechnology. *35*, 133, 2017.

134. Groebe K, Mueller-Klieser W. On the relation between size of necrosis and diameter of tumor spheroids. International Journal of Radiation Oncology*Biology*Physics. *34*, 395–401, 1996.

135. Zimmermann JA, Mcdevitt TC. Pre-conditioning mesenchymal stromal cell spheroids for immunomodulatory paracrine factor secretion. Cytotherapy. *16*, 331–45, 2014.

136. Kelm JM, Timmins NE, Brown CJ, Fussenegger M, Nielsen LK. Method for generation of homogeneous multicellular tumor spheroids applicable to a wide variety of cell types. Biotechnology and Bioengineering. *83*, 173–80, 2003.

137. Foty R. A simple hanging drop cell culture protocol for generation of 3D spheroids. Journal of Visualized Experiments : JoVE. *51*, 2720, 2011.

138. Tung Y-C, Hsiao AY, Allen SG, Torisawa Y, Ho M, Takayama S. High-throughput 3D spheroid culture and drug testing using a 384 hanging drop array. The Analyst. *136*, 473–8, 2011.

139. Okuyama T, Yamazoe H, Mochizuki N, Khademhosseini A, Suzuki H, Fukuda J. Preparation of arrays of cell spheroids and spheroid-monolayer cocultures within a microfluidic device. Journal of Bioscience and Bioengineering. *110*, 572–6, 2010.

140. Lin RZ, Chou LF, Chien CCM, Chang HY. Dynamic analysis of hepatoma spheroid

formation: Roles of E-cadherin and beta1-integrin. Cell and Tissue Research. *324*, 411–22, 2006.

141. Bao B, Jiang J, Yanase T, Nishi Y, Morgan JR. Connexon-mediated cell adhesion drives microtissue self-assembly. FASEB Journal : Official Publication of the Federation of American Societies for Experimental Biology. *25*, 255–64, 2011.

142. Robinson EE, Foty RA, Corbett SA. Fibronectin matrix assembly regulates alpha5beta1-mediated cell cohesion. Molecular Biology of the Cell. *15*, 973–81, 2004.

143. Shimazui T, Schalken JA, Kawai K, Kawamoto R, van Bockhoven A, Oosterwijk E, Akaza H. Role of complex cadherins in cell-cell adhesion evaluated by spheroid formation in renal cell carcinoma cell lines. Oncology Reports. *11*, 357–60, 2004.

144. Ivascu A, Kubbies M. Diversity of cell-mediated adhesions in breast cancer spheroids. International Journal of Oncology. *31*, 1403–13, 2007.

145. Sabol RA, Bowles AC, Côté A, Wise R, Pashos N, Bunnell BA. Therapeutic Potential of Adipose Stem Cells. Advances in Experimental Medicine and Biology. 2018.

146. Egger D, Tripisciano C, Weber V, Dominici M, Kasper C. Dynamic Cultivation of Mesenchymal Stem Cell Aggregates. Bioengineering. *5*, 48, 2018.

147. Bartosh TJ, Ylöstalo JH, Mohammadipoor A, Bazhanov N, Coble K, Claypool K, Lee RH, Choi H, Prockop DJ. Aggregation of human mesenchymal stromal cells (MSCs) into 3D spheroids enhances their antiinflammatory properties. Proceedings of the National Academy of Sciences of the United States of America. *107*, 13724–9, 2010.

148. Ylöstalo JH, Bartosh TJ, Coble K, Prockop DJ. Human mesenchymal stem/stromal cells cultured as spheroids are self-activated to produce prostaglandin E2 that directs stimulated macrophages into an anti-inflammatory phenotype. Stem Cells. *30*, 2283–96, 2012.

149. Kinney MA, Hookway TA, Wang Y, McDevitt TC. Engineering three-dimensional stem cell morphogenesis for the development of tissue models and scalable regenerative therapeutics. Annals of Biomedical Engineering. *42*, 352–67, 2014.

150. Zhang S, Liu P, Chen L, Wang Y, Wang Z, Zhang B. The effects of spheroid formation of adipose-derived stem cells in a microgravity bioreactor on stemness properties and therapeutic potential. Biomaterials. *41*, 15–25, 2015.

151. Kapur SK, Wang X, Shang H, Yun S, Li X, Feng G, Khurgel M, Katz a J. Human adipose stem cells maintain proliferative, synthetic and multipotential properties when suspension cultured as self-assembling spheroids. Biofabrication. *4*, 25004, 2012.

152. Yoon HH, Bhang SH, Shin J-Y, Shin J, Kim B-S. Enhanced cartilage formation via three-dimensional cell engineering of human adipose-derived stem cells. Tissue Engineering. Part A. *18*, 1949–56, 2012.

153. Zhang K, Yan S, Li G, Cui L, Yin J. In-situ birth of MSCs multicellular spheroids in poly(l -glutamic acid)/chitosan scaffold for hyaline-like cartilage regeneration. Biomaterials. *71*, 24–34, 2015.

154. Murata D, Tokunaga S, Tamura T, Kawaguchi H, Miyoshi N, Fujiki M, Nakayama K, Misumi K. A preliminary study of osteochondral regeneration using a scaffold-free three-dimensional construct of porcine adipose tissue-derived mesenchymal stem cells. Journal of Orthopaedic Surgery and Research. *10*, 35, 2015.

155. Langenbach F, Naujoks C, Smeets R, Berr K, Depprich R, Kübler N, Handschel J.

Scaffold-free microtissues: differences from monolayer cultures and their potential in bone tissue engineering. Clinical Oral Investigations. *17*, 9–17, 2013.

156. Gentile C. Filling the Gaps between the In Vivo and In Vitro Microenvironment: Engineering of Spheroids for Stem Cell Technology. Current Stem Cell Research & Therapy. *11*, 652–65, 2016.

157. Norotte C, Marga FS, Niklason LE, Forgacs G. Scaffold-free vascular tissue engineering using bioprinting. Biomaterials. *30*, 5910–7, 2009.

158. Ho VHB, Guo WM, Huang CL, Ho SF, Chaw SY, Tan EY, Ng KW, Loo JSC. Manipulating Magnetic 3D Spheroids in Hanging Drops for Applications in Tissue Engineering and Drug Screening. Advanced Healthcare Materials. *2*, 1430–4, 2013.

159. Olsen TR, Mattix B, Casco M, Herbst A, Williams C, Tarasidis A, Simionescu D, Visconti RP, Alexis F. Manipulation of cellular spheroid composition and the effects on vascular tissue fusion. Acta Biomaterialia. *13*, 188–98, 2015.

160. Bateman ME, Strong AL, Gimble JM, Bunnell BA. Concise Review: Using Fat to Fight Disease: A Systematic Review of Nonhomologous Adipose-Derived Stromal/Stem Cell Therapies. Stem Cells. *36*, 1311–28, 2018.

161. Frith JE, Thomson B, Genever PG. Dynamic three-dimensional culture methods enhance mesenchymal stem cell properties and increase therapeutic potential. Tissue Engineering Part C: Methods. *16*, 735–49, 2009.

162. Stricker S, Knaus P, Simon H-G. Putting Cells into Context. Frontiers in Cell and Developmental Biology. *5*, 32, 2017.

163. Casey RC, Burleson KM, Skubitz KM, Pambuccian SE, Oegema TR, Ruff LE, Skubitz APN. B1-Integrins Regulate the Formation and Adhesion of Ovarian Carcinoma Multicellular Spheroids. American Journal of Pathology. *159*, 2071–80, 2001.

164. Miyamoto Y, Ikeuchi M, Noguchi H, Yagi T, Hayashi S. Enhanced Adipogenic Differentiation of Human Adipose-Derived Stem Cells in an In Vitro Microenvironment: The Preparation of Adipose-Like Microtissues Using a Three-Dimensional Culture. Cell Medicine. *9*, 35–44, 2016.

165. Wang W, Itaka K, Ohba S, Nishiyama N, Chung U il, Yamasaki Y, Kataoka K. 3D spheroid culture system on micropatterned substrates for improved differentiation efficiency of multipotent mesenchymal stem cells. Biomaterials. *30*, 2705–15, 2009.

166. Scadden DT. The stem-cell niche as an entity of action. Nature. *441*, 1075–9, 2006.

167. Watt FM, Hogan BLM. Out of Eden: stem cells and their niches. Science. *287*, 1427–30, 2000.

168. Mouw JK, Ou G, Weaver VM. Extracellular matrix assembly: a multiscale deconstruction. Nature Reviews. Molecular Cell Biology. *15*, 771–85, 2014.

169. Murphy KC, Whitehead J, Falahee PC, Zhou D, Simon SI, Leach JK. Multifactorial Experimental Design to Optimize the Anti-Inflammatory and Proangiogenic Potential of Mesenchymal Stem Cell Spheroids. Stem Cells. *35*, 1493–504, 2017.

170. Xu Y, Shi T, Xu A, Zhang L. 3D spheroid culture enhances survival and therapeutic capacities of MSCs injected into ischemic kidney. Journal of Cellular and Molecular Medicine. *20*, 1203–13, 2016.

171. Wang K, Yu L-Y, Jiang L-Y, Wang H-B, Wang C-Y, Luo Y. The paracrine effects of

adipose-derived stem cells on neovascularization and biocompatibility of a macroencapsulation device. Acta Biomaterialia. *15*, 65–76, 2015.

172. Muhr C. Establishment and Characterization of a Human 3-D Fat Model. Doctoral thesis. 2012.

173. Studer D, Lischer S, Jochum W, Ehrbar M, Zenobi-Wong M, Maniura-Weber K. Ribosomal protein l13a as a reference gene for human bone marrow-derived mesenchymal stromal cells during expansion, adipo-, chondro-, and osteogenesis. Tissue Engineering. Part C, Methods. *18*, 761–71, 2012.

174. Cheng N-C, Wang S, Young T-H. The influence of spheroid formation of human adipose-derived stem cells on chitosan films on stemness and differentiation capabilities. Biomaterials. *33*, 1748–58, 2012.

175. Robinson EE. Alpha5Beta1 Integrin Mediates Strong Tissue Cohesion. Journal of Cell Science. *116*, 377–86, 2003.

176. Yeh HY, Liu BH, Hsu SH. The calcium-dependent regulation of spheroid formation and cardiomyogenic differentiation for MSCs on chitosan membranes. Biomaterials. *33*, 8943–54, 2012.

177. Bartosh TJ, Ylöstalo JH, Bazhanov N, Kuhlman J, Prockop DJ. Dynamic compaction of human mesenchymal stem/precursor cells into spheres self-activates caspase-dependent IL1 signaling to enhance secretion of modulators of inflammation and immunity (PGE2, TSG6, and STC1). Stem Cells. *31*, 2443–56, 2013.

178. Huang G-S, Dai L-G, Yen BL, Hsu S. Spheroid formation of mesenchymal stem cells on chitosan and chitosan-hyaluronan membranes. Biomaterials. *32*, 6929–45, 2011.

179. Yeh H-Y, Liu B-H, Sieber M, Hsu S-H. Substrate-dependent gene regulation of self-assembled human MSC spheroids on chitosan membranes. BMC Genomics. *15*, 10, 2014.

180. Lee WY, Chang YH, Yeh YC, Chen CH, Lin KM, Huang CC, Chang Y, Sung HW. The use of injectable spherically symmetric cell aggregates self-assembled in a thermo-responsive hydrogel for enhanced cell transplantation. Biomaterials. *30*, 5505–13, 2009.

181. Sottile J, Hocking DC. Fibronectin Polymerization Regulates the Composition and Stability of Extracellular Matrix Fibrils and Cell-Matrix Adhesions. Molecular Biology of the Cell. *13*, 3546–59, 2002.

182. Bachman H, Nicosia J, Dysart M, Barker TH. Utilizing Fibronectin Integrin-Binding Specificity to Control Cellular Responses. Advances in Wound Care. *4*, 501–11, 2015.

183. Wittmann K, Storck K, Muhr C, Mayer H, Regn S, Staudenmaier R, Wiese H, Maier G, Bauer-Kreisel P, Blunk T. Development of volume-stable adipose tissue constructs using polycaprolactone-based polyurethane scaffolds and fibrin hydrogels. Journal of Tissue Engineering and Regenerative Medicine. *10*, E409–18, 2016.

184. Noro A, Sillat T, Virtanen I, Ingerpuu S, Bäck N, Konttinen YT, Korhonen M. Laminin Production and Basement Membrane Deposition by Mesenchymal Stem Cells upon Adipogenic Differentiation. Journal of Histochemistry & Cytochemistry. *61*, 719–30, 2013.

185. Zhang K, Song L, Wang J, Yan S, Li G, Cui L, Yin J. Strategy for constructing vascularized adipose units in poly(l -glutamic acid) hydrogel porous scaffold through inducing in-situ formation of ASCs spheroids. Acta Biomaterialia. *51*, 246–57, 2017.

186. Verseijden F, Posthumus-van Sluijs SJ, van Neck JW, Hofer SOP, Hovius SER, van Osch GJVM. Vascularization of prevascularized and non-prevascularized fibrin-based human adipose tissue constructs after implantation in nude mice. Journal of Tissue Engineering and Regenerative Medicine. *6*, 169–78, 2012.

187. Hynes RO. Stretching the boundaries of extracellular matrix research. Nature Reviews. Molecular Cell Biology. *15*, 761–3, 2014.

188. Costa EC, de Melo-Diogo D, Moreira AF, Carvalho MP, Correia IJ. Spheroids Formation on Non-Adhesive Surfaces by Liquid Overlay Technique: Considerations and Practical Approaches. Biotechnology Journal. *13*, 1700417, 2018.

189. Friedrich J, Seidel C, Ebner R, Kunz-Schughart LA. Spheroid-based drug screen: Considerations and practical approach. Nature Protocols. *4*, 309–24, 2009.

190. Nakajima I, Muroya S, Tanabe R-I, Chikuni K. Positive effect of collagen V and VI on triglyceride accumulation during differentiation in cultures of bovine intramuscular adipocytes. Differentiation; Research in Biological Diversity. *70*, 84–91, 2002.

191. Aratani Y, Kitagawa Y. Enhanced synthesis and secretion of type IV collagen and entactin during adipose conversion of 3T3-L1 cells and production of unorthodox laminin complex. Journal of Biological Chemistry. *263*, 16163–9, 1988.

192. Chaubey A, Burg KJL. Extracellular Matrix Components as Modulators of Adult Stem Cell Differentiation in an Adipose System. Journal of Bioactive and Compatible Polymers. *23*, 20–37, 2008.

193. Hausman GJ, Wright JT, Richardson RL. The Influence of Extracellular Matrix Substrata on Preadipocyte Development in Serum-Free Cultures of Stromal-Vascular Cells. Journal of Animal Science. *74*, 2117–28, 1996.

194. Vaicik MK, Thyboll Kortesmaa J, Movérare-Skrtic S, Kortesmaa J, Soininen R, Bergström G, Ohlsson C, Chong LY, Rozell B, Emont M, Cohen RN, Brey EM, Tryggvason K. Laminin α4 deficient mice exhibit decreased capacity for adipose tissue expansion and weight gain. PloS One. *9*, 109854, 2014.

195. Hausman GJ, Wright JT, Thomas GB. Vascular and cellular development in fetal adipose tissue: Lectin binding studies and immunocytochemistry for laminin and type IV collagen. Microvascular Research. *41*, 111–25, 1991.

196. Turner PA, Gurumurthy B, Bailey JL, Elks CM, Janorkar A V. Adipogenic differentiation of human adipose-derived stem cells grown as spheroids. Process Biochemistry. *59*, 312–20, 2017.

197. Wiesner M, Berberich O, Hoefner C, Blunk T, Bauer-Kreisel P. Gap junctional intercellular communication in adipose-derived stromal/stem cells is cell density-dependent and positively impacts adipogenic differentiation. Journal of Cellular Physiology. *233*, 3315–29, 2018.

198. Baraniak PR, Mcdevitt TC. Scaffold-free culture of mesenchymal stem cell spheroids in suspension preserves multilineage potential. Cell Tissue Res. *347*, 701–11, 2012.

199. McBeath R, Pirone DM, Nelson CM, Bhadriraju K, Chen CS. Cell shape, cytoskeletal tension, and RhoA regulate stem cell lineage commitment. Developmental Cell. *6*, 483–95, 2004.

200. Weiser B, Prantl L, Schubert TEO, Zellner J, Fischbach-Teschl C, Spruss T, Seitz AK, Tessmar J, Goepferich A, Blunk T. In vivo development and long-term survival of

engineered adipose tissue depend on in vitro precultivation strategy. Tissue Engineering. Part A. *14*, 275–84, 2008.

201. Mekhileri N V, Lim KS, Brown GCJ, Mutreja I, Schon BS, Hooper GJ, Woodfield TBF. Automated 3D bioassembly of micro-tissues for biofabrication of hybrid tissue engineered constructs. Biofabrication. *10*, 24103, 2018.

202. McMaster R, Hoefner C, Hrynevich A, Blum C, Wiesner M, Wittmann K, Dargaville TR, Bauer-Kreisel P, Groll J, Dalton PD, Blunk T. Tailored Melt Electrowritten Scaffolds for the Generation of Sheet-Like Tissue Constructs from Multicellular Spheroids. Advanced Healthcare Materials. *8*, e1801326, 2019.

203. Timpl R. Macromolecular organization of basement membranes. Current Opinion in Cell Biology. *8*, 618–24, 1996.

204. Hoshiba T, Kawazoe N, Tateishi T, Chen G. Development of extracellular matrices mimicking stepwise adipogenesis of mesenchymal stem cells. Advanced Materials. *22*, 3042–7, 2010.

205. Niimi T, Kumagai C, Okano M, Kitagawa Y. Differentiation-dependent expression of laminin-8 (alpha 4 beta 1 gamma 1) mRNAs in mouse 3T3-L1 adipocytes. Matrix Biology : Journal of the International Society for Matrix Biology. *16*, 223–30, 1997.

206. Yurchenco PD, O'Rear JJ. Basement membrane assembly. Methods in Enzymology. *245*, 489–518, 1994.

207. Matsui C, Wang CK, Nelson CF, Bauer EA, Hoeffler WK. The assembly of laminin-5 subunits. The Journal of Biological Chemistry. *270*, 23496–503, 1995.

208. Li J, Zhou L, Tran HT, Chen Y, Nguyen NE, Karasek MA, Marinkovich MP. Overexpression of laminin-8 in human dermal microvascular endothelial cells promotes angiogenesis-related functions. The Journal of Investigative Dermatology. *126*, 432–40, 2006.

209. Yurchenco PD, Patton BL. Developmental and pathogenic mechanisms of basement membrane assembly. Current Pharmaceutical Design. *15*, 1277–94, 2009.

210. Hsueh Y-S, Chen Y-S, Tai H-C, Mestak O, Chao S-C, Chen Y-Y, Shih Y, Lin J-F, Shieh M-J, Lin F-H. Laminin-Alginate Beads as Preadipocyte Carriers to Enhance Adipogenesis In Vitro and In Vivo. Tissue Engineering. Part A. *23*, 185–94, 2017.

211. Lee J, Abdeen AA, Tang X, Saif TA, Kilian KA. Matrix directed adipogenesis and neurogenesis of mesenchymal stem cells derived from adipose tissue and bone marrow. Acta Biomaterialia. *42*, 46–55, 2016.

212. Vaicik MK, Blagajcevic A, Ye H, Morse MC, Yang F, Goddi A, Brey EM, Cohen RN. The Absence of Laminin α4 in Male Mice Results in Enhanced Energy Expenditure and Increased Beige Subcutaneous Adipose Tissue. Endocrinology. *159*, 356–67, 2018.

213. Noro A, Sillat T, Virtanen I, Ingerpuu S, Bäck N, Konttinen YT, Korhonen M. Laminin production and basement membrane deposition by mesenchymal stem cells upon adipogenic differentiation. The Journal of Histochemistry and Cytochemistry : Official Journal of the Histochemistry Society. *61*, 719–30, 2013.

214. Nauta AJ, Fibbe WE. Immunomodulatory properties of mesenchymal stromal cells. Blood. *110*, 3499–506, 2007.

215. Caplan AI, Dennis JE. Mesenchymal stem cells as trophic mediators. Journal of Cellular Biochemistry. *98*, 1076–84, 2006.

216. Follin B, Juhl M, Cohen S, Perdersen AE, Kastrup J, Ekblond A. Increased Paracrine Immunomodulatory Potential of Mesenchymal Stromal Cells in Three-Dimensional Culture. Tissue Engineering. Part B, Reviews. *22*, 322–9, 2016.

217. Baker BM, Chen CS. Deconstructing the third dimension – how 3D culture microenvironments alter cellular cues. Journal of Cell Science. *125*, 3015–24, 2012.

218. Lee RH, Pulin AA, Seo MJ, Kota DJ, Ylostalo J, Larson BL, Semprun-Prieto L, Delafontaine P, Prockop DJ. Intravenous hMSCs improve myocardial infarction in mice because cells embolized in lung are activated to secrete the anti-inflammatory protein TSG-6. Cell Stem Cell. *5*, 54–63, 2009.

219. Madrigal M, Rao KS, Riordan NH. A review of therapeutic effects of mesenchymal stem cell secretions and induction of secretory modification by different culture methods. Journal of Translational Medicine. *12*, 260, 2014.

220. Garcia MA, Nelson WJ, Chavez N. Cell-Cell Junctions Organize Structural and Signaling Networks. Cold Spring Harbor Perspectives in Biology. *10*, a029181, 2018.

221. Franke WW. Discovering the molecular components of intercellular junctions--a historical view. Cold Spring Harbor Perspectives in Biology. *1*, a003061, 2009.

222. Costa P, Parsons M. New Insights into the Dynamics of Cell Adhesions. International Review of Cell and Molecular Biology. *283*, 57–91, 2010.

223. Smith SC, Theodorescu D. Learning therapeutic lessons from metastasis suppressor proteins. Nature Reviews Cancer. *9*, 253–64, 2009.

224. Valiunas V, Doronin S, Valiuniene L, Potapova I, Zuckerman J, Walcott B, Robinson RB, Rosen MR, Brink PR, Cohen IS. Human mesenchymal stem cells make cardiac connexins and form functional gap junctions. The Journal of Physiology. *555*, 617–26, 2004.

225. Rossello RA, Kohn DH. Gap junction intercellular communication: a review of a potential platform to modulate craniofacial tissue engineering. Journal of Biomedical Materials Research. Part B, Applied Biomaterials. *88*, 509–18, 2009.

226. Fukunaga I, Fujimoto A, Hatakeyama K, Aoki T, Nishikawa A, Noda T, Minowa O, Kurebayashi N, Ikeda K, Kamiya K. In Vitro Models of GJB2-Related Hearing Loss Recapitulate Ca2+ Transients via a Gap Junction Characteristic of Developing Cochlea. Stem Cell Reports. *7*, 1023–36, 2016.

227. Kamiya K, Fujinami Y, Hoya N, Okamoto Y, Kouike H, Komatsuzaki R, Kusano R, Nakagawa S, Satoh H, Fujii M, Matsunaga T. Mesenchymal stem cell transplantation accelerates hearing recovery through the repair of injured cochlear fibrocytes. The American Journal of Pathology. *171*, 214–26, 2007.

228. Oviedo-Orta E, Howard Evans W. Gap junctions and connexin-mediated communication in the immune system. Biochimica et Biophysica Acta. *1662*, 102–12, 2004.

229. Oviedo-Orta E, Gasque P, Evans WH. Immunoglobulin and cytokine expression in mixed lymphocyte cultures is reduced by disruption of gap junction intercellular communication. FASEB Journal : Official Publication of the Federation of American Societies for Experimental Biology. *15*, 768–74, 2001.

230. Runkle EA, Mu D. Tight junction proteins: from barrier to tumorigenesis. Cancer Letters. *337*, 41–8, 2013.

231. Yoon AY, Yun S, Yang H, Lim YH, Kim H. Expression of tight junction molecule in the human serum-induced aggregation of human abdominal adipose-derived stem cells in vitro. Development & Reproduction. *18*, 213–24, 2014.

232. Luissint A-C, Nusrat A, Parkos CA. JAM-related proteins in mucosal homeostasis and inflammation. Seminars in Immunopathology. *36*, 211–26, 2014.

233. Ebnet K. Junctional adhesion molecules (JAMs): more molecules with dual functions? Journal of Cell Science. *117*, 19–29, 2004.

234. Kummer D, Ebnet K. Junctional Adhesion Molecules (JAMs): The JAM-Integrin Connection. Cells. *7*, 25, 2018.

235. Alimperti S, Andreadis ST. CDH2 and CDH11 act as regulators of stem cell fate decisions. Stem Cell Research. *14*, 270–82, 2015.

236. Kawaguchi J, Kii I, Sugiyama Y, Takeshita S, Kudo A. The Transition of Cadherin Expression in Osteoblast Differentiation from Mesenchymal Cells: Consistent Expression of Cadherin-11 in Osteoblast Lineage. Journal of Bone and Mineral Research. *16*, 260–9, 2001.

List of Figures

List of Tables

List of Abbreviations

The specification of physical quantities is based on the guidelines of the international system of units. Special abbreviations for technical terms that are not included in the list are explained in the text.

Abbreviation	Prefix	Factor
p	pico-	10^{-12}
n	nano-	10^{-9}
µ	micro-	10^{-6}
m	milli-	10^{-3}
c	centi-	10^{-2}
k	kilo-	10^{3}

2D	two-dimensional
3D	three-dimensional
°C	degrees celsius
AFG	autologous fat grafting
ANOVA	analysis of variance
aP2	adipocyte protein 2/ fatty acid binding protein 4 (FABP4)
ASC	adipose-derived stem cell(s)
AT	adipose tissue
BAT	brown adipose tissue
BM	basement membrane or basal medium
BMSC	bone marrow-derived mesenchymal stem cell(s)
BODIPY	4,4-difluoro-4-bora-3a,4a-diaza-s-indacene
BSA	bovine serum albumin
cAMP	cyclic adenosine monophosphate
cDNA	coding deoxyribonucleic acid
C/EBPα,β,δ	CCAAT-enhancer-binding protein alpha, beta, delta
CLDN	claudin
CO_2	carbon dioxide

COL	collagen
COX	cyclooxygenase
CREB	cAMP response element-binding protein
Cx	connexin protein(s)
DAT	decellularized adipose tissue
dH_2O	distilled water
DAPI	4’,6-diamidino-2-phenylindole
DM	differentiation medium
DMEM/F-12	Dulbecco’s Modified Eagle’s Medium/Ham’s F-12
DMSO	dimethyl sulfoxide
DNA	deoxyribonucleic acid
DNase	deoxyribonuclease
DPBS	Dulbecco´s phosphate-buffered saline
ECM	extracellular matrix
EDHB	ethyl-3, 4-dihydroxybenzoate
EDTA	ethylenediaminetetraacetic acid
EGTA	Ethylenglycol-bis-(β-aminoethyl ether)-N,N,N´,N´-tetraacetic acid
EF1α	elongation factor-1 alpha
e.g.	exempli gratia (Latin “for example”)
FACIT	fibril-associated collagen with interrupted triple-helices
FAK	focal adhesion kinase
FAT	fatty acid transporter
FBS	fetal bovine serum
FN	fibronectin
ESC	embryonic stem cell(s)
EthD-III	ethidium bromide homodimer III
g	gram
GAPDH	glyceraldehyde-3-phosphate dehydrogenase
GF	growth factor
GJ	gap junction
GLUT4	glucose transporter 4

GM	growth medium
GPDH	glycerol-3-phosphate dehydrogenase
GTP	guanosine triphosphate
HPRT	hypoxanthine-guanine-phosphoribosyltransferase
IBMX	3-isobutyl-1-methylxanthine
i.e.	id est (Latin “that is”)
IGF-1	insulin-like growth factor 1
IgG	immunoglobulin G
IHC	immunohistochemistry
IL	interleukin(s)
JAM	junctional adhesion molecule
KD	knockdown
L	liter
LAM	laminin
LPL	lipoprotein lipase
M	molarity
m	meter
MAPK	mitogen-activated protein kinase
MCE	mitotic clonal expansion
MM	maintenance medium
MMP	matrix metalloproteinase(s)
mRNA	messenger ribonucleic acid
MSC	mesenchymal stem cell(s)
NC	non-collagenous
ORO	Oil Red O
PBM-2	preadipocyte basal medium 2
PBS	phosphate-buffered saline
PCR	polymerase chain reaction
PGA	poly(glycolic acid)
PGE2	prostaglandin E2
PLA	poly(lactic acid)
PLGA	poly(lactic-co-glycolic acid)

PPAR γ	peroxisome proliferator-activated receptor gamma
Pref-1	preadipocyte factor-1;
PU	polyurethane
qRT-PCR	quantitative reverse transcription-polymerase chain reaction
RNA	ribonucleic acid
RNase	ribonuclease
rpm	revolutions per minute
SD	standard deviation
SDF-1	stem cell-derived factor 1
SOI	start of induction
SREBP-1/ADD-1	sterol regulatory element binding protein 1/adipocyte determination and differentiation-dependent factor 1
STC-1	stanniocalcin-1
SVF	stromal-vascular fraction
TE	tissue engineering
TG	triglyceride(s)
TJP	tight junction protein
TNF- α	tumor-necrosis factor-alpha
TRAIL	TNF-α related apoptosis inducing ligand
TSG-6	(TNF)-α-stimulated gene/protein 6
U	unit
WAT	white adipose tissue
w/o	without
x g	fold gravitational acceleration (g = 9.81 m/s^2)

Affidavit

I hereby confirm that my thesis entitled “Human adipose-derived mesenchymal stem cells in a 3D spheroid culture system – Extracellular matrix development, adipogenic differentiation, and secretory properties” is the result of my own work. I did not receive any help or support from commercial consultants. All sources and/or materials applied are listed and specified in the thesis.

Furthermore, I confirm that this thesis has not been submitted as part of another examination process neither in identical nor in similar form.

_____ _____

Place, date Signature

Eidesstattliche Erklärung

Hiermit erkläre ich an Eides statt, die Dissertation „Humane mesenchymale Stammzellen aus dem Fettgewebe in einem 3D Sphäroid Kultursystem – Entwicklung der Extrazellulärmatrix, adipogene Differenzierung und sekretorische Eigenschaften“ eigenständig, d.h. insbesondere selbständig und ohne Hilfe eines kommerziellen Promotionsberaters, angefertigt und keine anderen als die von mir angegebenen Quellen und Hilfsmittel verwendet zu haben.

Ich erkläre außerdem, dass die Dissertation weder in gleicher noch in ähnlicher Form bereits in einem anderen Prüfungsverfahren vorgelegen hat.

_____ _____

Ort, Datum Unterschrift

Statement on Copyright and Self-plagiarism

The data presented in this thesis has been partially submitted to the Journal Tissue Engineering Part A as an original article entitled “Human ASC spheroids possess high adipogenic capacity and acquire an adipose tissue-like ECM pattern”. In accordance with the regulations of the parent publisher Mary Ann Liebert, Inc., data, text passages and illustrations from the manuscript were used in identical or modified form in this thesis.

Statement of individual author contributions and of legal second publication rights

Hoefner, C., Muhr, C., Wiesner, M., Wittmann, K., Lukaszyk, D., Radeloff, K., Winnefeld, M., Becker, M., Blunk, T., and Bauer-Kreisel, P. Human ASC spheroids possess high adipogenic capacity and acquire an adipose tissue-like ECM pattern. Tissue Engineering Part A, submitted in 08/2019.					
Participated in	**Authors** - Responsibility decreasing from left to right				
Study Design	C. Hoefner	P. Bauer-Kreisel	T. Blunk	M. Winnefeld	K. Radeloff
Methods Development	C. Hoefner	C. Muhr	K. Wittmann	D. Lukaszyk	
Data Collection	C. Hoefner	M. Wiesner	C. Muhr	K. Wittmann	D. Lukaszyk
Data Analysis and Interpretation	C. Hoefner	P. Bauer-Kreisel	T. Blunk	M. Becker	M. Winnefeld K. Radeloff
Manuscript Writing	C. Hoefner	P. Bauer-Kreisel	T. Blunk	M. Becker	

Explanations

I, C. Höfner, have done the main work of this study. I planned it, carried out the experiments, evaluated and interpreted the data and wrote the manuscript. P. Bauer-Kreisel contributed to the study design, data interpretation, and revised the manuscript together with me. C. Muhr, K. Wittmann, and D. Lukaszyk were involved in method development. M. Wiesner assisted in data collection, together with C. Muhr, K. Wittmann and D Lukaszyk. M Becker participated in data interpretation and the proofreading of the manuscript. M. Winnefeld and K. Radeloff were further involved in the study design and data interpretation. T. Blunk is the principal investigator and was involved in the study design, data interpretation, writing of the manuscript, and did the proofreading.

Acknowledgement

Curriculum Vitae